

Greener on the Other Side: Inequity and Tax Compliance*

Michael Carlos Best[†] Luigi Caloi[‡] François Gerard[§] Evan Plous Kresch[¶]
Joana Naritomi^{||} Laura Zoratto^{**}

This version: February 16, 2025

Abstract

Governments frequently use proxies for deservingness—tags—to implement progressive tax and transfer policies. These proxies are often imperfect, leading to misclassification and inequities among equally deserving individuals. This paper studies the efficiency effects of such misclassification in the context of the property tax system in Manaus, Brazil. We leverage quasi-experimental variation in inequity generated by the boundaries of geographic sectors used to compute tax liabilities and a large tax reform in a series of augmented boundary discontinuity designs. We find that inequities significantly reduce compliance. The elasticity of compliance with respect to inequity is between 0.12 and 0.25, accounting for half of the observed change in compliance. A simple model of presumptive property taxation shows how mistagging affects the optimal tax schedule, highlighting the opposite implications of responses to the level of taxation and to inequity for optimal tax progressivity. Interpreting our findings through the lens of the model implies that optimal progressivity is around 50% lower than it would be absent inequity responses. These results highlight the importance of inequity for public policy design, especially in contexts with low fiscal capacity.

*We are grateful to Katarzyna Bilicka, Nadja Dwenger, Bill Hoyt, Henrik Kleven, Ilyana Kuziemko, Ben Lockwood, Victor Poulouen, Joel Slemrod, Johannes Spinnewijn and numerous seminar and conference participants at the CEPR Public Economics Symposium, Duke, FGV-EESP, Fordham, Georgetown, INSPER, University of Kentucky, IFS-STICERD, Mannheim, Munich, the National Tax Association Conference, Northwestern, Oxford, Princeton, PUC-Rio, SITE, UFPE, UC Chile, Universitat Pompeu Fabra, and Wharton. We are grateful to Amanda Awadey, Carlota Loran Lopez, Malavika Mani, Samira Noronha, Maggie Shi, and Thaissa Sousa for excellent research assistance. We thank *Secretaria Municipal de Finanças e Tecnologia da Informação* (SEMEF), who provided access anonymized administrative data. This study has been funded by JPAL and the World Bank. All remaining errors are ours.

[†]michael.best@columbia.edu. Columbia University, BREAD, CEPR, IFS & NBER.

[‡]luigi.caloi@columbia.edu. Columbia University.

[§]f.gerard@ucl.ac.uk. University College London, BREAD, CEPR, & IFS.

[¶]ekresch@oberlin.edu. Oberlin College.

^{||}J.Naritomi@lse.ac.uk. London School of Economics, BREAD, CEPR, & IFS.

^{**}lzoratto@worldbank.org. World Bank.

1 Introduction

Views on equity have important implications for policy design. They influence economic decisions such as labor supply (Card *et al.*, 2012), policy preferences (Hvidberg *et al.*, 2023), and political stability (Keen & Slemrod, 2021). As a result, public policy is seldom designed without accounting for individual differences. Governments aim to ensure that the burden of taxation falls more heavily on those with a greater ability to pay. Transfer programs are designed to target benefits exclusively to needy beneficiaries. However, welfare-relevant attributes such as earning ability are hard, if not impossible, to observe directly. Thus, governments often rely on proxies: observable attributes correlated with individuals' unobserved types. These (often coarse) tags can facilitate the implementation of policies intended to be progressive (Akerlof, 1978). Nevertheless, proxies are inherently imperfect and can themselves generate inequities through misclassification.¹ In low- and middle-income countries, these challenges are further exacerbated by a lack of reliable data to differentiate between individuals.

This paper studies whether this misclassification has direct efficiency effects, and how policy should respond. Misclassification may generate resentment among those treated less favorably than their welfare-relevant type merits, causing them to reduce their voluntary compliance with a policy's mandates.² In particular, we focus on the effects of inequities among equally deserving taxpayers caused by the use of tags in property taxation on tax compliance. We argue that inequities induced by mistagging reduce tax morale and generate strong decreases in voluntary tax compliance. This additional behavioral response has implications for public policy's optimal design which are different from those of individuals' responses to the overall size of the taxes/transfers they receive.

We study these issues in the context of the property tax in the city of Manaus, Brazil. Like most cities', Manaus' property tax is presumptive, based on properties' observable characteristics rather than an assessment of their market values.³ As is common, the presumptive tax formula features an assessed price of land that is different in different sectors of the city. The boundaries of these sectors generate inequity: houses on one side of the boundary would have

¹With imperfect tags, individuals with differing welfare-relevant types, but who share the same policy-relevant attributes will be treated equally, and individuals who have the same welfare-relevance but differing levels of the policy-relevant attributes will be treated differently. Adam Smith (Smith 1776) invokes this inequity in objection to the "Window Tax", an English presumptive property tax:

"The principal objection to all such taxes is their inequality, an inequality of the worst kind, as they must frequently fall much heavier upon the poor than upon the rich. A house of ten pounds rent in a country town may sometimes have more windows than a house of five hundred pounds rent in London; and though the inhabitant of the former is likely to be a much poorer man than that of the latter, yet so far as his contribution is regulated by the window-tax, he must contribute more to the support of the state."

²In principle, those treated more advantageously than intended may feel impelled to reciprocate, but as we show in section 6.3, we see no evidence for this response in our setting. Similarly, Dube *et al.* (2019a) show that responses to peer wages are driven by higher-paid peers

³Table 1 shows a majority of the global population lives under this type of presumptive property tax scheme, as opposed to one based on market value.

discretely different tax liabilities if they had happened to be located on the other side of the boundary they face. These discontinuous changes also provide a source of quasi-experimental variation in both tax liabilities and the extent of mistagging.

We show that the overall change in compliance at tax sector boundaries is large: Compliance is 8% lower on the side with the higher land price, though this combines responses to the higher tax liability with responses to greater inequity. Using a range of extensions to the Boundary Discontinuity Design (BDD) (Black, 1999; Bayer *et al.*, 2007), we show that behavioral responses to inequity are strong. Both cross-sectional variation in the extent of inequity and time-series variation from a 2011 reform suggest that the elasticity of compliance with respect to inequity is at least 0.12, accounting for around half of the total effect at the boundary. Comparing responses to reductions in overtagging (in our context, being located on the high-price side of a boundary) to responses to reductions in undertagging suggests that responses to inequity are driven entirely by resentment of overtagging.

To draw out the implications of these results, we develop a simple model of the optimal design of a presumptive property tax. The model highlights the different implications of responses to the overall tax liability and responses to inequity for the degree to which the optimal policy differentiates between taxpayers. Responses to inequity push towards less differentiation, while responses to the size of the tax liability suggest greater differentiation. Distinguishing between these responses is, therefore, a crucial input into policy design. Our results suggest that optimal policy is 50% less progressive than if responses were solely driven by the level of the tax liability. Conversely, this suggests that the returns to investment in the fiscal capacity with which to accurately differentiate between properties are sizable, both in terms of raising additional revenue, and for reducing inequity.

Manaus, the capital city of the state of Amazonas in Brazil, is divided into 63 tax sectors, exclusively for the purposes of property taxation. Each of these sectors is associated with a sector-specific land price, a key input into the presumptive formula that determines each property's tax liability. These sector-specific land prices are tags for the value of properties in different parts of the city. However, this also means that at the boundaries of the tax sectors there are geographic discontinuities in tax bills. Two identical properties on the same street face different tax rates if they fall in different tax sectors. This provides us with an opportunity to construct a sharp measure of inequity: For each property our measure of the inequity they face takes the ratio of their tax liability to the counterfactual tax liability their property would have had had it been located across the street—and hence been tagged with a different tax sector.

We develop a simple model of presumptive property tax design to frame our analysis. In the model, properties are of two types (market values), but the government cannot observe properties' true types. Instead, the government observes a *tag* that proxies for the properties' types and uses these tags as the basis for its presumptive tax. Taxpayers, however, know their property type. When they receive the incorrect tag, this creates inequity, affecting their tax compliance decisions and creating a novel source of efficiency costs of taxation.

We derive sufficient statistics expressions characterizing the optimal tax schedule. Mistagging affects the optimal tax schedule through three channels. First, mistagging affects the composition of taxpayers. Some of the taxpayers paying the high-tag tax, have low-type houses. Second, behavioral responses to inequity increase the efficiency costs of raising revenue. Third, mistagging raises the marginal utility of consumption of mistagged households, aggravating the welfare costs of taxation.

Importantly, the two channels of behavioral responses—to the size of the tax liability, and to inequity—have opposite implications for the degree of progressivity of the optimal tax schedule. The standard elasticity of compliance with respect to the tax liability pushes in favor of more progressive taxes. By contrast the more elastic compliance is with respect to inequity, the less progressive the optimal tax schedule is. As a result, it is critical to disentangle the sources of behavioral responses in order to draw welfare and policy conclusions. Our empirical analysis provides a number of empirical strategies with which to achieve this.

We begin our empirical analysis by documenting a large change in compliance at the tax sector boundaries. Using a Boundary Discontinuity Design (BDD) (Black, 1999; Bayer *et al.*, 2007), we estimate that compliance is 8% lower on the side of the boundary with the higher land-price tag than on the side with the lower tag. However, this compliance change combines the responses to two changes at the boundary. First, tax liabilities are on average 13% higher. Second, inequity is 62% higher.

To disentangle these two effects, we develop a series of augmented BDD strategies that complement the BDD with two additional sources of variation. Our first set of strategies exploits the fact that the inequity we focus on is driven by the way that land enters the presumptive tax formula, rather than the contribution of the built structure. As a result, *expansive* properties with a lot of land and relatively little built structure face more inequity. This is true even conditional on properties' tax liability, allowing us to hold tax liabilities fixed and exploit the variation in expansiveness to estimate the effects of inequity.

We present two augmented BDD strategies that leverage this variation in expansiveness. First, we show that under a restrictive set of assumptions that we later relax, the BDD is identified for every level of the tax liability and at every level of expansiveness. These assumptions imply that after controlling flexibly for the tax liability on either side of the boundary, the augmented BDD recovers the average elasticity of compliance with respect to inequity. Implementing this design, we estimate that the elasticity is between 0.19 and 0.23. Second, we relax the assumptions required for identification. Instead of requiring a valid BDD for all levels of expansiveness, we instead require that the bias in the BDD is uncorrelated with expansiveness, akin to the parallel trends assumption used in difference in differences designs. Implementing this strategy, we estimate that the elasticity of compliance with respect to inequity is between 0.23 and 0.29.

Our second set of strategies leverages a large reform to the property tax implemented in 2011. The reform made large changes to the tax sectors' land prices and the other parameters of the

presumptive tax formula, but left the map of the tax sectors unchanged. This allows us to hold any time-invariant determinants of property tax compliance fixed and relate *changes* in compliance to changes in the tax liability and changes in inequity.

A first approach that leverages the reform in an augmented BDD assumes that after controlling flexibly for the change in the tax liability, an augmented BDD estimating the impact of changes in inequity on changes in compliance identifies the average elasticity of compliance with respect to inequity. Our second approach does not require that changes in potential compliance over time vary smoothly around the boundaries but instead allows the low-tax and high-tax sides of the boundaries to have different time trends. Combining the reform with variation in expansiveness, we show that an augmented BDD akin to a triple-differences design is able to recover the elasticity of compliance with respect to inequity. This approach makes the weakest assumptions of all of our designs, and our results here suggest that the elasticity of compliance with respect to inequity is between 0.11 and 0.12.

The final part of our empirical analysis develops an approach that allows us to separately identify the impacts of overtagging on the high-tax side of the tax sector boundaries and the impacts of undertagging on the low-tax side of the boundaries. Invoking a “strong parallel trends” assumption (Callaway *et al.*, 2024), we show that the responses to inequity are driven exclusively by households resenting being overtaxed on the high-tax side of the boundaries. We are unable to reject a null effect of undertagging on the low-tax side of the boundaries.

Our empirical analysis deploys a number of distinct strategies to estimate the impacts of inequity on tax compliance. They uniformly suggest that these responses are strong, with an elasticity of compliance with respect to inequity between 0.11 and 0.29. This suggests that around half of the 8% drop in compliance we observe on average at the tax sector boundaries is driven by the increase in inequity at the boundaries rather than the increase in tax liabilities. Viewed through the lens of a calibration of our model, this suggests that the optimal property tax schedule is around 50% less progressive than would be the case if behavioral responses operated exclusively through the level of the tax liability, as is commonly presumed.

Our paper contributes to four strands of literature. First, we contribute to the literatures on presumptive taxation and tagging in public finance. Akerlof (1978) and Nichols & Zeckhauser (1982) made seminal contributions showing how tagging can relax the incentive-compatibility constraints faced by redistributive policies. Despite these powerful theoretical arguments, Mankiw & Weinzierl (2010) argue that tagging is not as prevalent a feature of real-world policy as one might expect, possibly do to equity considerations Saez & Stantcheva (2016). Subsequent literature incorporates moral hazard considerations into the standard tagging framework (Besley & Coate, 1992; Gaubert *et al.*, 2021). We explore an additional channel: efficiency effects of inequity from imperfect tagging.

Second, we contribute to the literature on fairness and tax compliance and tax morale. Recent contributions here include Cruces *et al.* (2013); Giacobasso *et al.* (2022); Kuziemko *et al.* (2015); Hvidberg *et al.* (2023), see Luttmer & Singhal (2014); Slemrod (2019) for surveys. In the context of

property taxes, [Cabral & Hoxby \(2012\)](#) show that the more salient property taxes are, the lower governments set rates and limits. [Nathan et al. \(2023, 2025\)](#) study property tax appeals in Texas, showing experimentally that hassle costs and perceptions of the property tax system’s fairness affect appeal behavior. We contribute quasi-experimental estimates of the impact of inequity on compliance behavior and draw out the implications for policy design.

Third, we contribute to a growing literature on property taxation in low- and middle-income countries ([Castro & Scartascini, 2015](#); [Del Carpio, 2016](#); [Weigel, 2020](#); [Balan et al., 2022](#); [Okunogbe, 2023](#); [Ajzenman et al., 2024](#); [Bergeron et al., 2024a](#); [Dzansi et al., 2024](#); [Bergeron et al., 2024b](#); [Kapon et al., 2024](#)). [Brockmeyer et al. \(2023\)](#) provide evidence on the impact of enforcement activities and tax rates on compliance with Mexico City’s property tax, and explore the implications for how policy should trade off between the two instruments. Building on their work, we study a distinct channel: inequity, and draw out its implications for optimal policy.

Fourth, we contribute to the literature using boundary discontinuity designs to study public policy. Seminal contributions here include [Black \(1999\)](#); [Bayer et al. \(2007\)](#). More recent work has used augmented boundary discontinuity designs to study the valuation of local jurisdictions ([Schönholzer, 2022](#)) and the impacts of wealth taxation on saving ([Ring, 2024](#)). We show how the boundary discontinuity design can be augmented to incorporate cross-section differences in the intensity of treatment and changes over time in treatment.

Our paper proceeds as follows. Section 2 presents the context we study in Manaus, the data we use, and how we use it to measure inequity. Section 3 develops our resumptive property tax model, showing conceptually how mistagging and inequity affect the optimal tax schedule. Section 4 presents our Boundary Discontinuity Design (BDD) to study the overall changes in compliance that we see at the boundaries of Manaus’ tax sectors, documenting an 8% overall reduction in compliance. Section 5 presents our identification arguments and results for our augmented BDD leveraging variation in the expansiveness of properties. Section 6 presents our identification arguments and results for the augmented BDD leveraging Manaus’ 2011 reform, and our strategy to separately estimate the effects of overtagging and undertagging. Finally, section 7 concludes.

2 Context & Data

2.1 Property Tax (IPTU)

The property tax (IPTU: *Imposto Predial e Territorial Urbano*) is one of the two main tax instruments assessed by municipal governments in Brazil. The tax authority of Manaus (SEMEF; *Secretaria Municipal de Finanças e Tecnologia da Informação*) informs households of their liability in mid-January of the relevant tax year. Taxpayers can choose between making a single payment or paying their tax bill in installments. Failure to pay the IPTU bill results in fines, interest, or legal recourse. The imposition of fines is automatically triggered on any household delinquent in their payment on January 1 of the year after the IPTU issuance, with no discretion by SEMEF to

levy fines on particular households.⁴

Like all municipalities in Brazil, Manaus employs a presumptive formula to calculate the property tax liability. This differs from the market value-based assessment used in the United States but is in line with how property tax is calculated in most large urban centers around the world (see table 1). As with many cities employing a presumptive formula, the calculation of property tax in Manaus is in part a function of geography, with rates differing depending on where the property is located within the city.

By statute, the effective property tax rate—defined as the IPTU bill as a percent of a property’s market value—is set at 0.9%.⁵ However, average IPTU bills as a fraction of advertised sales prices imply an effective tax rate closer to 0.46%. Using the 2010 census, we estimate that the average residential IPTU bill in Manaus for a given year represents a roughly 2.6% share of annual household income.⁶ This property tax burden as a share of annual income is similar to property taxes in the United States, which range from 1.5% to 5%, and is nearly identical to the burden faced by residents of California.⁷ The estimated effective tax rate places Manaus among the lowest effective rates in the United States, which range from 0.4% to 3% (Twait & Langley, 2024).

The IPTU of a given property i in year y is calculated based on estimates of the property value (T_{isy} ; *valor venal*), which is the sum of an estimate for land value (a_{isy} ; *valor do terreno*) and estimates of the house’ value (b_{isy} ; *valor da edificação*) multiplied by a tax rate according to a schedule (α_y) based on the type of property.

$$T_{isy} = \alpha_y [p_{s(i)}a_{iy} + b_{iy}] = \alpha_y [p_{s(i)}f(\mathbf{A}'_{iy}\boldsymbol{\xi}_y^A) + f(\mathbf{B}'_{iy}\boldsymbol{\xi}_y^B)] \quad (1)$$

The value a_{iy} is based on four observable land characteristics for the property (\mathbf{A}_{iy}), each with an associated corrective factor ξ_y^A . In addition to these land characteristics (e.g., whether the land is flat or hilly), T_{isy} accounts for the sector of the city where the property is located. Each sector s is assigned a sector-specific price per square meter $p_{s(i)}$ based on municipal estimates of housing prices (see figure 1). Similarly, b_{iy} is based on characteristics of the building or house (with associated factors ξ_y^B): the type of construction, the materials used in the construction, the size of the property, among other characteristics.

Crucially for our identification, the tax sectors are not used for other policy or administrative purposes beyond property tax, and only a few of the sector boundaries overlap with neighborhood boundaries (see appendix A, figure A.1). The use of geography is ubiquitous in presumptive property taxes around the world (see table 1), and Manaus is not unique in having tax sectors that do not align with municipal administrative divisions. All properties within a sector are assigned the same square meter value (General Plan for Standardize Property Value; *Planta*

⁴See <https://www.manaus.am.gov.br/pgm/divida-ativa-servico/>

⁵Lei No 1.628/2011, article 2

⁶This figure is calculated using the average household income in Manaus from the 2010 census tracts. Note that this figure is likely to be an upper bound, as we are likely underestimating household income.

⁷Source: USAFacts. <https://usafacts.org/articles/where-do-people-pay-the-most-and-least-in-property-taxes/>

Genérica de Valores), which were set when the tax authority first created the city-wide tax sectors in 1983. Despite the growth of the city, the boundaries of these sectors have not changed, leading to arbitrary changes in the square-meter values for very similar properties in close proximity to each other but across a tax sector boundary (see figure 2).

2.2 2011 Tax Reform

In an effort to reflect the significant changes in the city over nearly three decades, Manaus passed a major reform in its property tax system (Law 1.628/2011) that was introduced in 2012. One of the main goals of the reform was to update the policy parameters used to estimate land and house values. In 1983, a government committee divided Manaus into 62 sectors (see figure 1), with the square-meter values ($p_{s(i)}$) based on property valuations in the city in 1983. These values did not change in subsequent decades and by 2011 these policy parameters were out of date as Manaus experienced substantial sprawl of the city outward from the historic core (see appendix B, figure B.1). The population in 1983 was only 30 percent of the current population of Manaus, and its remarkable growth led to entirely new housing developments in previously uninhabited forest. However, these uninhabited areas were still assigned a tax sector in 1983, resulting in areas of the city with house values that were unrelated to the established sector rates.

As a result of not updating the tax code, property taxes became less progressive over time. Although households in wealthier census tracts still had a larger tax bill in 2010, the difference across census tracts with different household incomes flattened considerably (see appendix B, figure B.3a). Insofar as the parameters for a_{iy} and b_{iy} were set in 1983 to target wealthier households, an inability to revise the city's General Plan for Standardize Property Value to reflect the shifting socioeconomic geography of the city led to a deterioration in the usefulness of the tags.

To address these concerns about progressivity, the 2011 reform adjusted rates across the city, with the amount resulting from the additional IPTU phased in over five years. Each year, 20% of the additional amount was added to the tax bill (from 2012 to 2016).⁸ The reform raised tax liabilities for almost every property with striking heterogeneity in size of the tax increase to address the inequities in the previous system (see appendix B, figure B.2).

Although the 2012 property tax system was still based on presumptive estimates of the value of the property, it was considered more fair by the municipal government as it was more aligned with the actual current property values than the previous estimates from 1983.⁹ Panel B of figure B.3 shows the improvement in targeting as a result of the reform; not only did the reform increase the average IPTU across census tracts, it also led to a larger change in tax bills for richer households (see appendix B, figure B.3b). It should be noted that while the 2011 reform led to an improvement in targeting, the system was still based on a presumptive formula that did not

⁸This phase-in was meant to avoid a backlash from the some sharp increases in the IPTU bill. The first attempt to update IPTU's tax rates and revise the Municipal General Plan for Standardize Property Value was made in 2006, but the reform failed and was never fully implemented.

⁹The online portal of one of the main Brazilian newspaper *O Globo* (G1) highlighted that the updated property value estimates were more fair given how outdated the 1983 values were [link to article](#).

eliminate the potential for mistagging - especially for otherwise identical households on sector boundaries - which we use as our main source of identification throughout the rest of the paper.

2.3 Data

In collaboration with SEMEF, we have access to de-identified property registry information (cadaster) for 613,131 properties that includes a recent snapshot of the building characteristics, lot size and land characteristics. This data is geo-referenced and matched to the road network of the city. We also have GIS maps for all relevant boundaries (tax sector, neighborhood, city block, parcel), which we use to measure a household's distance to a tax sector boundary, and hence to the discontinuity in the per-square meter rate.

In addition to the cadaster, we have data on IPTU liabilities from 2004–2019 and IPTU payments from 2004–2019 for the universe of taxpayers in Manaus, including fines and legal follow-up due to delinquency. This allows us to directly observe both the household's tax liability in a given year and whether a given property was compliant with IPTU payments. We also have data on property transfers and sales from the property transfer tax system (ITBI; *Imposto sobre transmissão de bens imóveis*).

Our main outcome of interest for studying the behavioral response to mistagging is compliance—share of a household's IPTU bill that they pay within 18 months of receiving their bill. Since a household's property tax bill is mechanically determined by its characteristics in the cadaster, there is no self-declaration of the tax base.¹⁰ Thus, we do not measure the moral hazard response of households attempting to change their “tags”, but rather the response of households *after* receiving their tax bill.

Compliance with the property tax in Manaus is relatively low and stable over time (see appendix A, figure A.3). Two features of tax compliance in Manaus are worth noting. First, compliance is driven almost entirely on the extensive margin, with households paying their entire IPTU bill if they decide to pay. Second, compared to other large cities in Brazil, Manaus has a markedly lower collection rate, although this is consistent with the fact that poorer cities throughout the country tend to have lower collection rates (see appendix A, figure A.4).

2.4 Measuring Distance to Sector Boundary

Our identification strategy relies in part on the discontinuous changes in the square-meter rate across the tax sector boundaries in a regression discontinuity setting. We restrict our sample of interest to properties within 300 meters of a tax sector boundary. The distance from the boundary is measured as the closest point of a given lot to the boundary line, where properties on the boundary are defined as having a distance of zero. Appendix C provides additional details on the construction of the distance measure. We define households as being on the “high side” of

¹⁰There is a mechanism by which a household can petition SEFAZ to update the cadaster, but this is almost never used. SEFAZ can update the cadaster (and did so in 2011), but this is generally done on the city-wide stock of housing inventory and is exogenous from the point of view of households.

the boundary if the square-meter rate is higher than the sector rate on the other side of the given boundary.

To refine our dataset for the boundary discontinuity analysis, we narrowed our focus to properties within 300 meters of the tax sector boundaries, excluding those exempt from tax, without construction, or not designated as residential. Properties on sector boundaries that overlap with neighborhood boundaries were also excluded from the boundary discontinuity design to control for changes in municipal public provision. After these adjustments, our analysis centers on 27,356 properties, resulting in 415,546 property-year observations from 2004 to 2019.¹¹

2.5 Measuring Inequity: σ

To create a measure for the degree of inequity in the IPTU system, we take advantage of two features of our setting. First, we are able to observe both the true (i.e., statutory) tax liability for a given property, as well as its compliance in every year. Second, we use the discontinuous jumps in the value of the price per square meter $p_{s(i)}$ across tax sectors.

For a given property i in tax sector s , we identify the nearest neighboring tax sector \hat{s} and define the inequity measure σ_i as

$$\sigma_{iy} = \frac{T_{iy}}{\hat{T}_{iy}}$$

where T_{iy} is the true tax liability faced by property i in a given year y . We define \hat{T} as the counterfactual tax liability $\hat{T}_{iy} := \alpha [p_{\hat{s}} a_{iy} + b_{iy}]$. That is, \hat{T}_{iy} represents the property tax bill that household i would have received if were located on the other side of the tax sector boundary, with all other land (a_{iy}) and building (b_{iy}) characteristics being the same.

Defining inequity in this way has a few advantages. First, since we are computing the counterfactual tax bill using the household’s own characteristics, the link between inequity and mistagging is fairly straightforward; $|\sigma|$ is larger for households that live on the boundary of two tax sectors with larger difference in the square meter rate ($p_{s(i)}$). Additionally, as σ is defined using only household i ’s characteristics, we can be agnostic about peer group selection. This is in contrast to papers such as [Dube et al. \(2019b\)](#), [Card et al. \(2012\)](#), and [Hvidberg et al. \(2023\)](#) that define the peer group needed for comparisons of inequity. Our measure of inequity is therefore a “selfish” measure, where the household’s response is driven by whether they feel that they have been treated by the system, and does not capture whether a household cares about whether other people are treated fairly.

Two attributes of our measure of σ make it useful for studying the behavioral response to inequity inherent in the tax system, as discussed in more detail in appendix E. First, there is significant variation in σ for households across the city (see appendix E, figure E.37), implying that individuals respond to a markedly different counterfactual of what their IPTU would have been

¹¹See appendix D for more details on the sample selection process.

if taxed on the other side of the sector boundary. Second, the measures for the counterfactual tax liability (σ) and true tax liability (τ) are not collinear (see appendix E, figure E.38). This allows us to separately estimate the behavioral response to changes in both the direct effect (changes in τ) and the effect driven by changes in the relative inequity of imperfect tagging in the system.

3 Conceptual Framework

This section presents a simple model of the welfare effects of property taxation. There are a mass 1 of each of two *types* of houses: $\theta \in \{H, L\}$. These houses generate flows of housing consumption $y_H > y_L$. Actual house types θ are not observable to the government. Instead, the government observes a *tag* ϕ : either h or l for each house. When houses are correctly tagged, the H -type houses receive the tag $\phi = \phi(H) = h$ and the L -type houses receive the tag $\phi = \phi(L) = l$. However, when a house receives the incorrect tag ($\phi \neq \phi(\theta)$) this generates inequity for the occupant. We model this inequity as $\sigma_{\theta\phi} = T_\phi/T_{\phi(\theta)}$. Whenever $\sigma_{\theta\phi} > 1$ the house is said to be *overtagged* while if $\sigma_{\theta\phi} < 1$ the house is *undertagged*. Households have a distaste for paying an inequitable tax $d(\sigma_{\theta\phi})$. We assume that when they are correctly tagged they have no distaste for inequity: $d(1) = 0$ and that $d(\cdot)$ is continuous, but place no additional restrictions on $d(\cdot)$.¹²

Households decide whether to pay their property tax T_ϕ . If they pay, this reduces their consumption and they bear the disutility of inequity. If they don't pay, they face a cost of being a tax delinquent γ . This cost is idiosyncratic in the population with a distribution $F(\gamma)$. A household will pay its taxes whenever their cost of delinquency is high enough:

$$u_{\theta\phi}^{\text{pay}} > u_{\theta\phi}^{\text{evade}} \leftrightarrow u(y_\theta - T_\phi) - d(\sigma_{\theta\phi}) > u(y_\theta) - \gamma \leftrightarrow \gamma > u(y_\theta) - u(y_\theta - T_\phi) + d(\sigma_{\theta\phi}) = \gamma_{\theta\phi}^*$$

and as a result, compliance amongst households of type θ with tag ϕ is $c_{\theta\phi} = 1 - F(\gamma_{\theta\phi}^*)$.

For simplicity, we will assume that there is only overtaging: All H -type houses are correctly tagged with $\phi = h$, but a fraction ψ of the L -type houses are incorrectly given the $\phi = h$ tag. In section 3.3.1 and appendix K we present the extension to incorporate undertagging, but in section 6.3 we provide empirical evidence that there is no behavioral response to undertagging in our setting, so this simplification is warranted in our context.

Tax revenue $r = \psi c_{Lh} T_h + (1 - \psi) c_{Ll} T_l + c_{Hh} T_h$ is used to finance the provision of local public goods with social benefits of $B(r)$ and marginal benefits $b(r)$. Social welfare combines the welfare of a unit mass of each type of household and the benefits of the public good:

$$W = \psi \omega_L V_{Lh} + (1 - \psi) \omega_L V_{Ll} + \omega_H V_{Hh} + B(r)$$

¹²Households may have different distaste for inequity depending on whether they are undertagged ($\sigma_{\theta\phi} < 1$) or overtaged ($\sigma_{\theta\phi} > 1$), analogously to Dube *et al.* (2019b). For example, we might use a piecewise linear function $d(\sigma_{\theta\phi}) = (\sigma_{\theta\phi} - 1)(d_1 + (\delta - d_1)\mathbf{1}[\sigma_{\theta\phi} > 1])$ where $\delta > d_1 \geq 0$.

where ω_θ are Pareto weights on the welfare of the two types of households, and

$$V_{\theta\phi} = \int_{-\infty}^{\gamma_{\theta\phi}^*} [u(y_\theta) - \gamma] dF(\gamma) + \int_{\gamma_{\theta\phi}^*}^{\infty} [u(y_\theta - T_\phi) - d(\sigma_{\theta\phi})] dF(\gamma)$$

is the private welfare of θ -type houses with the ϕ tag.

3.1 Benchmark: Perfect Tagging, No Inequity

As a benchmark, first consider the case in which tagging is perfect ($\psi = 0$ and so $\phi = \phi(\theta)$ for all houses). In this case, there is no inequity and so households' compliance behavior is driven only by the level of taxation they face. Changes in compliance in response to marginal changes in taxes generate fiscal externalities so that the increase in tax revenue from marginal increases in the l -tag tax is $dr/dT_l = c_{Ll}(1 - \varepsilon)$, where $\varepsilon \equiv -\frac{\partial c}{\partial T} \frac{T}{c}$ is the elasticity of compliance with respect to the tax liability. Analogously, the effect of a marginal increase in the h -tag tax is $dr/dT_h = c_{Hh}(1 - \varepsilon)$.

The optimal property tax trades off the benefits of additional revenue for public goods against the costs of reducing private welfare and the fiscal externality from changes in compliance. The following lemma characterizes this optimal balance.

Proposition 1 (Property Taxes Under Perfect Tagging). *With perfect tagging ($\phi = \phi(\theta)$ for all houses), the optimal property tax satisfies*

$$\frac{T_l}{y_L} = \frac{1 - \varepsilon - g_L}{\rho g_L} \quad (2)$$

$$\frac{T_h}{y_H} = \frac{1 - \varepsilon - g_H}{\rho g_H} \quad (3)$$

where $g_\theta = \omega_\theta u'(y_\theta) / b(r)$ is the generalized social marginal welfare weight of type θ (Saez & Stantcheva, 2016) and $\rho \equiv -u''(y) y / u'(y)$ is the coefficient of relative risk aversion.

The level of taxation is lower the stronger are behavioral responses to the tax liability: $\partial T_\phi / \partial \varepsilon < 0$. Moreover, the optimal property tax is more progressive the stronger society's preference for redistribution g_L / g_H , and the larger the elasticity of compliance with respect to the tax liability ε :

$$\frac{\partial \left(\frac{T_h / y_H}{T_l / y_L} \right)}{\partial g_L / g_H} > 0 \quad \& \quad \frac{\partial \left(\frac{T_h / y_H}{T_l / y_L} \right)}{\partial \varepsilon} > 0$$

Proof. See appendix I □

These simple expressions relate taxes to the parameters in intuitive ways. The larger are the utility costs of reducing consumption (governed by the g_θ and the curvature of utility ρ), the lower are taxes; and similarly the larger are the behavioral responses and the corresponding fiscal externalities (governed by the elasticity of compliance ε) the lower are taxes. Perhaps less

obviously, the progressivity of the tax is steeper the stronger are behavioral responses. Consider an increase in ε that costs the government \$1 in lost revenue. Recovering this revenue from the h -tax reduces social welfare by g_H , while recovering it from an increase in the l -tax costs $g_L > g_H$ and so naturally the burden falls more heavily on the h -tax, increasing progressivity.

3.2 Imperfect Tagging and Inequity Aversion

We now consider a model that also features the key force that our empirical analysis seeks to study: Households are mistagged ($\psi > 0$) and they have a distaste for the resulting inequity ($d(\sigma)$). This creates a third group of households: L -type houses incorrectly tagged with the h tag. These households face inequity $\sigma_{Lh} > 1$, adding two new channels to the optimal policy tradeoff.

First, the disutility from inequity creates first-order welfare losses for Lh households. Second, Lh households' compliance decisions depend both on their tax liability T_h and on the inequity they face $\sigma_{Lh} = T_h/T_l$. This creates a new source of fiscal externalities of both the high tax T_h and the low tax T_l governed by the strength of the elasticity of compliance with respect to inequity $\eta \equiv -\frac{\partial c}{\partial \sigma} \frac{\sigma}{c}$. As a result, the elasticity of compliance by Lh households with respect to the h tax is $\frac{dc_{Lh}}{dT_h} \frac{T_h}{c_{Lh}} = -\varepsilon - \eta < 0$ and with respect to the l tax (which they do not face but which affects inequity) is $\frac{dc_{Lh}}{dT_l} \frac{T_l}{c_{Lh}} = \eta > 0$.¹³

The following proposition characterizes the optimal tax schedule and how the presence of mistagging and inequity aversion affect the optimal policy:

Proposition 2 (Property Taxes with Imperfect Tagging and Inequity Aversion). *The optimal property tax schedule satisfies*

$$\frac{T_l}{y_L} = \frac{1 - g_L - \varepsilon + \varphi_l \frac{\eta}{\varepsilon} \sigma (g_L + \varepsilon)}{g_L \rho (1 - \varphi_l \frac{\eta}{\varepsilon} \sigma^2)} \quad (4)$$

$$\frac{T_h}{y_H} = \frac{1 - \bar{g}_h - \varepsilon - \varphi_h \frac{\eta}{\varepsilon} (g_L + \varepsilon)}{\rho \left[\bar{g}_h + \varphi_h g_L \left(\frac{y_H}{y_L} \left(1 + \frac{\eta}{\varepsilon} \right) - 1 \right) \right]} \quad (5)$$

where $\sigma = \sigma_{Lh} = T_h/T_l$; $\varphi_l = \psi c_{Lh}/(1 - \psi)c_{Ll}$ is the number of mistagged L taxpayers relative to the number of l -tax taxpayers; $\varphi_h = \psi c_{Lh}/(\psi c_{Lh} + c_{Hh})$ is the number of mistagged L taxpayers relative to the number of h -tax taxpayers, and $\bar{g}_h = \varphi_h g_L + (1 - \varphi_h) g_H$ is the average social marginal welfare weight of h -tax taxpayers.

Relative to a benchmark with perfect tagging, imperfect tagging reduces optimal property tax revenues. In particular,

1. The greater the extent of mistagging ψ the lower optimal property tax revenues;
2. The stronger the behavioral response to inequity η the lower optimal property tax revenues;

¹³To see these, note that $\frac{dc_{Lh}}{dT_h} \frac{T_h}{c_{Lh}} = \left(\frac{\partial c_{Lh}}{\partial T_h} + \frac{\partial c_{Lh}}{\partial \sigma} \frac{\partial \sigma}{\partial T_h} \right) \frac{T_h}{c_{Lh}} = \frac{\partial c_{Lh}}{\partial T_h} \frac{T_h}{c_{Lh}} + \frac{\partial c_{Lh}}{\partial \sigma} \frac{\sigma}{c_{Lh}} \frac{\partial \sigma}{\partial T_h} \frac{T_h}{\sigma} = -\varepsilon - \eta$ and, analogously, that $\frac{dc_{Lh}}{dT_l} \frac{T_l}{c_{Lh}} = \frac{\partial c_{Lh}}{\partial \sigma} \frac{\sigma}{c_{Lh}} \frac{\partial \sigma}{\partial T_l} \frac{T_l}{\sigma} = \eta$.

3. The stronger the behavioral response to the tax liability ε , the lower optimal property tax revenues.

Relative to a benchmark with perfect tagging, imperfect tagging lessens the optimal degree of progressivity of the property tax. In particular,

1. The greater the extent of mistagging ψ the less progressive the property tax;
2. The stronger the behavioral response to inequity η the less progressive the property tax;
3. The stronger the behavioral response to the tax liability ε , the more progressive the property tax.

Proof. See appendix J □

Comparing the characterization of the optimal property tax schedule in (4) & (5) to the benchmark with perfect tagging characterized in (2) & (3), the presence of imperfect tagging and inequity aversion adds three new effects. First, a fraction φ_h of the households paying the h tax are not H -types (the tax's intended targets) but rather mistagged L -types. This raises the average social marginal welfare weight of the h -taxpayers from g_H to \bar{g}_h , lowering the h tax.

Second, inequity aversion $d(\sigma)$ directly reduces the utility of mistagged types and increases the fiscal externality of compliance responses to T_h . Conversely, increasing T_l reduces inequity, increasing the utility of mistagged types and reducing the fiscal externality of their compliance responses. The $\varphi_\phi \frac{\eta}{\varepsilon}$ terms in the numerators of (4) & (5) account for these effects. They increase T_l and reduce T_h , making the tax system less progressive.

Third, mistagged L households pay a higher tax than their correctly tagged counterparts, raising the marginal utility at which their consumption losses are evaluated. The φ_ϕ terms in the denominators of (4) & (5) account for these effects. They also increase T_l and reduce T_h , making the tax system less progressive.

While these additional effects push in the intuitive directions, proposition 2 highlights the importance of understanding the mechanisms behind behavioral responses to property taxes. In particular, the proposition shows that ε and η can have opposite implications for optimal tax progressivity. In general, empirical estimates of behavioral responses to taxes will contain a mixture of the two channels (in section 4 we show how this issue affects the interpretation of estimates from our reduced-form boundary discontinuity design), with unclear implications for policy. In sections ?? and 6 we show how to disentangle the two channels empirically. Before turning to these empirical challenges, however, we present some extensions of the model to highlight the robustness of the qualitative conclusions in proposition 2.

3.3 Extensions

3.3.1 Mistagging of Both House Types

Appendix K presents an extension to the model in which both L - and H -type houses can be mistagged. It incorporates two changes to the baseline model. First, a fraction $\psi_{Hl} \geq 0$ of H -type houses is mistagged with the l tag (in addition to a fraction $\psi_{Lh} \geq 0$ of mistagged L -types

as in the baseline model in section 3.2). Second, the elasticity of compliance with respect to inequity of the undertagged, η_{Hl} need not equal the elasticity of the overtagged η_{Lh} . With these additions, we can characterize the optimal tax schedule:

$$\frac{T_l}{y_L} = \frac{1 - \varepsilon - \bar{g}_l + \varphi_{Ll} \frac{\eta_{Lh}}{\varepsilon} \sigma (g_L + \varepsilon) - \varphi_{Hl} \frac{\eta_{Hl}}{\varepsilon} (g_H + \varepsilon)}{\rho \left(\bar{g}_l + g_H \varphi_{Hl} \left[\left(1 + \frac{\eta_{Hl}}{\varepsilon} \right) \frac{y_L}{y_H} - 1 \right] - g_L \varphi_{Ll} \frac{\eta_{Lh}}{\varepsilon} \sigma^2 \right)} \quad (6)$$

$$\frac{T_h}{y_H} = \frac{1 - \varepsilon - \bar{g}_h + \varphi_{Hh} \frac{\eta_{Hl}}{\varepsilon} \frac{1}{\sigma} (g_H + \varepsilon) - \varphi_{Lh} \frac{\eta_{Lh}}{\varepsilon} (g_L + \varepsilon)}{\rho \left(\bar{g}_h + g_L \varphi_{Lh} \left[\left(1 + \frac{\eta_{Lh}}{\varepsilon} \right) \frac{y_H}{y_L} - 1 \right] - g_H \varphi_{Hh} \frac{\eta_{Hl}}{\varepsilon} \frac{1}{\sigma^2} \right)} \quad (7)$$

where $\sigma = T_h/T_l$; $\bar{g}_l = \frac{(1-\psi_{Lh})c_{Ll}g_L + \psi_{Hl}c_{Hl}g_H}{(1-\psi_{Lh})c_{Ll} + \psi_{Hl}c_{Hl}}$ is the average social marginal welfare weight of l -tax taxpayers, and analogously $\bar{g}_h = \frac{\psi_{Lh}c_{Lh}g_L + (1-\psi_{Hl})c_{Hh}g_H}{\psi_{Lh}c_{Lh} + (1-\psi_{Hl})c_{Hh}}$ is the average social marginal welfare weight of h -tax taxpayers; and the $\varphi_{\theta\phi}$ terms are the number of mistagged θ -types as a fraction of the number of ϕ -tax taxpayers (e.g. $\varphi_{Lh} = \frac{\psi_{Lh}c_{Lh}}{\psi_{Lh}c_{Lh} + (1-\psi_{Hl})c_{Hh}}$).

The three forces discussed in proposition in the context of the baseline model with only mistagging of L -types are present now also for the mistagged H -types. The lower social marginal welfare weight of the l -tax taxpayers ($\bar{g}_l < g_L$) also pushes towards more progressive taxes, but the two effects due to the behavioral response to inequity now have opposite signs: they push towards more progresssive taxes.¹⁴ This suggests that the overall effect on the tax schedule is ambiguous and depends on the magnitudes of the parameters (the extent of mistagging of the two types $\psi_{\theta\phi}$, the elasticities $\eta_{\theta\phi}$, and the property values y_{θ}). However, for given parameter values, all three forces are weaker for the mistagged H -types than for the mistagged L -types, suggesting that the net effects will still be in the directions highlighted by proposition 2.¹⁵ Moreover, as we show in section 6.3, our empirical evidence suggests that the elasticity of compliance with respect to undertagging, η_{Lh} is zero, so these additional terms are not empirically relevant in our context.

3.3.2 Location Choice and House-Price Capitalization

Appendix L presents a modified model in which L -type households can choose to move between L -type houses in locations with l and h tags.¹⁶ As is common in spatial models (Redding &

¹⁴These are: First, the $\varphi_{\theta\phi}$ terms in the numerators to account for direct utility losses and the fiscal externality. The $\varphi_{L\phi}$ terms push towards less progressive taxes while the $\varphi_{H\phi}$ terms suggest more progressive taxes. Second, the $\varphi_{\theta\phi}$ terms in the denominators to account for the higher marginal utility of consumption of mistagged households. Again, the $\varphi_{L\phi}$ terms push towards less progressive taxes while the $\varphi_{H\phi}$ terms suggest more progressive taxes.

¹⁵To see this, consider the case of the $\varphi_{\theta\phi}$ terms in the numerator of equation (6) for T_l . These push towards a less progressive tax (as in the baseline case in proposition 2) whenever the φ_{Lh} term is larger than the φ_{Hl} term. This is likely because first, the positive φ_{Lh} term is multiplied by $\sigma \geq 1$ while the negative φ_{Hl} term is not; and second, because the φ_{Lh} term depends on the social marginal welfare weight of the L -types, g_L , which is larger than the social marginal welfare weight of the H -types, g_H , appearing in the negative φ_{Hl} . As a result, for the force from the mistagged H -types to dominate, it would need to be the case that they are a large group (large φ_{Hl}) and/or that they are much more sensitive to inequity than the mistagged L -types ($\eta_{Hl} > \eta_{Lh}$). In section 6.3 we show that our evidence suggests that $\eta_{Hl} = 0$, suggesting that the forces from the mistagged L -types will dominate. Analogous reasoning applies to the numerator of (7) and to the $\varphi_{\theta\phi}$ terms in the denominators of (6) and (7).

¹⁶For simplicity, we assume that the H -type households all live in houses with h tags and do not move.

Rossi-Hansberg, 2017), households have idiosyncratic preferences for houses in each location ξ_ϕ . Households take house prices $p_{L\phi}$ and property taxes T_ϕ as given and choose where to live, anticipating whether or not they will pay their property tax. Given house prices and taxes, these household choices determine which households live in which location and which ones pay their property taxes. House prices then adjust to equilibrate housing demand and an exogenous supply of houses in each sector.

In this model, households' distaste for tax inequities is net of the extent to which tax differences are capitalized into house prices. To capture this we model the disutility of inequity as $d(\tilde{\sigma})$ where $\tilde{\sigma} = \left(1 + \frac{p_{Lh} - p_{Ll}}{T_h - T_l}\right) \frac{T_h}{T_l}$, where $p_{L\phi}$ is the price of an L -type house taxed at T_ϕ . In the extreme, when tax differences are fully capitalized into house prices, households no longer experience inequity and the impacts of mistagging on optimal policy described in section K disappear. However, whenever tax differences are less than fully capitalized into house prices, misclassification still generates inequity and affects tax compliance decisions, shaping the optimal policy schedule.

L -type households will choose to live in the sector with the h tax whenever $V_h(\gamma, \xi_h; p_{Lh}, T_h) > V_l(\gamma, \xi_l; p_{Ll}, T_l)$, where $V_\phi = \max\{u(v_L - p_{L\phi} - T_\phi) - d(\tilde{\sigma}) + \xi_\phi, u(v_L - p_{L\phi}) - \gamma + \xi_\phi\}$ is their value from living in the sector with the ϕ tax, incorporating their optimal choice of whether to pay the corresponding property tax. Whenever households all share the same tastes for the two sectors ($\text{Var}(\xi_\phi) = 0$), households must be indifferent between living in the two sectors and tax differences are fully capitalized into prices.¹⁷ But whenever there are idiosyncratic tastes for living in each sector, this will lead to incomplete capitalization of property taxes, and hence inequity.

Marginal changes in property taxes now also cause households to move. However, by the envelope theorem, these moves have no first-order effect on movers' utility. Nevertheless, moves affect house-prices, with first-order effects on home buyers' welfare.¹⁸ Moreover, the compliance elasticities now also incorporate a composition effect as some households move between sectors. These compliance elasticities are still, however, the relevant sufficient statistics for welfare and optimal policy, alongside an additional sufficient statistic: $\kappa \equiv -\partial p_{L\phi} / \partial T_\phi$ governing the extent to which property taxes are capitalized into house prices.

¹⁷To see this, let $\xi_h = \xi_l = 0$ for all households and consider compliant households. Whenever they are not indifferent between the two sectors, they all choose the same sector and the aggregate demand for houses in the sectors will not equal supply. For them to be indifferent it must be the case that $v_L - p_{Ll} - T_l = v_L - p_{Lh} - T_h - d(\tilde{\sigma})$. If $T_h > T_l$ and this is not fully capitalized into house prices, $d(\tilde{\sigma}) > 0$ so households cannot be indifferent. They can only be indifferent when taxes are fully capitalized into house prices: $p_{Lh} = p_{Ll} - T_h + T_l$. p_{Ll} then adjusts such that the aggregate demand for houses in each sector equals supply.

¹⁸There are no sellers in the model. If there were and they had the same welfare weights as the buyers, changes in house prices would merely be transfers between the buyer and the seller with no welfare impact

The modified optimal tax formulas incorporating house price changes are:

$$\frac{T_l}{\tilde{y}_{Ll}} = \frac{1 - \varepsilon - g_L + \varphi_l \frac{\eta}{\varepsilon} \sigma (g_L + \varepsilon) + \kappa \frac{g_L}{c_{Ll}}}{\rho g_L (1 - \kappa) \left[1 - \varphi_l \frac{\eta}{\varepsilon} \sigma^2 (1 - \tilde{\kappa}) \right]} \quad (8)$$

$$\frac{T_h}{\tilde{y}_{Hh}} = \frac{1 - \varepsilon - \bar{g}_h - \varphi_h \frac{\eta}{\varepsilon} (g_L + \varepsilon) + \kappa \frac{\tilde{g}_h}{\tilde{c}_h}}{\rho (1 - \kappa) \left[\bar{g}_h + \varphi_h g_L \left(\frac{\tilde{y}_{Hh}}{\tilde{y}_{Ll}} \left(1 + \frac{\eta}{\varepsilon} \right) (1 - \tilde{\kappa}) - 1 \right) + \varphi_h g_L \frac{\kappa}{c_{Lh}} \tilde{\kappa} \frac{\tilde{y}_{Hh}}{\tilde{y}_{Ll}} \right]} \quad (9)$$

where $\tilde{\kappa} = \frac{\kappa}{1-\kappa} \left(1 - \frac{1}{\sigma} \right)$ governs the increase in marginal utility from the loss in house value from being taxed at T_h rather than T_l ; $\tilde{g}_h = (g_H + \psi g_L) / (1 + \psi)$ is the average marginal social welfare weight of those asked to pay the h tax (note this is not the same as the average social marginal welfare weight of those who *do* pay the h -tax \bar{g}_h); and $\tilde{c}_h = (c_{Hh} + \psi c_{Lh}) / (1 + \psi)$ is the fraction of those asked to pay the h tax who comply.

The equations look much as before, but with some new terms. In the numerators we have the $\kappa g/c$ terms. These account for the fact that when taxes reduce property prices, all households benefit from access to cheaper housing.¹⁹ The $(1 - \kappa)$ term in the denominators is similarly there to account for the decrease in marginal utility of consumption coming from the lower house prices. The $(1 - \tilde{\kappa})$ terms in the denominators account for the dampening of the effects of tax differences on the disutility from inequity. Finally, the final term in the denominator in (9) accounts for the lower marginal utility of all overtagged households from their higher house prices.

Notably, these effects interact with one of the channels highlighted for mistagging: The $(1 - \tilde{\kappa})$ terms dampen (but do not eliminate) the forces that made the mistagging make taxes less progressive. In sum, incorporating household mobility and endogenous house prices with partial tax capitalization dampens a key channel through which mistagging makes taxes less progressive, but the other two channels are unaffected. House price changes have first-order welfare effects of their own, and so the quantitative impacts will depend on the compliance elasticities and the extent of house price capitalization, but the qualitative impacts of mistagging remain as in the baseline model in section 3.2.

4 Overall Compliance Responses: Boundary Discontinuity Evidence

We begin our empirical exploration of the forces highlighted by the conceptual framework in section 3 by studying differences in compliance behavior around the boundaries of Manaus' tax sectors (described in section 2). To do this, we develop a Boundary Discontinuity Design (BDD) (Black, 1999; Bayer *et al.*, 2007) that captures the overall effect of facing a tax schedule with a high price of land rather than a schedule with a lower price. Naturally, this combines both the fact that taxes are higher on the high-tax side of the boundary, and the fact that those on the

¹⁹As noted above, the model does not account for the welfare of the incumbent owners of the properties. If their welfare weights are the same as the houses' new occupants, these terms represent transfers between households with equal welfare weights and so they disappear from the expressions.

high-tax side face greater inequity. As the framework in section 3 shows, the welfare and policy implications of mistagging are very different depending on whether this reduced form effect is driven by responses to inequity or responses to the level of property’s tax liabilities. Sections 5 and 6 then take up the identification challenge of separately identifying behavioral responses to inequity and to the tax liability.

4.1 Boundary Discontinuity Design

Figure 2 sets the stage for our BDD approach, highlighting tax sector boundaries. The introduction of sector-specific prices per square meter in the tax formula 1 leads to differential taxation of identical properties across the boundary. This creates quasi-experimental variation allowing us to study the impacts of this differential taxation on tax compliance.

We focus on the year immediately preceding the 2011 tax reform, 2010, when the inequities in the tax system were at their most pronounced. And we restrict our analysis to properties facing a non-trivial degree of inequity ($|\sigma_i| > 0.05$). For each tax sector boundary, we split the street into 500-meter long segments, $s(i)$, which are used to ensure we are comparing properties close to each other. To study the impact of the discontinuous change in taxation on compliance, we estimate the following equation for compliance c_i by taxpayer i :

$$c_i = \gamma_{s(i)} + f(d_i) + \beta_0 HTS_i + h(d_i) \times HTS_i + \varepsilon_i \quad (10)$$

where $\gamma_{s(i)}$ are boundary-segment fixed effects, HTS_i is an indicator for being on the high-tax side of the boundary ($d_i > 0$); $f_0(d_i)$ and $f_1(d_i)$ control for distance to the boundary on the low- and high-tax sides of the boundary, respectively; and ε_i is the residual.

The presence of a discontinuity in the tax schedule at the boundaries may induce sorting around the boundaries. To the extent that this sorting is driven by the property tax, it is a component of the compliance elasticities we seek to estimate, since they contribute to the fiscal externality of behavioral responses to the property tax, as discussed in section 3.3.2. However, as shown in Bayer *et al.* (2007), when sorting is driven by other forces, this can meaningfully change the interpretation of the BDD. In our setting, the boundaries that we study are used exclusively for taxation. They do not determine access to public goods or which part of the government delivers them. Moreover, we remove any boundaries that overlap with neighborhood (“bairro”) boundaries from our analysis to ensure that any differences between neighborhoods are not driving our results. Notwithstanding this, both the tax liability and inequity change discontinuously at the boundaries, and so our results should be interpreted as the causal effects of the change in the combination of the two tax incentives.

4.2 Results

Figure 3 shows the results of estimating (10). The figure shows our point estimate of the change in compliance at the boundary, computed using local linear controls for distance, the MSE-

minimizing bandwidth, and triangular weighting kernels (Calonico *et al.*, 2014, 2018, 2019, 2020). To help visualize the design, the figure also shows an estimated conditional expectation over the full -300 meter – +300 meter window, estimated using decile-spaced bins of distance on either side of the boundary and the triangular kernel used to estimate the point estimate, censoring the kernel at its tenth percentile to still give positive weight to observations outside the MSE-optimal bandwidth. Bins containing the optimal bandwidth are shown in blue while bins outside the optimal bandwidth are shown in grey.

Three key findings emerge. First, there is a sharp drop in compliance precisely at the boundary, suggesting that compliance behavior is responsive to the tax system. Second, the drop in compliance is economically meaningful. Compliance is 6 percentage-points lower on the high-tax side of the boundary. Since average compliance is 0.75 just on the low-tax side of the boundary, this is an 8% drop in compliance. Figure 4 is constructed analogously to figure 3 but shows the corresponding first stages for the tax liability and inequity. It shows that the discontinuity in the tax liability increases tax liabilities by 13%. If all behavior is driven by the tax liability, combining this with the 8% drop in compliance implies an elasticity of compliance with respect to the tax liability of 0.615. This elasticity is large. For example Brockmeyer *et al.* (2023) employ a range of difference-in-differences and regression discontinuity approaches in Mexico City and estimate compliance elasticities between 0.24 and 0.46.

Third, as figure 4 makes clear, the tax sector boundaries generate quasi-experimental variation in two distinct first-stages: Tax liabilities are 13% higher on the high-tax side of the tax sector boundaries, but inequity is also 62% higher. The compliance effect we see in figure 3 potentially combines responses to both incentives. As we showed in the model in section 3, the behavioral responses to the two incentives have opposite implications for the progressivity of the optimal tax schedule, and so our next sections turn to disentangling the two mechanisms.

5 Boundary Discontinuity Design Based on Property Expansiveness

As discussed in section 4, at the tax sector boundaries, both the tax liability and inequity change discontinuously. This poses an identification challenge in recovering the elasticity of compliance with respect to inequity alone. The insight that allows us to disentangle the two things is that even once we condition on the tax liability that a house has, there is still variation in the inequity it faces. That variation comes from the property’s *expansiveness* — the ratio of the property’s land area to its built structure.

The source of the quasi-experimental variation in inequity that we seek to isolate is the discontinuous change in the price at which land is taxed. A property featuring a small house on a large lot — an expansive property — has a tax liability that is primarily due to the land it encompasses, and hence faces a high degree of inequity. Conversely, a property with the same tax liability, but a large house on a small lot has a tax liability that is primary due to the built structure on the property, and hence faces a smaller degree of inequity. To see this mathemat-

ically, note that the inequity faced by a property on the high-tax side of a boundary where the land price jumps from p_l to p_h is given by

$$\sigma = \frac{T_h}{T_l} = \frac{b + p_h a}{b + p_l a} = \frac{1 + p_h e}{1 + p_l e}$$

where the property's expansiveness $e = a/b$.²⁰ Properties with high expansiveness e will face a greater degree of inequity than properties with low expansiveness, even if they share the same (log) tax liability τ .²¹

To leverage this source of quasi-experimental variation in inequity, we need to augment our boundary discontinuity design in two ways. First, we need to incorporate conditioning on the properties' tax liability to be able to isolate the discontinuous change in inequity at the boundary. To do this, we adapt the methods in [Frölich & Huber \(2019\)](#) who show how to incorporate conditioning covariates into a standard regression discontinuity design. Second, the classic regression discontinuity design studies the causal effect of a binary treatment, but in our setting, inequity is a continuous function of expansiveness, complicating the interpretation of the regression discontinuity estimates. Here we follow the approach in [Dong *et al.* \(2023\)](#) who show how to achieve identification of Local Average Treatment Effects (LATEs) at quantiles of the distribution of expansiveness and how to aggregate them to weighted (local) average treatment effects.

In section 5.1 we provide a set of assumptions under which we can identify and estimate the causal effect of inequity on compliance. These assumptions are strong, amounting to assuming that after conditioning on the tax liability, we have a valid boundary discontinuity design at each quantile of the expansiveness distribution. In subsequent sections, we progressively relax the required assumptions, show how identification is achieved, and estimate the effect of inequity. In section 5.2 we do not require a valid BDD for every quantile of expansiveness. Instead, we require that the bias in the BDD at different quantiles doesn't covary with expansiveness, akin to a parallel trends assumption in a difference in differences design. In section 6, we relax the required assumptions further still by incorporating Manaus' 2011 property tax reform, allowing us to hold all time-varying unobservable determinants of compliance fixed, and allowing for differential time-trends in compliance on the low- and high-tax sides of the boundary.

5.1 Augmented Boundary Discontinuity Design

As a first exercise, in this section we provide a set of assumptions under which a Boundary Discontinuity Design (BDD) augmented to control flexibly for the tax liability achieves identification of the causal effect of inequity on compliance. These assumptions effectively require that the BDD is identified for every level of expansiveness, conditional on the tax liability. These

²⁰In all of the discussion in this section we implicitly condition, without any loss in generality, on properties located at a particular boundary so that we can hold p_h and p_l fixed.

²¹And, naturally, analogous derivations lead to the same conclusion for properties on the low-tax side of a boundary. For them $\sigma = (1 + p_l e) / (1 + p_h e)$.

are strong assumptions, but they provide transparent conditions for identification and allow us to be precise about which Local Average Treatment Effect (LATE) we can identify. Subsequent assumptions show that identification is preserved under more palatable assumptions, and our results are similar under all of these designs.

5.1.1 Identification

Our approach builds on the advances in Frölich & Huber (2019) and Dong *et al.* (2023) who adapt the regression discontinuity design to settings with controls, and continuous treatments, respectively. We denote our compliance outcome $C \in [0, 1]$ as the fraction of a taxpayer's liability that they pay in response to the treatment we are interested in: inequity $\sigma \in \mathbb{R}^+$. The running variable in our regression discontinuity design is distance to the boundary of a tax sector $D \in \mathcal{D} \subset \mathbb{R}$. Compliance is determined by potential outcomes given by $C = G(\sigma, \tau, D, \nu)$ where τ is the (log) tax liability, and ν are other, potentially unobserved, determinants of compliance.²²

It is useful to think of crossing the boundary as an instrument $Z = \mathbf{1}[D > 0]$ giving properties potential treatments when Z is exogenously set to z of $\sigma_z \equiv q_z(E_z) = (-1)^{1-z} \log \left(\frac{1+p_H E_z}{1+p_L E_z} \right)$, where E_z is a property's potential expansiveness when the instrument is $Z = z$. Since we will invoke a rank invariance assumption, it is convenient to study quantiles of the treatment distribution.²³ Our first assumption allows us to map 1-to-1 between quantiles of expansiveness and inequity:

Assumption 1 (Quantile representation). *The conditional distribution of E_z given distance $D = d$ and tax liability $\tau = t$ is continuous with a strictly increasing CDF $F_{E_z|\tau,D}(e, t, d)$.*

This assumption allows us to define the inequity faced by the property at the u th conditional quantile of expansiveness as²⁴

$$q_z(d, u, t) = (-1)^{1-z} \log \left(\frac{1 + p_H F_{E_z|t,d}^{-1}(u)}{1 + p_L F_{E_z|t,d}^{-1}(u)} \right)$$

More substantively, we make a set of four smoothness assumptions:

Assumption 2 (Smoothness). *$q_z(d, u, t)$, $z = 0, 1$, is continuous in $d \in \mathcal{D}$ for any $u \in [0, 1]$ and $t \in \mathcal{T} \subset \mathbb{R}^+$. Either $G(\sigma, \tau, D, \nu)$ is continuous in all its arguments, or it is a.e. continuous and bounded. $f_{\nu|U_z, \tau, D}(v, u, t, d)$ is continuous in $d \in \mathcal{D}$ for any $u \in [0, 1]$, $t \in \mathcal{T}$, and $v \in \mathcal{V}$, where \mathcal{V} is compact. $f_{D|\tau}(d, t)$ is continuous and strictly positive around $d = 0$.*

This assumption requires that inequity, taxes, distance, and unobservables all generate smooth impacts on compliance. It also assumes that for a given rank in the expansiveness distribution,

²²We allow these determinants $\nu \in \mathcal{V} \subset \mathbb{R}^{\dim \nu}$ to have arbitrary dimension.

²³This is also convenient since it offers a natural way to pool across tax sector boundaries.

²⁴Note that while the reduced form only depends on expansiveness, it now depends on τ also because the distribution of expansiveness we are using to normalize with is conditional on distance and τ .

the distribution of unobservables is smooth near the boundaries. These are strong assumptions, and in sections 5.2 and 6 we show how we can relax both of them while still achieving identification. The assumption that distance has a smooth effect on potential treatments is easily satisfied as long as assumption 2 holds. The assumption that distance is continuous and has positive density at the boundary is standard in BDD designs.

Our final assumption requires that properties stay at approximately the same rank in the potential expansiveness distribution on either side of the tax sector boundaries.²⁵ Formally,

Assumption 3 (Local expansiveness rank invariance or similarity). *Conditional on $D = 0$ and $\tau = t \in \mathcal{T}$, 1. $U_0 = U_1$; or, more generally, 2. $U_0|\nu \sim U_1|\nu$*

Assumption 3 implies that crossing the boundary (our instrument) does not affect properties' rank in the expansiveness distribution.²⁶ Notably, this assumption does not require properties to have the same potential expansiveness on either side of the boundary. The relative, after-tax price of land a is higher on the high-tax side of the boundary and so we might expect property owners to substitute towards built structure. Assumption 3 permits this, but requires that the unobservables are not correlated with the elasticity of substitution between land a and built structure b in such a way that it would reverse ranks in the potential expansiveness distribution.

Together with the smoothness of the distribution of ν in assumption 2, assumption 3 means that at the boundary, we can use U as a control variable (Imbens & Newey, 2009) — conditional on U , the change in inequity at the tax sector boundary is exogenous (unrelated to ν) (Dong et al., 2023).²⁷

With these assumptions we can show that a boundary regression discontinuity design that conditions on tax liability identifies the treatment effect of inequity:

Proposition 3 (Identification of LATEs conditional on U and τ). *Define the $Q\tau$ -LATE:*

$$\begin{aligned}\eta(u, t) &\equiv \int \frac{G(\sigma_1(u, t), t, 0, v) - G(\sigma_0(u, t), t, 0, v)}{\sigma_1(u, t) - \sigma_0(u, t)} F_{\nu|U, \tau, D}(dv, u, t, 0) \\ &= \mathbb{E} \left[\frac{C_{\sigma_1(u, t)} - C_{\sigma_0(u, t)}}{\sigma_1(u, t) - \sigma_0(u, t)} \middle| U = u, \tau = t, D = 0 \right]\end{aligned}$$

This is the average causal effect of inequity for taxpayers with expansiveness rank $U = u$ and tax liability $\tau = t$.

Under Assumptions 1, 2 & 3, for any $u \in \mathcal{U}$, the set of u for which there is a first stage (non-zero expansiveness), and for any $t \in \mathcal{T}$, $Q\tau$ -LATE $\eta(u, t)$ is identified and is given by

$$\eta(u, t) = \frac{m^+(u, t) - m^-(u, t)}{q^+(u, t) - q^-(u, t)} \quad (11)$$

²⁵Note that this does not require properties to have the same expansiveness, only that their rank is similar.

²⁶The more general formulation of the assumption permits random slippages from a property's rank in the expansiveness distribution just on either side of the boundary (Chenozhukov & Hansen, 2005; Dong et al., 2023).

²⁷See the proof of proposition 3 in appendix M for details.

where the limits in the denominator are defined by $q^+(u, t) \equiv \lim_{d \rightarrow 0^+} q(d, u, t)$ and $q^-(u, t) \equiv \lim_{d \rightarrow 0^-} q(d, u, t)$. Also let $m(s, t, d) \equiv \mathbb{E}[C | \sigma = s, \tau = t, D = d]$, and define $m^+(u, t) \equiv \lim_{d \rightarrow 0^+} m(q^+(u, t), t, d)$ and $m^-(u, t) \equiv \lim_{d \rightarrow 0^-} m(q^-(u, t), t, d)$. All of these can be consistently estimated from the data.

Further, the W-LATE $\bar{\eta}(w) = \int_{\mathcal{U}} \int_{\mathcal{T}} \eta(u, t) w(t, u) dt du$ is identified for any known or estimable weighting function $w(t, u)$ such that $w(t, u) \geq 0$ and $\int_{\mathcal{U}} \int_{\mathcal{T}} w(t, u) dt du = 1$.

Proof. See appendix M □

The proposition shows that under assumptions 1–3, we have a valid BDD for every expansiveness rank and every tax liability. A property’s tax liability and expansiveness rank pin down its dose of the treatment, the denominator in the LATE. The smoothness assumptions allow us to identify the reduced form effect in the numerator. Assumptions 1–3 are strong, but proposition 3 shows transparently how identification is achieved and which LATEs can be estimated, and so we think of it as a good starting point in analyzing the effects of inequity on compliance.

Proposition 3 also shows that we can estimate weighted averages of the causal effects of inequity on compliance at different expansiveness quantiles and tax liabilities. To implement this in practise, we use regression weights and estimate the following regression:

$$c_i = \gamma_{s(i)} + g(\tau_i, e_i) + f(d_i) + \beta_0 HTS_i + h(d_i) \times HTS_i + \varepsilon_i \quad (12)$$

where $\gamma_{s(i)}$ are fixed effects for 500-meter segments along the boundaries to ensure we are comparing properties who are nearby each other; $g(\tau_i, e_i)$ are flexible controls for property i ’s (log) tax liability τ_i and expansiveness e_i (our baseline estimates use τ splines and expansiveness deciles); $f(d_i)$ and $h(d_i)$ control flexibly for distance to the boundary on the low- and high-tax sides of the boundary respectively; and HTS_i is an indicator for properties on the high-tax side of the boundary ($d_i > 0$).

5.1.2 Results

Figure 5 shows the results of estimating equation (12) with (log) inequity σ as the outcome. The figure is constructed analogously to the baseline BDD discussed in section 4. It shows that we have a strong first-stage impact on inequity of 0.519 (down from 0.618 in figure 4) even after controlling flexibly for the tax liability and expansiveness (using cubic splines of the tax liability and fixed effects for deciles of expansiveness). Similarly, figure 6 shows the results of estimating equation (12) with compliance as the outcome. It shows that there is a strong impact of inequity on compliance. Compliance is 7.5 percentage points lower on the high-tax side of the boundaries even after controlling flexibly for the tax liability and expansiveness.

Table 2 shows the results of estimating equation (12) using a variety of approaches to controlling flexibly for the tax liability and expansiveness. In column (1) we control for cubic splines of the tax liability and fixed effects for deciles of expansiveness. In column (2) we replace the expansiveness deciles with cubic splines of expansiveness while column (3) replaces the splines

of the tax liability with deciles. Columns (4)–(6) additionally interact the tax liability controls with the expansiveness controls. The table shows remarkably consistent results: the implied elasticity of compliance with respect to inequity ranges from 0.25 to 0.27.

5.1.3 Saliency

In this section, we have shown that compliance decreases discontinuously at the border sector boundaries, even for properties with the same tax liability, τ_{it} . To interpret this decrease as a causal effect of inequity on compliance, we must assume that property owners are aware of their counterfactual tax bill, $\hat{\tau}_{it}$. Here, we provide evidence that the BDD results are stronger where the inequity σ_i is more salient.

While the formula for tax bill is publicly available to all citizens, citizens can also learn about $\hat{\tau}_{it}$ by comparing their tax bill to the ones from similar properties on the other side of the boundary.²⁸ Thus, we define our measure of saliency for each property i as the density of $\hat{\tau}_i$ in the tax liability distribution of the other side of the boundary. Appendix F describes in more detail how we measure saliency. We then split our sample into five disjoint groups using the quintiles of our saliency measure and estimate 12 in each group. The results are displayed in figure 7. The figure shows that our results are strongly decreasing in the saliency of the property tax. In the bottom quintile the estimated effect is zero, but then the effect is negative in the higher quintiles of saliency.

5.2 Difference in Boundary Discontinuities Design

One disadvantage of the approach in section 5.2 is that we have to assume that compliance potential outcomes evolve smoothly around the boundaries, even conditional on the tax liability.²⁹ However, this assumption may well be violated. For example, conditional on a tax liability, properties on the side of the boundary with the higher land price are smaller (either smaller lots, smaller buildings, or both).³⁰ Moreover, the lower taxes on land on the low-tax side of the boundary may attract different households and/or affect investment incentives. All of these may be correlated with unobserved determinants of compliance.

In this section we relax this assumption, allowing for discontinuities in compliance at the boundaries. Our relaxed assumptions, akin to a parallel trends assumption, is that the discontinuities in compliance at the boundaries are the same for different levels of expansiveness Callaway *et al.* (2024). In section 6 we relax this assumption as well by introducing the reform to the property tax in 2011.

²⁸The amount of the tax bill is commonly displayed in real estate websites such as Viva Real.

²⁹Specifically, we assume that potential outcomes $G(\sigma, \tau, D, \nu)$ are continuous in all arguments (including distance D), and that the distribution of the unobserved determinants of compliance ν conditional on expansiveness rank U , tax liability τ and distance D is continuous at the boundary $D = 0$.

³⁰To see this, consider a boundary where the price of land jumps from p_L to $p_H > p_L$. To share the same tax liability τ it must be the case that $b_L + p_L a_L = b_H + p_H a_H$ so properties on the high-tax side must have lower $b_H < b_L$ or $a_H < a_L$, or both.

5.2.1 Identification

In our modified approach, we separate the potential outcomes into an untreated component G_0 capturing potential compliance in the absence of inequity, and a treatment effect G_1 capturing the impact of compliance on inequity. We also partition the unobserved determinants of compliance ν into those that influence the treatment effect ν_1 and those that only affect the untreated potential outcomes ν_0 .

$$C = G(\sigma, \tau, D, \nu) = G_0(\tau, D, \nu_0) + G_1(\sigma, \tau, D, \nu_1) \quad (13)$$

The difference in boundary discontinuity design allows for discontinuities in the untreated potential outcomes G_0 at the boundaries, and for the distribution of ν_0 to be discontinuous at the boundary, substantially relaxing the smoothness assumption (Assumption 2) required in section ???. Instead, we assume that

Assumption 4 (Smoothness). $q_z(d, u, t)$, $z = 0, 1$, is continuous in $d \in \mathcal{D}$ for any $u \in [0, 1]$ and $t \in \mathcal{T} \subset \mathbb{R}^+$. Either $G_1(\sigma, \tau, D, \nu_1)$ is continuous in all its arguments or it is a.e. continuous and bounded. $G_0(\tau, D, \nu_0)$ is right and left continuous in D at $D = 0$ for any $t \in \mathcal{T}$ and $\nu_0 \in \mathcal{V}_0$. $f_{\nu_1|U_z, \tau, D}(v_1, u, t, d)$ is continuous in D for any $u \in [0, 1]$, $t \in \mathcal{T}$ and $v_1 \in \mathcal{V}_1$ where \mathcal{V}_1 is compact. $f_{\nu_0|U_z, \tau, D}(v_0, u, t, d) = f_{\nu_0|\tau, D}(v_1, t, d)$ for any $u \in [0, 1]$. $f_{\nu_0|\tau, D}(v_1, t, d)$ is left and right continuous at $D = 0$ for any $t \in \mathcal{T}$ and $v_0 \in \mathcal{V}_0$ where \mathcal{V}_0 is compact. $f_{D|\tau}(d, t)$ is continuous and strictly positive around $d = 0$.

This is akin to a parallel trends assumption, but modified to allow for a continuous treatment (Callaway *et al.*, 2024). We allow for selection at the boundary in the untreated potential outcomes such that the right- and left limits of $\mathbb{E}[G_0(t, d, \nu_0) | \tau = t, D = d]$ at $D = 0$ need not be the same. However, we require that the gap be constant across potential treatment levels σ_z .

We can also weaken our assumption about the expansiveness ranks to condition only on the subcomponent of ν that affects the treatment effects:

Assumption 5 (Local expansiveness rank invariance or similarity). Conditional on $D = 0, 1$. $U_0 = U_1$; or more generally, 2. $U_0 | \nu_1 \sim U_1 | \nu_1$

With these modified assumptions, we can show that the difference in the LATEs between any pair of levels of expansiveness are identified:

Proposition 4 (Identification of Differences in LATEs). Define the $Q\tau DD$ -LATE:

$$\begin{aligned} \eta(\underline{u}, \bar{u}, t) &\equiv \frac{\int G(\sigma_1(\bar{u}, t), t, 0, v) - G(\sigma_0(\bar{u}, t), t, 0, v) F_{\nu|U, \tau, D}(dv, \bar{u}, t, 0) \\ &\quad - \int G(\sigma_1(\underline{u}, t), t, 0, v) - G(\sigma_0(\underline{u}, t), t, 0, v) F_{\nu|U, \tau, D}(dv, \underline{u}, t, 0)}{[\sigma_1(\bar{u}, t) - \sigma_0(\bar{u}, t)] - [\sigma_1(\underline{u}, t) - \sigma_0(\underline{u}, t)]} \\ &= \frac{\mathbb{E}[C_{\sigma_1(\bar{u}, t)} - C_{\sigma_0(\bar{u}, t)} | U = \bar{u}, \tau = t, D = 0] - \mathbb{E}[C_{\sigma_1(\underline{u}, t)} - C_{\sigma_0(\underline{u}, t)} | U = \underline{u}, \tau = t, D = 0]}{[\sigma_1(\bar{u}, t) - \sigma_0(\bar{u}, t)] - [\sigma_1(\underline{u}, t) - \sigma_0(\underline{u}, t)]} \end{aligned} \quad (14)$$

This is the difference in the average causal effect of inequity for taxpayers with tax liability $\tau = t$ between taxpayers with expansiveness rank $U = \bar{u}$ and taxpayers with expansiveness rank $U = \underline{u}$. Under Assumptions 1, 4 & 5, for any $\bar{u}, \underline{u} \in \mathcal{U}$, and for any $t \in \mathcal{T}$, $Q\tau DD$ -LATE $\eta(\underline{u}, \bar{u}, t)$ is identified and is given by

$$\eta(\underline{u}, \bar{u}, t) = \frac{[m^+(\bar{u}, t) - m^-(\bar{u}, t)] - [m^+(\underline{u}, t) - m^-(\underline{u}, t)]}{[q^+(\bar{u}, t) - q^-(\bar{u}, t)] - [q^+(\underline{u}, t) - q^-(\underline{u}, t)]} \quad (15)$$

where the limits are as defined in proposition 3, all of which can be consistently estimated from the data.

Further, the weighted WDD-LATE $\bar{\eta}_{QDD}(w) = \int_{\mathcal{U}} \int_{\mathcal{U}} \int_{\mathcal{T}} \eta(\underline{u}, \bar{u}, t) w(\underline{u}, \bar{u}, t) dt d\bar{u} d\underline{u}$ is identified for any known or estimable weighting function $w(\underline{u}, \bar{u}, t)$ such that $w(\underline{u}, \bar{u}, t) \geq 0$ and $\int_{\mathcal{U}} \int_{\mathcal{U}} \int_{\mathcal{T}} w(\underline{u}, \bar{u}, t) dt d\bar{u} d\underline{u} = 1$.

Proof. See appendix N □

Proposition 4 shows that we are able to identify the difference in the treatment effects of crossing the boundary experienced by properties at any pair of levels of expansiveness ranks \underline{u} and \bar{u} (and hence between any pair of levels of inequity since by assumption 1 there is a one-to-one mapping between expansiveness ranks u and potential treatments $q_z(d, u, t)$). Since we permit discontinuities in compliance at the boundary, neither the treatment effect experienced by properties with expansiveness rank \underline{u} nor the treatment effect at \bar{u} is identified. However, the difference between the two, and hence the shape of the relationship between inequity and treatment effects, is identified.

The second part of the proposition shows that any weighted average of the pairwise differences in the treatment effects is also identified. In our empirical analysis, we estimate such a weighted LATE through linear regression, whose weights are estimable and hence identified by proposition 4. Specifically, we estimate

$$c_i = \gamma_{s(i)} + g_0(\tau_i, e_i) + f(d_i) + HTS_i \times [\beta_0 + \eta \log(\sigma) + h(d_i) + g_1(\tau_i, e_i)] + \varepsilon_i \quad (16)$$

where terms are as defined above for equation (12) and now we also permit the controls for the tax liability τ and expansiveness e_i to be different on each side of the boundary.

One of the main advantages of this identification strategy is that it allows for selection at the boundary in the untreated potential outcomes. However, we still require that the gap in potential outcomes be constant across potential treatment levels σ_z . To test this assumption, we constructed a placebo test using sector boundaries where there is no high tax side, and therefore for all properties $\sigma_i = 0$. We then construct a dataset in which we stack the properties of each sector boundary with the properties of the closest sector boundary with a different sector rate. Using these placebo boundaries, we construct a placebo measure of the inequity and estimate 16. Details of the dataset construction are in Appendix G, and the results are shown in Table G.1.

5.2.2 Results

We begin by demonstrating how the impact of inequity on compliance differs across subgroups of the sample determined by the extent of inequity they face. In figure 8 we show the first-stage discontinuity in inequity estimated using (12) in two groups. The top quartile of $|\sigma|$ (high inequity) and all other properties (low inequity). Figure 8 demonstrates that the first stage is significantly stronger for the high inequity group.

Figure 9 then turns to estimating compliance effects in these two groups. Consistent with our strategy, we see no significant change in compliance at the boundary in the low inequity group in panel A. However, we see a very strong effect in the top quartile of inequity in panel B. To further investigate the relationship between the compliance jump and σ , we divide the data into seven finer groups: the first three quartiles of $|\sigma|$ and four equally sized subgroups of the top quartile. The decision to split the top quartile stems from the fact that the distribution of $|\sigma|$ is heavily concentrated near zero, with significant variation appearing only in the last quartile. Figure 10 presents the RD estimates from 12 for each group, revealing a clear, negative relationship between the compliance jump and the magnitude of inequity.

To formally quantify the relationship in a single parameter, we estimate η from 16, varying the controls for τ and expansiveness. The results, presented in Table 3, consistently confirm the negative relationship between compliance and inequity. In column (1), we control for cubic splines of the tax liability and fixed effects for deciles of the expansiveness distribution. In column (2) we control separately for the tax liability and expansiveness on either side of the boundary. Column (3) replaces the expansiveness deciles with cubic splines in expansiveness while column (4) replaces the tax liability deciles with cubic splines. Columns (5)–(7) control for these separately on either side of the boundary. Importantly, the estimated elasticities remain robust across specifications and closely align with the findings discussed in section ???. In this case, we estimate elasticities of compliance with respect to inequity between 0.25 and 0.27.

6 Dynamic Boundary Discontinuity Design Based on 2011 Reform

The analysis in section 5 exploited purely cross-sectional variation in data from 2010: We augmented the boundary discontinuity design to control for the tax liability and to leverage variation in inequity induced by differences in properties' expansiveness. While our difference in BDD design in section 5.2 required significantly weaker assumptions, concerns may remain about unobserved determinants of compliance that vary discontinuously around the boundaries and that are correlated with expansiveness.³¹

However, these unobservables are likely to be fixed over time, at least in the short run, and so in this section we show how to augment the BDD to incorporate Manaus' 2011 property tax reform and in the process hold fixed all time-invariant determinants of compliance. Our approach

³¹For example, the discontinuity in the size of the built structure and the land under the property may be correlated with expansiveness.

in section 6.1 studies the causal effect of changes in inequity on changes in compliance, while controlling for changes in taxes. This approach requires a parallel trends assumption at the tax sector boundaries, analogously to the assumption in ?? that unobserved determinants of compliance vary smoothly at the boundaries. The approach we develop in section 6.2 relaxes this assumption and instead develops a triple-differences design to estimate the impact of changes in inequity. Finally, in section 6.3, we make a “strong” parallel trends assumption (Callaway *et al.*, 2024) which permits us to separately identify the impacts of undertagging ($\sigma < 1$) and overtagging ($\sigma > 1$).

6.1 Dynamic Boundary Discontinuity Design

Our approach here mirrors the augmented boundary discontinuity design in ?? with one key difference: The outcomes we are interested in now are *changes* in compliance over time, which we relate to changes in inequity over time.

Formally, we assume that potential compliance outcomes in year y are given by $C_y = G(\sigma_y, \tau_y, D, \mu, \nu_y, y)$. As before, compliance depends on inequity σ , the tax liability τ , and distance to the boundary D . We augment the potential outcomes though to depend on a set of time-invariant unobservables μ , time-varying unobservables ν_y , and time y . We assume that the difference between potential compliance in 2010 (before the reform) and 2016 (after the reform is fully phased in) can be written as $\Delta C = \Delta G(\Delta\sigma, \Delta\tau, D, \Delta\nu)$ where, critically, by taking differences over time, we eliminate the dependence of the potential outcomes on the time-invariant unobservables μ .³²

From here, we proceed as in section ??, but replacing the level of compliance C with the change in compliance ΔC everywhere, and the levels of tax τ and inequity σ with their time-changes $\Delta\tau$ and $\Delta\sigma$. Applying proposition 3, we are able to identify the causal effect of changes in inequity $\Delta\sigma$ on changes in compliance ΔC at all levels of the change in tax liability $\Delta\tau$ and expansiveness rank U , and we can also identify weighted averages of these causal effects. We do so by estimating the regression-weighted causal effect through the following equation:

$$\Delta c_i = \gamma_{s(i)} + g(\Delta\tau_i, e_i) + f_0(d_i) + HTS_i \times [\beta_0 + f_1(d_i)] + \varepsilon_i \quad (17)$$

Figure 11 shows the first stage change in inequity in two groups. First, the group of properties for whom the reform meaningfully reduced inequity (either by reducing overtagging or by reducing undertagging), and second, the remaining properties who did not experience a reduction in inequity.³³ For the analysis in this section, we re-incorporate tax sector boundaries that overlap with neighborhood boundaries since our design is able to hold fixed any changes at the boundaries that don’t change over time, such as the difference between neighborhoods. We see

³²Moreover, the change in compliance depends on the *change* in the tax liability $\Delta\tau$ not on the levels of taxes in either year.

³³We first defined a divergence variable as $\Delta\sigma$ for properties on the high tax side and $-1 \times \Delta\sigma$ for properties on the low tax side. We then defined the group that the reform meaningfully reduced inequity as the first quartile of “divergence.”

that for the former group, overtagging decreased by 34% at the high-tax side of the boundary, while undertagging decreased by 14% at the low-tax side of the boundary. By contrast, the properties who did not experience a meaningful reduction in inequity experienced approximately equal, and small (under 10%) changes in inequity.

Figure 12 shows the effects of changes in inequity on changes in compliance in these two groups. In panel A, we see that in the group that did not experience a reduction in inequity, the discontinuity in the change in compliance is a precisely estimated zero, providing confidence in the validity of the design. Meanwhile, in panel B, we see that in the group experiencing a meaningful reduction in inequity, the change in compliance is 5.7 percentage-points higher on the high-tax side than the low-tax side, and precisely estimated, suggesting that households respond strongly to the removal of inequity.

Figure 13 extends the analysis to study the impacts of changes in inequity on changes in compliance in four groups defined by quartiles of the change in inequity they experience. We see that the impacts are driven by the group in which inequity changes are meaningful: the three higher quartiles experience inequity changes smaller than 10–15% which does not appear to be sufficient for them to respond meaningfully.

6.2 Dynamic Difference in Boundary Discontinuity Design

Our most robust design allows compliance on the low-tax and high-tax sides of the boundaries to be on different trends, which would invalidate our dynamic boundary discontinuity design in section 6.1 as the discontinuity in changes in compliance at the boundary conflates differences in trends and the causal effect of changes in inequity we seek to estimate. Analogously to the approach in section 5.2, we require that whatever difference in trends there is between the two sides of the boundary, it is orthogonal to properties' expansiveness, akin to a triple-differences design.

Applying proposition 4, replacing compliance, taxes, and inequity with their time-changes, we are able to identify the differences in the causal effects of changes in inequity on changes in compliance between any two pairs of expansiveness ranks. Moreover, we can identify any weighted average of these differences in causal effects. We do so by estimating the following regression-weighted average causal effect η :

$$\Delta c_i = \gamma_{s(u)} + g_0(\Delta \tau_i, e_i) + f_0(d_i) + HTS_i \times [\delta_0 + \eta \Delta \log(\sigma_i) + g_1(\Delta \tau_i, e_i) + f_1(d_i)] + \varepsilon_i \quad (18)$$

where all terms are as defined previously.

Table 4 shows the results of estimating equation (18) with different specifications of the controls for the change in the tax liability and expansiveness. Column (1) uses splines of the tax liability and fixed effects for deciles of expansiveness. Column (2) adds interactions of these with the high-tax side indicator and with each other. Column (3) replaces the expansiveness decile fixed effects with expansiveness splines, while column (4) instead replaces the tax liabil-

ity splines with fixed effects for deciles of the tax liability.

We see that the estimated coefficient on the interaction between the high-tax side indicator and the size of the change in inequity is strongly negative and highly statistically significant at around -0.07. Converting this to an elasticity of compliance with respect to inequity yields an elasticity of 0.11 in column (1). Moreover, the results are highly robust to alternative specifications of the controls, with the elasticity only varying between 0.106 and 0.121. This design requires the weakest assumptions and so we interpret it as our most robust, and hence preferred, estimate of the elasticity of compliance with respect to inequity.

6.3 Difference in Differences Design

Our final design is aimed at distinguishing between the effects of overtagging $\sigma > 1$ and the effects of undertagging $\sigma < 1$. It also permits us to evaluate the dynamics of the causal effects and evaluate the plausibility of our parallel trends assumptions by studying trends in compliance leading up to the 2011 reform.

Formally, we make a “strong” parallel trends assumption (Callaway *et al.*, 2024) to allow us to estimate the impact of changes in inequity separately for those on the high-tax side of the boundary (who were predominantly overtagged before the reform and for whom this overtagging was reduced) and those on the low tax side of the boundary (who were undertagged before the reform and for whom this undertagging was reduced through the reform):

Assumption 6 (Strong Parallel Trends).

$$\begin{aligned} & \mathbb{E} [G(s_y, t_y, d, \mu, \nu_y, y) - G(s_0, t_0, d, \mu, \nu_0, 0) | \sigma_y = s_y, \sigma_0 = s_0, \tau_y = t_y, \tau_0 = t_0, D = d] \\ &= \mathbb{E} [G(s_y, t_y, d, \mu, \nu_y, y) - G(s_0, t_0, d, \mu, \nu_0, 0) | \tau_y = t_y, \tau_0 = t_0, D = d] \quad \forall y \end{aligned} \quad (19)$$

where $G(s_y, \tau_y, D, \mu, \nu_y, y)$ are the compliance potential outcomes, and we choose the base year $y = 0$ to be 2010.

Assumption 6 requires parallel trends between any pair of inequity levels σ_y and σ_0 such that we can estimate effects of changes in inequity using dynamic difference in differences designs. Specifically, we are interested in estimating the effects of changes in inequity for the undertagged households on the low-tax side of tax sector boundaries and the undertagged households on the high-tax side. We do so by estimating the following equation:

$$\begin{aligned} c_{iy} = & \alpha_i + \gamma_{s(i)y} + \sum_{j \neq 2010} D_{jy} \times \left[f_{0j}(d_i) + \beta_{0j} \Delta \tau_i + \eta_{0j} \Delta \sigma_i \right. \\ & \left. + HTS_i \times (\delta_j + f_{1j}(d_i) + \beta_{1j} \Delta \tau_i + \eta_{1j} \Delta \sigma_i) \right] + \varepsilon_{iy} \end{aligned} \quad (20)$$

where $\gamma_{s(i)y}$ are segment-year fixed effects, $D_{jy} \equiv \mathbf{1}[y = j]$ are year dummies, and we include year-specific distance controls $f_{0j}(d_i)$ and $f_{1j}(d_i)$; and year-specific controls for property i 's tax

liability change due to the reform.

Figure 14 shows the impacts of the reform. Panel A shows the impacts on the high-tax side. It plots the η_{1j} coefficients from equation 20 along with their 95% confidence intervals. We see that the estimated coefficients in years before the reform are all indistinguishable from zero, so we have no evidence that properties receiving different-sized changes in inequity due to the reform are on differential trends before the reform. We also see that the coefficients become negative after the reform, indicating that compliance by properties receiving larger cuts to inequity improves relative to properties receiving smaller cuts to inequity. This suggests that the inequity generated by overtagging has strong effects on compliance. Somewhat surprisingly, the effects emerge immediately following the reform’s enactment in 2011 despite the fact that the reform was phased in over 5 years. This is likely due to the high salience of the reform as it was being implemented.

Panel B shows the impacts on the low-tax side. It plots the η_{0j} coefficients along with their 95% confidence intervals. If the effects of undertagging were symmetric to the effects of overtagging, we would expect to see a similar pattern in panel B as we see in panel A. However, we see that the post-reform coefficients in panel B are consistently indistinguishable from zero, suggesting no impact of undertagging and that all of the responses to inequity come from taxpayers resenting being overtagged. This is consistent with the findings in Dube *et al.* (2019a) studying labor market behavior in the US. They find that workers’ quit behavior is responsive to wage rises for their higher-paid peers (the analog of overtagging in our setting) but not to wage increases for their lower-paid peers.

In summary, across a range of augmented BDD designs, we find consistent evidence of the importance of inequity for tax compliance. The estimated elasticity of compliance with respect to inequity ranges from 0.11 to 0.29. Moreover, these responses are driven exclusively by resentment of overtagging. We cannot reject the hypothesis that undertagging has no effect on compliance.

7 Conclusion

Property taxes are an important source of government revenues, particularly for local governments, but they are seldom based on direct evaluations of market prices. Rather, they are overwhelmingly based on presumptive formulas that approximate properties’ values using a limited set of observable characteristics. Indeed, observable tags are used throughout tax codes, especially in low- and middle- income taxes where presumptive taxes are ubiquitous and eligibility for benefits is commonly based on proxy-means tests. A large literature has emphasized the consequences of the limited statistical precision of imperfect tags for eligibility (Besley & Kanbur, 1988) and the moral hazard presumptive taxes induce (Oates & Schwab, 2015; Gaubert *et al.*, 2021). We introduce a novel force into this discussion — direct behavioral responses to the inevitable inequity that imperfect tagging generates.

Our conceptual framework shows how imperfect tagging leads to both lower tax revenues overall, and less progressive taxation. In our empirical analysis of Manaus’ presumptive property tax we provide evidence that these behavioral responses are strong. Using a range of research designs extending the Boundary Discontinuity Design (BDD), we estimate that the elasticity of compliance is in the range of $(0.11 - -0.29)$. These estimates suggest that responses to inequity account for half of the overall reduction in compliance observed at the boundaries of tax sectors.³⁴

Figure 15 shows a calibration of the model presented in section 3.2.³⁵ In the figure, we hold the overall response to taxation, governed by $\varepsilon + \eta$ fixed and vary the fraction of the total response that is driven by the elasticity with respect to inequity η vs the elasticity with respect to the tax liability ε . We show the two optimal tax rates and the ratio of the two: the progressivity of the tax schedule. Since the two elasticities have opposite implications for progressivity, the larger the fraction of the response that comes from inequity, the less progressive the optimal tax schedule. Our estimates in table 4 suggest that η is 0.12, implying $\varepsilon = 0.33$ placing us at the dashed vertical line, and implying that optimal progressivity is around 50% of what it would be if all responses were driven by the tax liability and none by inequity.

Given the ubiquity of presumptive taxes throughout the world, these findings have profound implications for the design of tax systems. Imperfect tagging places severe constraints on governments’ ability to raise revenues, and on their ability to redistribute through the tax code. And as a result, our findings suggest that there are large returns to investments in fiscal capacity that can allow governments to use more precise tags, reducing the extent of mistagging, the resulting inequity, and the consequent behavioral responses that raise the efficiency cost of taxation.

Our measure of inequity is a “selfish” notion of inequity. That is, our measure captures the extent to which an individual taxpayer may feel that they are over/under-taxed relative to a benchmark of accurate tagging. This has the great advantage of being easily operationalized, but does not capture the extent to which taxpayers may care about how much *others* have to pay in taxes. In particular, it cannot capture traditional notions of horizontal equity, such as equal treatment of groups of normatively equivalent taxpayers (Kaplow, 1989; Auerbach & Hassett, 2002), or vertical equity (sharing the burden of taxation across groups of taxpayers equitably).

Indeed, the 2011 reform we study was intended to correct both the inequity that we study (mistagging taxpayers) and the vertical inequity of overtaxing neighborhoods that had become less desirable and undertaxing neighborhoods that had become highly desirable in the decades leading up to the reform. In fact, a traditional tax-reform approach relating the large changes in tax liabilities (the average increase was a doubling of the tax liability) to changes in compli-

³⁴To see this, note that the drop in compliance dc/c in figure 3 is $-0.06/0.75 = -0.08$. In figure 4 we see that $dT/T = 0.13$ and $d\sigma/\sigma = 0.62$. However, as we show in section 6.3, inequity responses are driven exclusively by overtaging and so the effective $d\sigma/\sigma$ is only half of this: 0.31. Combining these through the relationship $-dc/c = \varepsilon dT/T + \eta d\sigma/\sigma$, the responses to inequity account for half of the overall response.

³⁵We set the parameters as follows: $\psi = 0.05$, $\rho = 2$, $y_H/y_L = 1.8$ $b(r) = 1.3$ $g_H/g_L = 1.07$.

ance decisions (following the approach in [Gruber & Saez \(2002\)](#)) suggests a remarkably small elasticity of tax compliance of 0.08, entirely consistent with the compliance-enhancing response to the reduction in inequity pushing against the negative effects of increasing tax liabilities. A more comprehensive evaluation of these effects is beyond the scope of this paper, but suggests a promising direction for future research.

References

- AJZENMAN, NICOLAS, CRUCES, GUILLERMO, PEREZ-TRUGLIA, RICARDO, TORTAROLO, DARIO, & VAZQUEZ-BARE, GONZALO. 2024. From Flat to Fair? The Effects of a Progressive Tax Reform. *NBER Working Paper No. 33286*.
- AKERLOF, GEORGE A. 1978. The economics of "tagging" as applied to the optimal income tax, welfare programs, and manpower planning. *The American economic review*, **68**(1), 8–19.
- ALLCOTT, HUNT, & TAUBINSKY, DMITRY. 2015. Evaluating Behaviorally Motivated Policy: Experimental Evidence from the Lightbulb Market. *American Economic Review*, **105**, 2501–2538.
- AUERBACH, ALAN J., & HASSETT, KEVIN A. 2002. A New Measure of Horizontal Equity. *American Economic Review*, **92**(4), 1116–1125.
- BALAN, PABLO, BERGERON, AUGUSTIN, TOUREK, GABRIEL, & WEIGEL, JONATHAN. 2022. Local Elites as State Capacity: How City Chiefs use Local Information to Increase Tax Compliance in D.R. Congo. *American Economic Review*, **112**, 1–36.
- BAYER, PATRICK, FERREIRA, FERNANDO, & MCMILLAN, ROBERT. 2007. A Unified Framework for Measuring Preferences for Schools and Neighborhoods. *Journal of Political Economy*, **115**(4).
- BERGERON, AUGUSTIN, TOUREK, GABRIEL, & WEIGEL, JONATHAN. 2024a. The State Capacity Ceiling on Tax Rates: Evidence from Randomized Tax Abatements in the DRC. *Econometrica*, **92**, 1163–1193.
- BERGERON, AUGUSTIN, BESSONE, P, KABEYA, JK, TOUREK, GABRIEL, & WEIGEL, JONATHAN. 2024b. *Supermodular Bureaucrats: Evidence from Randomly Assigned Tax Collectors in the DRC*. forthcoming, *American Economic Review*.
- BESLEY, TIMOTHY, & COATE, STEPHEN. 1992. Workfare versus Welfare: Incentive Arguments for Work Requirements in Poverty-Alleviation Programs. *American Economic Review*, **82**, 249–261.
- BESLEY, TIMOTHY, & KANBUR, RAVI. 1988. Food Subsidies and Poverty Alleviation. *The Economic Journal*, **98**, 701–719.
- BLACK, SANDRA E. 1999. Do Better Schools Matter? Parental Valuation of Elementary Education. *The Quarterly Journal of Economics*, **114**(2), 577–599.
- BROCKMEYER, ANNE, ESTEFAN, ALEJANDRO, ARRAS, KARINA RAMÍREZ, & SERRATO, JUAN CARLOS SUÁREZ. 2023. *Taxing property in developing countries: theory and evidence from Mexico*. National Bureau of Economic Research Working Paper.
- CABRAL, MARIKA, & HOXBY, CAROLINE. 2012. *The hated property tax: salience, tax rates, and tax revolts*. Tech. rept. National Bureau of Economic Research.
- CALLAWAY, BRANTLY, GOODMAN-BACON, ANDREW, & SANT'ANNA, PEDRO H.C. 2024. *Difference-in-Differences with a Continuous Treatment*. Mimeo: Emory University: <https://doi.org/10.48550/arXiv.2107.02637>.
- CALONICO, SEBASTIAN, CATTANEO, MATIAS D., & TITIUNIK, ROCIO. 2014. Robust Nonparametric Confidence Intervals for Regression-Discontinuity Designs. *Econometrica*, **82**(6), 2295–2326.

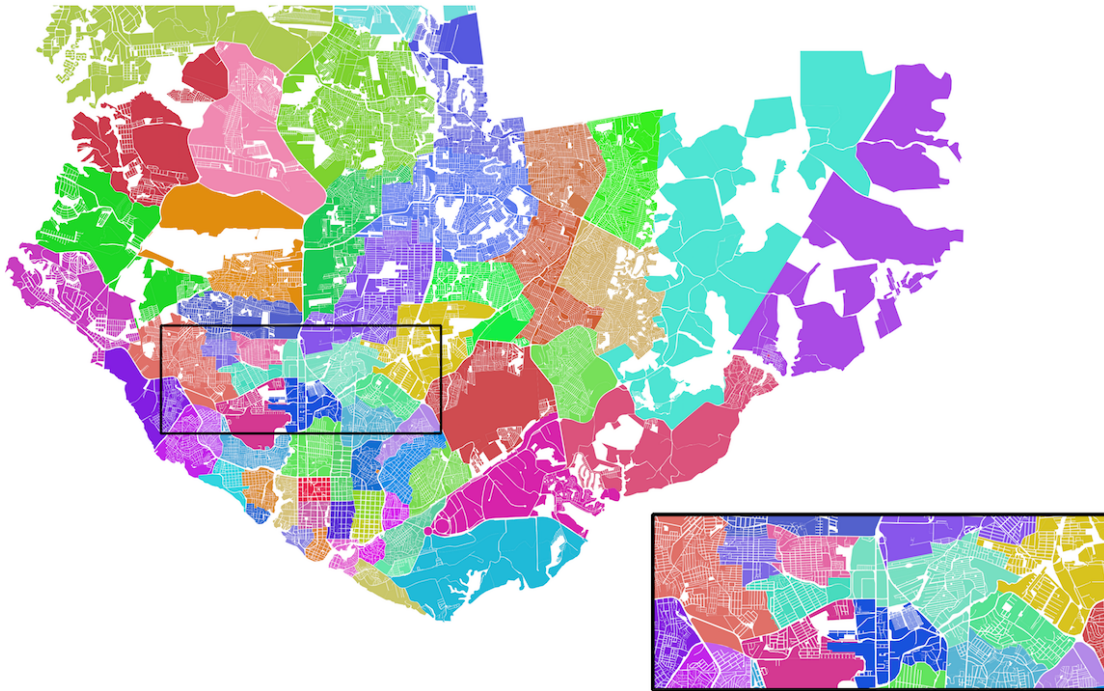
- CALONICO, SEBASTIAN, CATTANEO, MATIAS D., & FARRELL, MAX H. 2018. On the Effect of Bias Estimation on Coverage Accuracy in Nonparametric Inference. *Journal of the American Statistical Association*, **113**(522), 767–779.
- CALONICO, SEBASTIAN, CATTANEO, MATIAS D., FARRELL, MAX H., & TITIUNIK, ROCÍO. 2019. Regression Discontinuity Designs Using Covariates. *The Review of Economics and Statistics*, **101**(3), 442–451.
- CALONICO, SEBASTIAN, CATTANEO, MATIAS D., & FARRELL, MAX H. 2020. Optimal Bandwidth Choice for Robust Bias-Corrected Inference in Regression Discontinuity Designs. *Econometrics Journal*, **23**, 192–210.
- CARD, DAVID, MAS, ALEXANDRE, MORETTI, ENRICO, & SAEZ, EMMANUEL. 2012. Inequality at work: The effect of peer salaries on job satisfaction. *American Economic Review*, **102**(6), 2981–3003.
- CARVALHO JUNIOR, PEDRO HUMBERTO BRUNO. 2017. *Property tax performance and potential in Brazil*. Ph.D. thesis, University of Pretoria.
- CASTRO, LUCIA, & SCARTASCINI, CARLOS. 2015. Tax Compliance and Enforcement in the Pampas: Evidence from a Field Experiment. *Journal of Economic Behavior & Organization*, 65–82.
- CHENOZHUKOV, VICTOR, & HANSEN, CHRISTIAN. 2005. An IV Model of Quantile Treatment Effects. *Econometrica*, **73**, 245–261.
- CHETTY, RAJ. 2006. A General Formula for the Optimal Level of Social Insurance. *Journal of Public Economics*, **90**, 1879–1901.
- CRUCES, GUILLERMO, PEREZ-TRUGLIA, RICARDO, & TETAZ, MARTIN. 2013. Biased perceptions of income distribution and preferences for redistribution: Evidence from a survey experiment. *Journal of Public Economics*, **98**, 100 – 112.
- DEL CARPIO, LUCIA. 2016. *Are the Neighbors Cheating? Evidence from a Social Norm Experiment on Property Taxes in Peru*. mimeo: INSEAD.
- DONG, YINGYING, LEE, YING-YING, & GOU, MICHAEL. 2023. Regression Discontinuity Designs With a Continuous Treatment. *Journal of the American Statistical Association*, **118**, 208–221.
- DUBE, ARINDRAJIT, GIULIANO, LAURA, & LEONARD, JONATHAN. 2019a. Fairness and Frictions: The Impact of Unequal Raises on Quit Behavior. *American Economic Review*, **109**, 620–663.
- DUBE, ARINDRAJIT, GIULIANO, LAURA, & LEONARD, JONATHAN. 2019b. Fairness and frictions: The impact of unequal raises on quit behavior. *American Economic Review*, **109**(2), 620–663.
- DZANSI, JAMES, JENSEN, ANDERS, LAGAKOS, DAVID, & TELLI, HENRY. 2024. *Technology and Tax Capacity: Evidence from Local Governments in Ghana*. NBER working paper number 29923.
- FACK, GABRIELLE, & GRENET, JULIEN. 2010. When do better schools raise housing prices? Evidence from Paris public and private schools. *Journal of public Economics*, **94**(1-2), 59–77.
- FRÖLICH, MARKUS, & HUBER, MARTIN. 2019. Including Covariates in the Regression Discontinuity Design. *Journal of Business & Economic Statistics*, **37**, 736–748.

- GAUBERT, CECILE, KLINE, PATRICK, VERGARA, DAMIEN, & YAGAN, DANNY. 2021. *Place-Based Redistribution*. Mimeo: UC Berkeley.
- GIACCOBASSO, MATIAS, NATHAN, BRAD, PEREZ-TRUGLIA, RICARDO, & ZENTNER, ALEJANDRO. 2022. Where Do My Tax Dollars Go? Tax Morale Effects of Perceived Government Spending. *NBER Working Paper No. 29789*.
- GIBBONS, STEPHEN, MACHIN, STEPHEN, & SILVA, OLMO. 2013. Valuing school quality using boundary discontinuities. *Journal of Urban Economics*, **75**, 15–28.
- GRUBER, JON, & SAEZ, EMMANUEL. 2002. The Elasticity of Taxable Income: Evidence and Implications. *Journal of Public Economics*, **84**, 1–32.
- HVIDBERG, KRISTOFFER B, KREINER, CLAUS T, & STANTCHEVA, STEFANIE. 2023. Social positions and fairness views on inequality. *Review of Economic Studies*, **90**(6), 3083–3118.
- IMBENS, GUIDO, & NEWEY, WHITNEY. 2009. Identification and Estimation of Triangular Simultaneous Equations Models Without Additivity. *Econometrica*, **77**, 1481–1512.
- KAPLOW, LOUIS. 1989. Horizontal Equity: Measures in Search of a Principle. *National Tax Journal*, **42**, 139–154.
- KAPON, SAMUEL, DEL CARPIO, LUCIA, & CHASSANG, SYLVAIN. 2024. *Using Divide-and-Conquer to Improve Tax Collection*. forthcoming, *Quarterly Journal of Economics*.
- KEELE, LUKE J, & TITIUNIK, ROCIO. 2015. Geographic boundaries as regression discontinuities. *Political Analysis*, **23**(1), 127–155.
- KEEN, MICHAEL, & SLEMMOD, JOEL. 2021. *Rebellion, Rascals, and Revenue: tax follies and wisdom through the ages*. Princeton University Press.
- KUZIEMKO, ILYANA, NORTON, MICHAEL, SAEZ, EMMANUEL, & STANTCHEVA, STEFANIE. 2015. How Elastic are Preferences for Redistribution? Evidence from Randomized Survey Experiments. *American Economic Review*, **105**, 1478–1508.
- LIVY, MITCHELL R. 2018. Intra-school district capitalization of property tax rates. *Journal of Housing Economics*, **41**, 227–236.
- LUTTMER, ERZO, & SINGHAL, MONICA. 2014. Tax Morale. *Journal of Economic Perspectives*, **28**, 149–168.
- MANKIW, N GREGORY, & WEINZIERL, MATTHEW. 2010. The optimal taxation of height: A case study of utilitarian income redistribution. *American Economic Journal: Economic Policy*, **2**(1), 155–176.
- NATHAN, BRAD, PEREZ-TRUGLIA, RICARDO, & ZENTNER, ALEJANDRO. 2023. Paying Your Fair Share: Perceived Fairness and Tax Compliance. *NBER Working Paper No. 32588*.
- NATHAN, BRAD, PEREZ-TRUGLIA, RICARDO, & ZENTNER, ALEJANDRO. 2025. My Taxes Are Too Darn High: Why Do Households Protest Their Taxes? *American Economic Journal: Economic Policy*, **17**(1), 273–310.
- NICHOLS, ALBERT L, & ZECKHAUSER, RICHARD J. 1982. Targeting Transfers through Restrictions on Recipients. *American Economic Review*, **72**, 372–377.

- OATES, WALLACE E, & SCHWAB, ROBERT M. 2015. The window tax: A case study in excess burden. *Journal of Economic Perspectives*, **29**(1), 163–180.
- OKUNOGBE, OYEBOLA. 2023. *Becoming Legible to the State: The Role of Detection and Enforcement Capacity on Tax Compliance*. mimeo: World Bank.
- REDDING, STEPHEN J., & ROSSI-HANSBERG, ESTEBAN. 2017. Quantitative Spatial Economics. *Annual Review of Economics*, **9**, 21–58.
- RING, MARIUS AK. 2024. Wealth taxation and household saving: Evidence from assessment discontinuities in Norway. *Review of Economic Studies*, rdae100.
- SAEZ, EMMANUEL, & STANTCHEVA, STEFANIE. 2016. Generalized Social Marginal Welfare Weights for Optimal Tax Theory. *American Economic Review*, **106**, 24–45.
- SCHÖNHOLZER, DAVID. 2022. *Measuring Preferences for Local Governments*. Working Paper.
- SLEMROD, JOEL. 2019. Tax Compliance and Enforcement. *Journal of Economic Literature*, **57**, 904–954.
- SMITH, ADAM. 1776. *An Inquiry into the Nature and Causes of the Wealth of Nations*. London: W. Strahan and T. Cadell. Chap. Book V, Chapter 2: Of the Sources of the General or Public Revenue of the Society.
- TURNER, MATTHEW A, HAUGHWOUT, ANDREW, & VAN DER KLAUW, WILBERT. 2014. Land use regulation and welfare. *Econometrica*, **82**(4), 1341–1403.
- TWAIT, AARON, & LANGLEY, ADAM. 2024. *50-State Property Tax Comparison Study*. Lincoln Institute of Land Policy.
- WEIGEL, JONATHAN. 2020. The Participation Dividend of Taxation: How Citizens in Congo Engage More with the State When it Tries to Tax Them. *Quarterly Journal of Economics*, **135**, 1849–1903.

Figures & Tables

FIGURE 1: TAX SECTOR BOUNDARIES



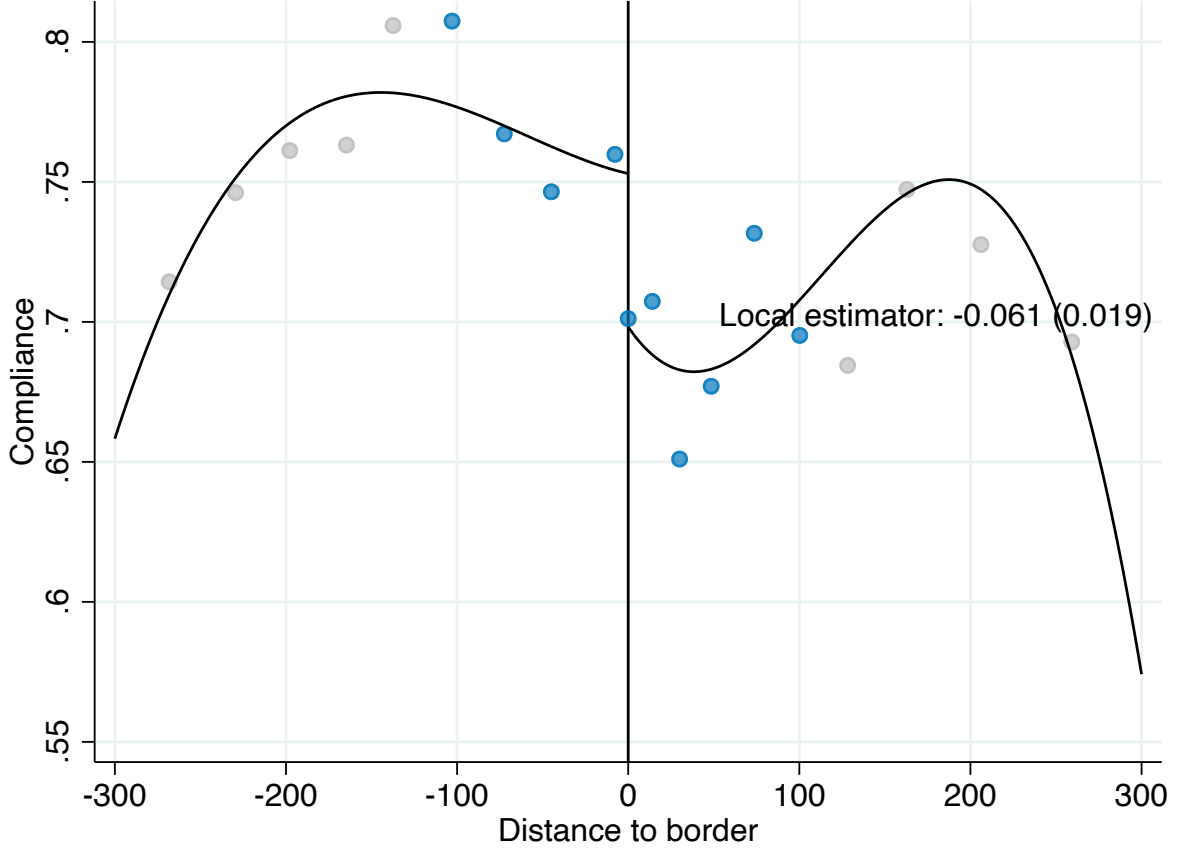
Notes: This is a map of the city of Manaus, and the colors highlight the different tax sectors created by SEMEF in 1983. Within each sector, properties are assigned the same square meter land value. The rectangle zooms in an area of the city to show more clearly the tax sector boundaries.

FIGURE 2: SECTORS CREATE ARBITRARY BOUNDARIES



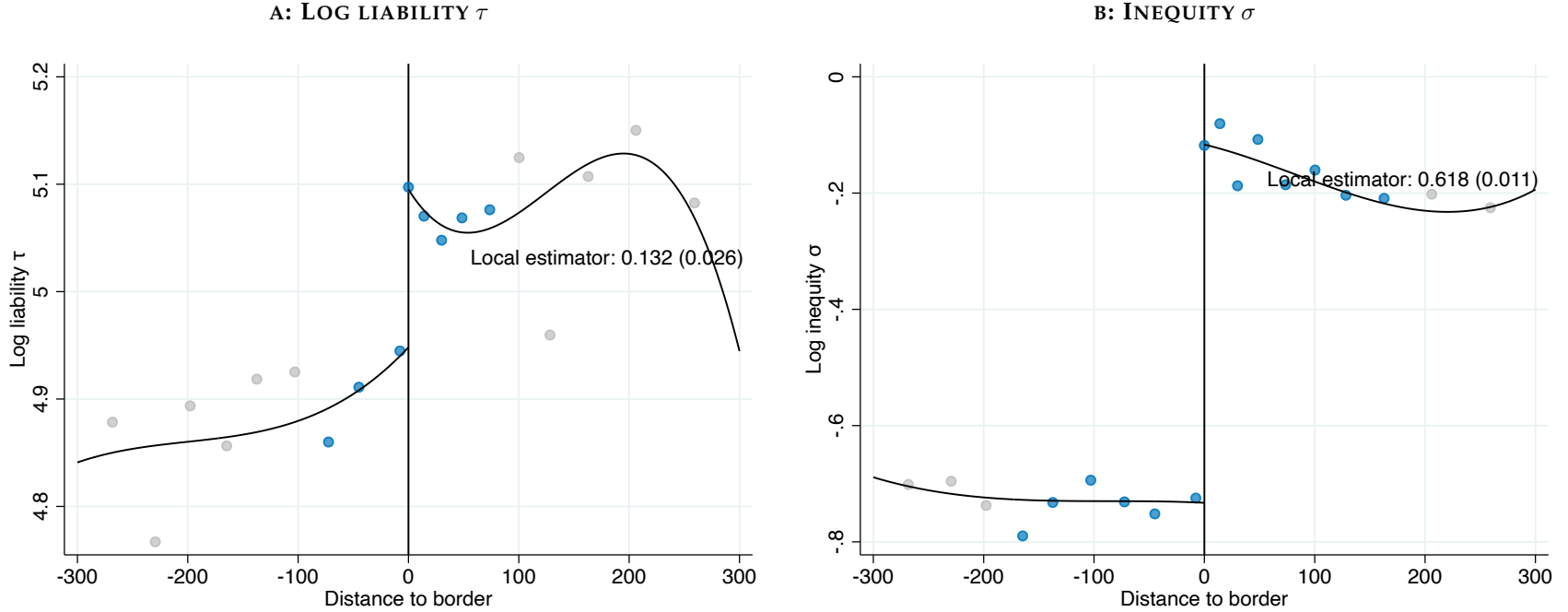
Notes: The tax sectors can create arbitrary boundaries where very similar houses are assigned different tax bills. This photo shows one of the boundaries highlighted in Figure 1. Map data: © 2018 Google.

FIGURE 3: OVERALL CHANGE IN COMPLIANCE AT TAX SECTOR BOUNDARIES



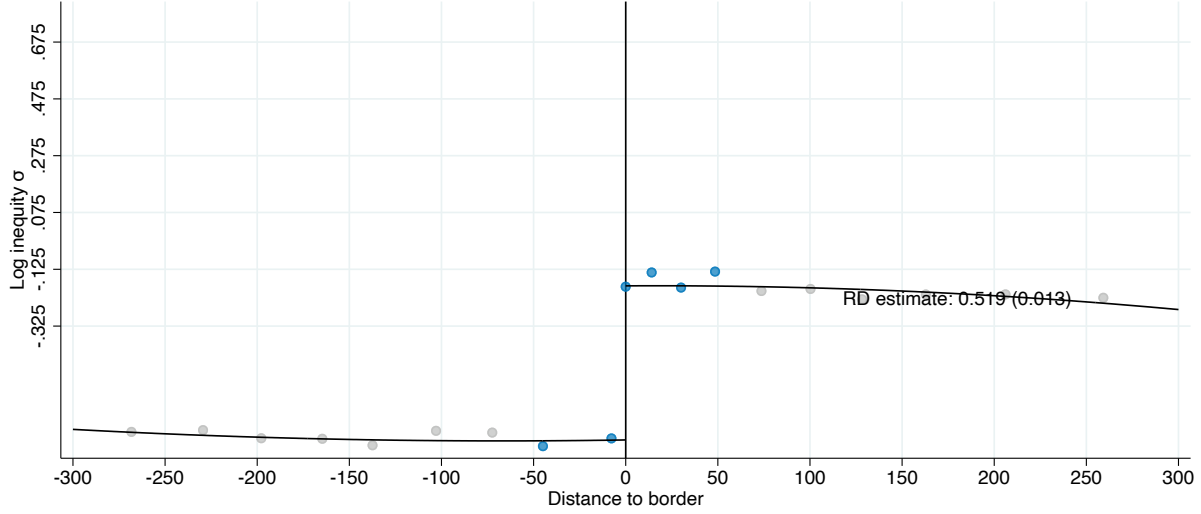
Notes: The figure shows the overall change in compliance at tax sector boundaries discussed in section 4.1. Specifically, we show the results of estimating the following equation for compliance (10): c_i by taxpayer i : $c_i = \gamma_{s(i)} + f(d_i) + \beta_0 HTS_i + h(d_i) \times HTS_i + \varepsilon_i$ where $\gamma_{s(i)}$ are boundary-segment fixed effects, HTS_i is an indicator for being on the high-tax side of the boundary ($d_i > 0$); $f_0(d_i)$ and $f_1(d_i)$ control for distance to the boundary on the low- and high-tax sides of the boundary, respectively; and ε_i is the residual. Overlaid on the figure, we show the point estimate of the discontinuity in compliance estimated using local linear distance controls, the MSE-minimizing bandwidth, and triangular kernel weights in distance. The dots in the figure show the coefficients from estimating (10) with fixed effects for decile-spaced bins of distance, using the same triangular kernel weights but censoring them at their tenth percentile to give non-zero weights to distances outside the optimal bandwidth. The bins in the optimal bandwidth are shown in blue while those outside are shown in grey. The black line is a global cubic polynomial fit in the same way.

FIGURE 4: OVERALL CHANGE IN INEQUITY AND LIABILITY AT TAX SECTOR BOUNDARIES



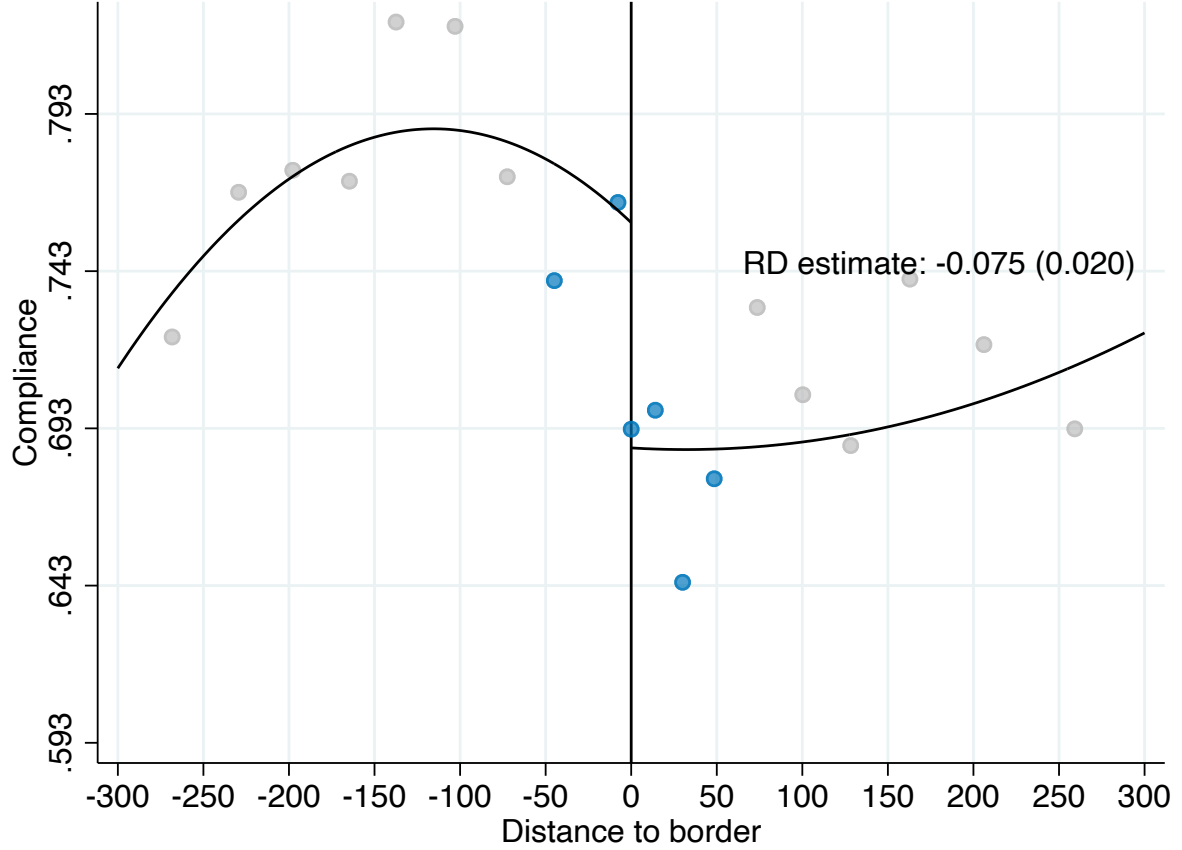
Notes: The figure shows the overall change in compliance at tax sector boundaries discussed in section 4. Specifically, we show the results of estimating the following equation (10) for log liability and inequity y_i by taxpayer i : $y_i = \gamma_{s(i)} + f(d_i) + \beta_0 HTS_i + h(d_i) \times HTS_i + \varepsilon_i$ where $\gamma_{s(i)}$ are boundary-segment fixed effects, HTS_i is an indicator for being on the high-tax side of the boundary ($d_i > 0$); $f_0(d_i)$ and $f_1(d_i)$ control for distance to the boundary on the low- and high-tax sides of the boundary, respectively; and ε_i is the residual. The outcome variable y_i is log liability τ in panel A and inequity σ in panel B. Overlaid on the figure, we show the point estimate of the discontinuity in the outcome variable estimated using local linear distance controls, the MSE-minimizing bandwidth, and triangular kernel weights in distance. The dots in the figure show the coefficients from estimating (10) with fixed effects for decile-spaced bins of distance, using the same triangular kernel weights but censoring them at their tenth percentile to give non-zero weights to distances outside the optimal bandwidth. The bins in the optimal bandwidth are shown in blue while those outside are shown in grey. The black line is a global cubic polynomial fit in the same way.

FIGURE 5: AUGMENTED BOUNDARY DISCONTINUITY DESIGN: FIRST STAGE



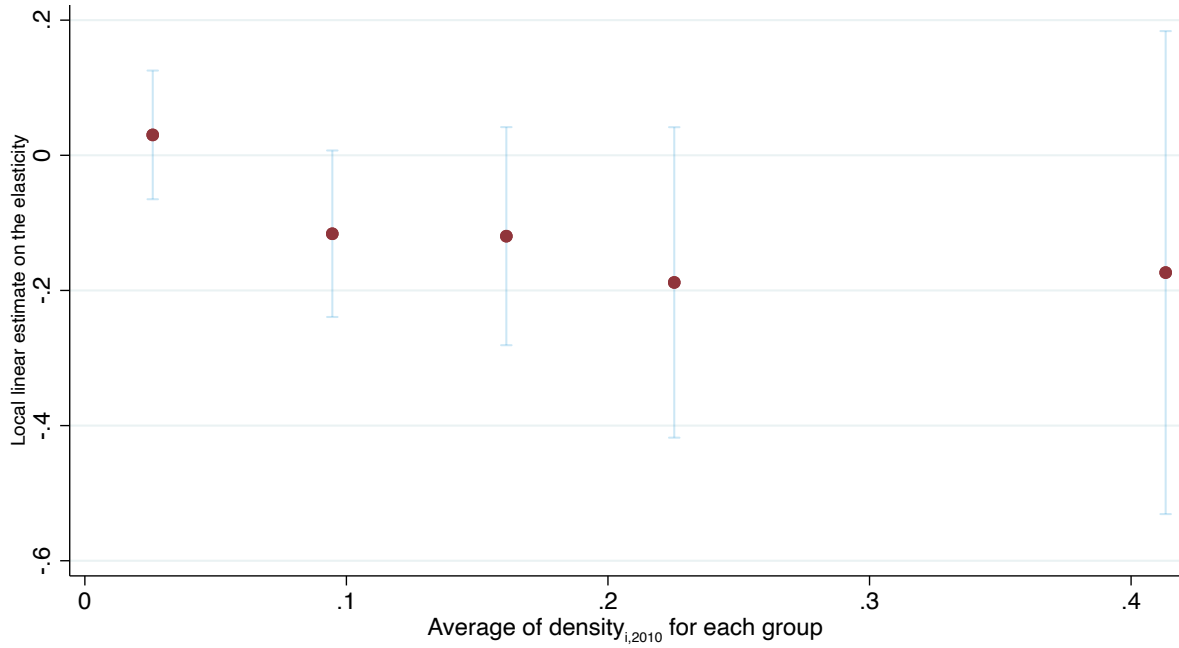
Notes: The figure shows the first stage impact on inequity in the augmented BDD discussed in section ?? . Specifically, we show the results of estimation of equation (12): $c_i = \gamma_{s(i)} + g(\tau_i, e_i) + f(d_i) + \beta_0 HTS_i + h(d_i) \times HTS_i + \varepsilon_i$ using log-inequity σ as the outcome variable, where $\gamma_{s(i)}$ are fixed effects for 500-meter segments along the boundaries to ensure we are comparing properties who are nearby each other; $g(\tau_i, e_i)$ are flexible controls for property i 's (log) tax liability τ_i and expansiveness e_i (our baseline estimates use τ splines and expansiveness deciles); $f(d_i)$ and $h(d_i)$ control flexibly for distance to the boundary on the low- and high-tax sides of the boundary respectively; and HTS_i is an indicator for properties on the high-tax side of the boundary ($d_i > 0$). Overlaid on the figure, we show the point estimate of the discontinuity in inequity estimated using local linear distance controls, the MSE-minimizing bandwidth, and triangular kernel weights in distance. The dots in the figure show the coefficients from estimating (12) with fixed effects for decile-spaced bins of distance, using the same triangular kernel weights but censoring them at their tenth percentile to give non-zero weights to distances outside the optimal bandwidth. The bins in the optimal bandwidth are shown in blue while those outside are shown in grey. The black line is a global cubic polynomial fit in the same way.

FIGURE 6: AUGMENTED BOUNDARY DISCONTINUITY DESIGN: COMPLIANCE EFFECTS



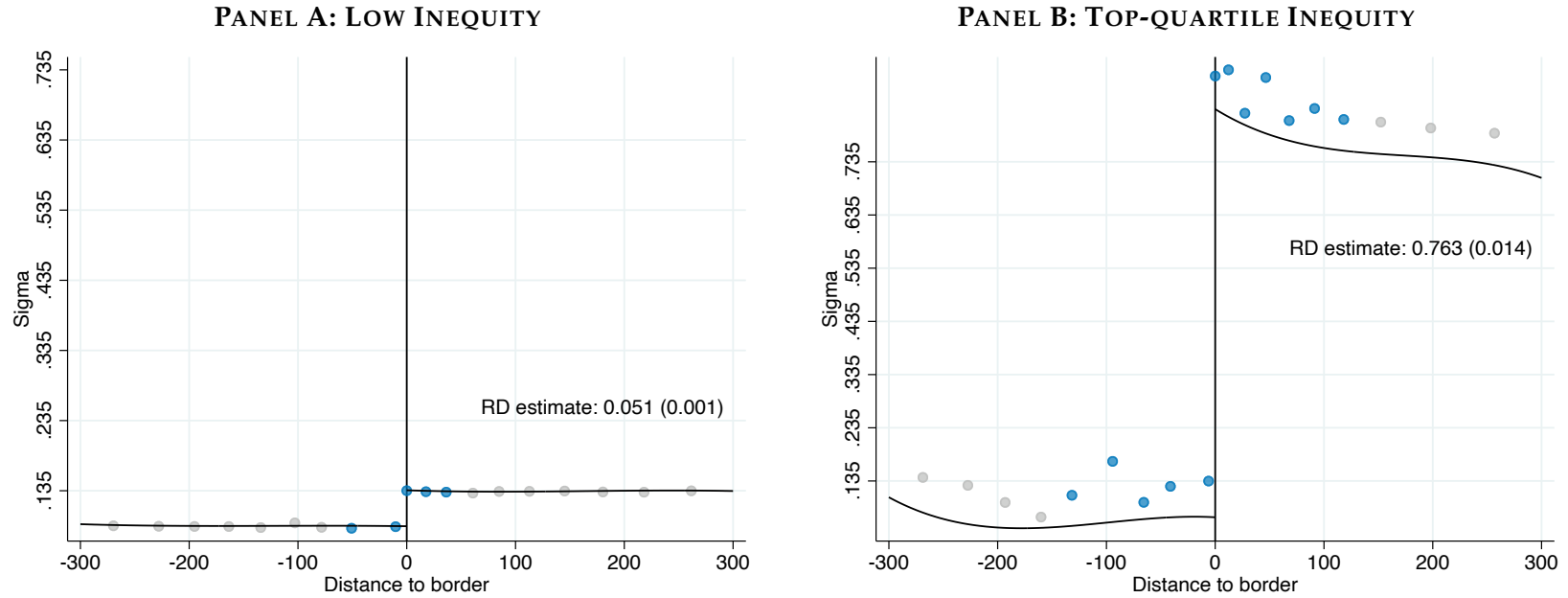
Notes: The figure shows the first stage impact on inequity in the augmented BDD discussed in section ???. Specifically, we show the results of estimation of equation (12): $c_i = \gamma_{s(i)} + g(\tau_i, e_i) + f(d_i) + \beta_0 HTS_i + h(d_i) \times HTS_i + \varepsilon_i$ using compliance as the outcome variable, where $\gamma_{s(i)}$ are fixed effects for 500-meter segments along the boundaries to ensure we are comparing properties who are nearby each other; $g(\tau_i, e_i)$ are flexible controls for property i 's (log) tax liability τ_i and expansiveness e_i (our baseline estimates use τ splines and expansiveness deciles); $f(d_i)$ and $h(d_i)$ control flexibly for distance to the boundary on the low- and high-tax sides of the boundary respectively; and HTS_i is an indicator for properties on the high-tax side of the boundary ($d_i > 0$). Overlaid on the figure, we show the point estimate of the discontinuity in inequity estimated using local linear distance controls, the MSE-minimizing bandwidth, and triangular kernel weights in distance. The dots in the figure show the coefficients from estimating (12) with fixed effects for decile-spaced bins of distance, using the same triangular kernel weights but censoring them at their tenth percentile to give non-zero weights to distances outside the optimal bandwidth. The bins in the optimal bandwidth are shown in blue while those outside are shown in grey. The black line is a global cubic polynomial fit in the same way.

FIGURE 7: HETEROGENEITY OF THE BOUNDARY DISCONTINUITY DESIGN CONTROLLING FOR TAX LIABILITY COMPLIANCE EFFECTS, BY QUINTILES OF THE SALIENCE MEASURE



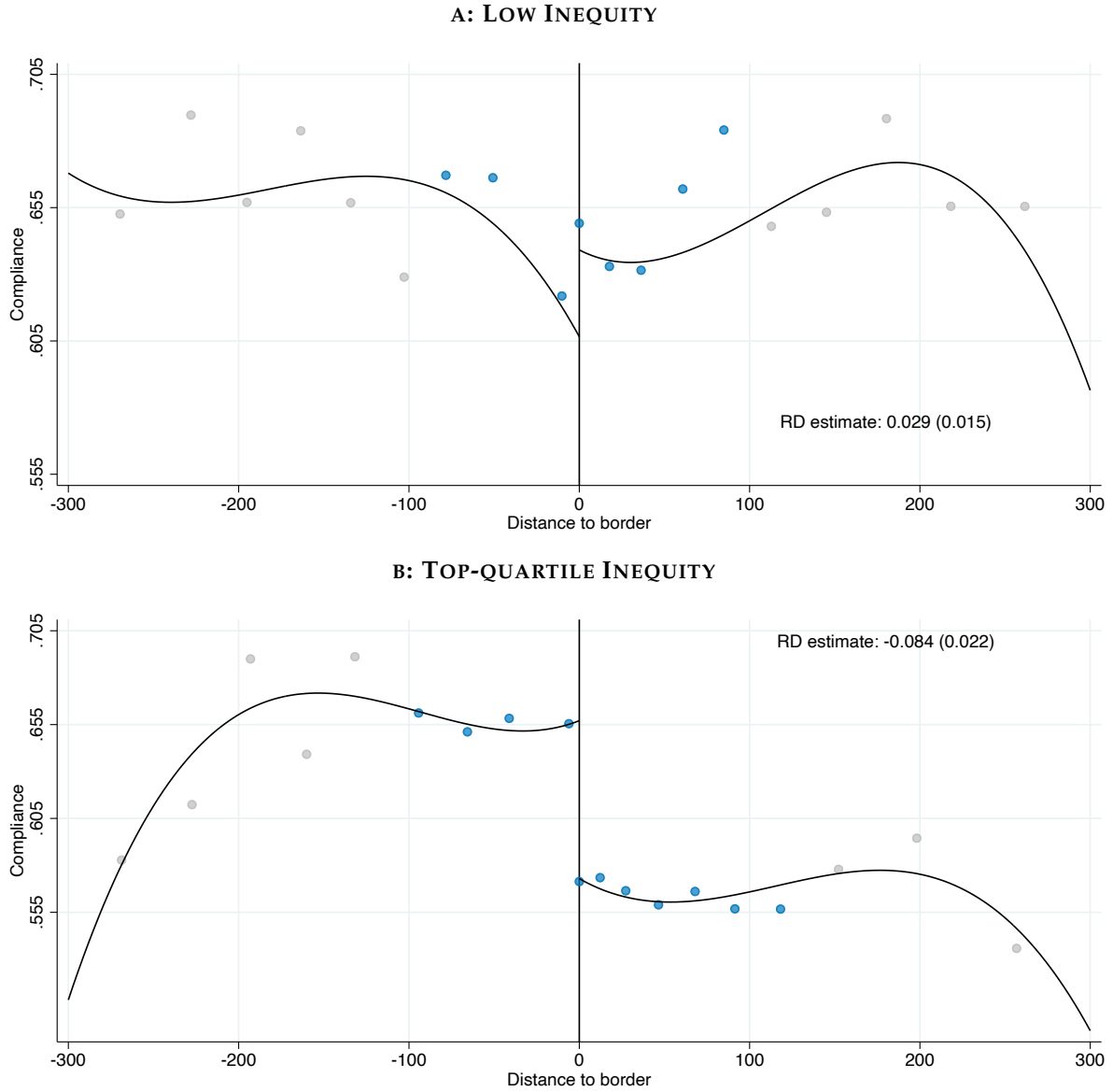
Notes: The figure shows the change in compliance at tax sector boundaries by groups of our salience measure, controlled by τ and expansiveness. Specifically, we split our sample into five disjoint groups using the quintiles of our salience measure, further explained in Appendix F. For each group, we show on the y-axis the results of the point estimate of the discontinuity in compliance estimated using local linear distance controls, the MSE-minimizing bandwidth, and triangular kernel weights in distance. On the x-axis, we show the average salience measure for each group. The figure shows that our results are strongly decreasing in the salience of the property tax. In the bottom quintile the estimated effect is zero, but then the effect is negative in the higher quintiles of salience.

FIGURE 8: DIFFERENCE IN BOUNDARY DISCONTINUITY DESIGN: FIRST STAGE



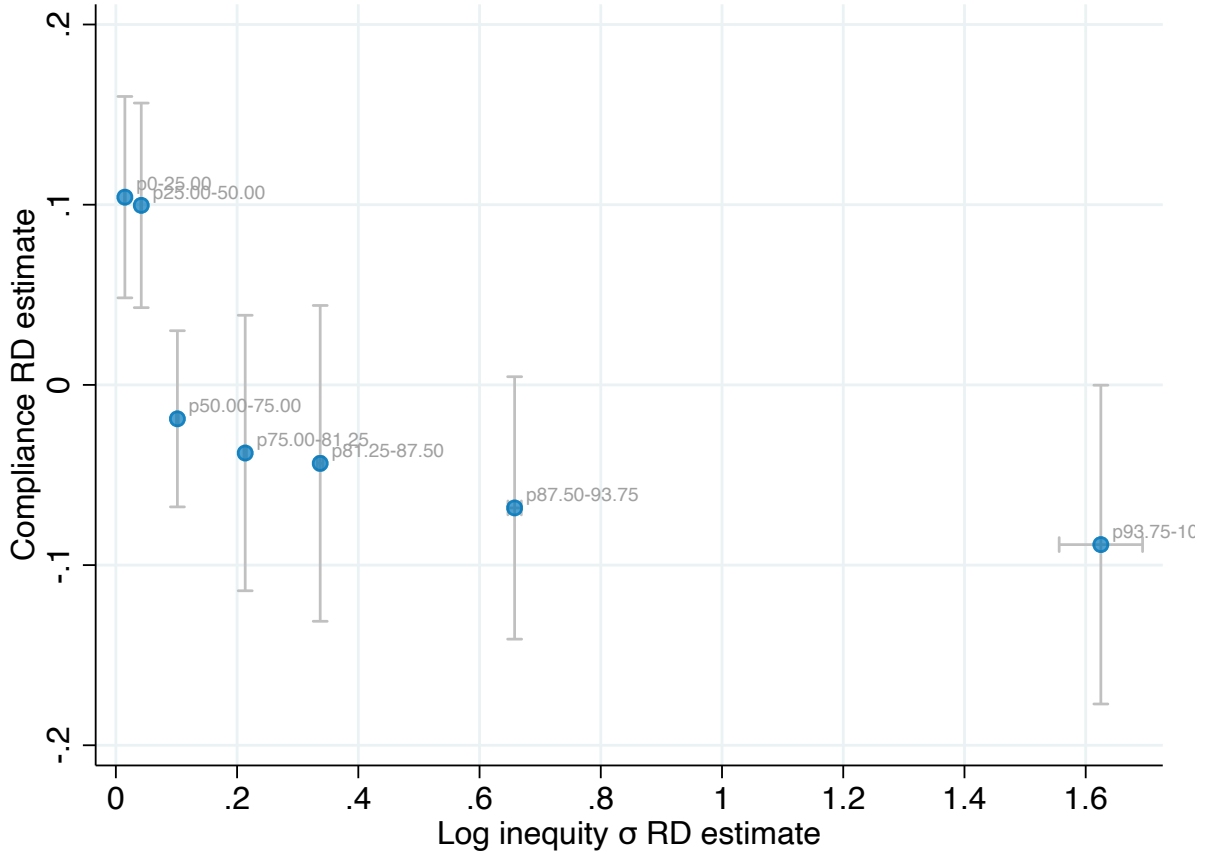
Notes: The figure shows the results of estimating equation (12): $c_i = \gamma_{s(i)} + g(\tau_i, e_i) + f(d_i) + \beta_0 HTS_i + h(d_i) \times HTS_i + \varepsilon_i$ with inequity as the outcome variable, where terms are as defined in the notes to figure 6. Panel A shows the estimates in the subsample of properties facing low inequity (defined as being in the bottom 3 quartiles of inequity). Panel B shows the estimates in the subsample of properties facing top-quartile inequity.

FIGURE 9: DIFFERENCE IN BOUNDARY DISCONTINUITY DESIGN: COMPLIANCE EFFECTS



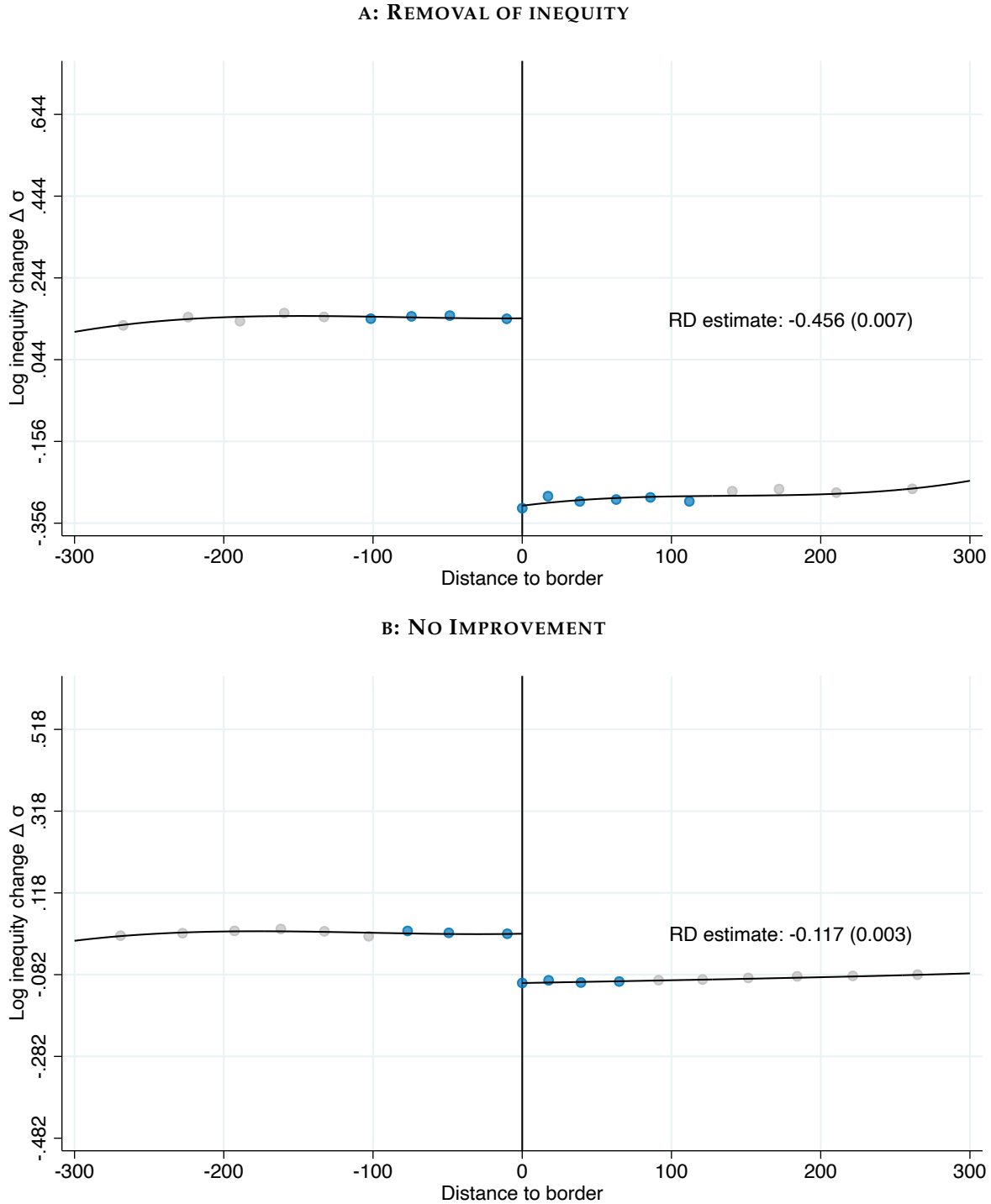
Notes: The figure shows the results of estimating equation (12): $c_i = \gamma_{s(i)} + g(\tau_i, e_i) + f(d_i) + \beta_0 HTS_i + h(d_i) \times HTS_i + \varepsilon_i$ with compliance as the outcome variable, where terms are as defined in the notes to figure 6. Panel A shows the estimates in the subsample of properties facing low inequity (defined as being in the bottom 3 quartiles of inequity). Panel B shows the estimates in the subsample of properties facing top-quartile inequity.

FIGURE 10: DIFFERENCE IN BOUNDARY DISCONTINUITY DESIGN: HETEROGENEITY



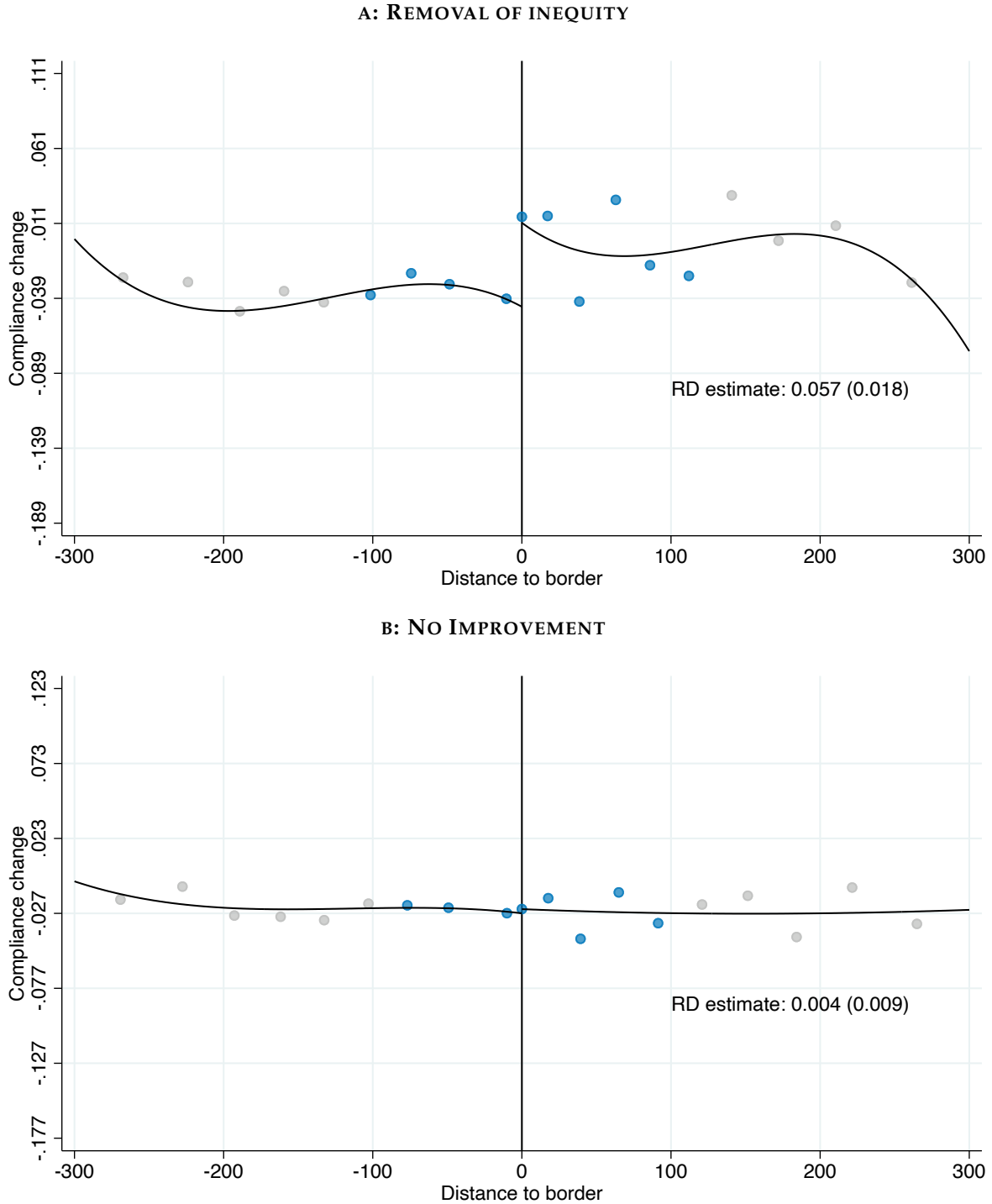
Notes: The figure shows the results of estimating equation (12): $c_i = \gamma_{s(i)} + g(\tau_i, e_i) + f(d_i) + \beta_0 HTS_i + h(d_i) \times HTS_i + \varepsilon_i$ where terms are as defined in the notes to figure 6. Each dot represents a different subsample. The three leftmost dots represent the three bottom quartiles of inequality. The remaining dots split the top quartile of inequality into 4 equally-sized subgroups. The vertical position and vertical grey bars of the dots display the estimated compliance effect and its 95% confidence interval. The horizontal position and horizontal grey bars of the dots display the estimated inequality change and its 95% confidence interval.

FIGURE 11: DYNAMIC BOUNDARY DISCONTINUITY DESIGN: REMOVAL OF INEQUITY VS NO IMPROVEMENT



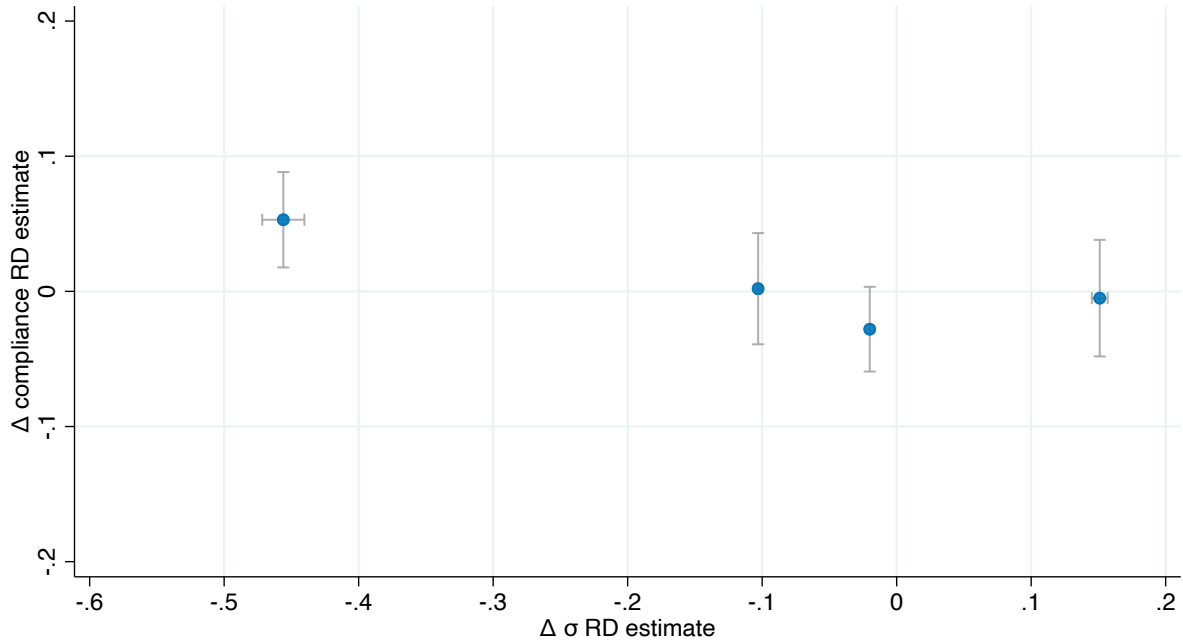
Notes: The figure shows the results of estimating equation (17) $\Delta\sigma_i = \gamma_{s(i)} + g(\Delta\tau_i) + f_0(d_i) + HTS_i \times [\beta_0 + f_1(d_i)] + \varepsilon_i$ where the outcome variable is the change in inequality, $\gamma_{s(i)}$ are boundary-segment fixed effects, HTS_i is an indicator for being on the high-tax side of the boundary ($d_i > 0$); $f_0(d_i)$ and $f_1(d_i)$ control for distance to the boundary on the low- and high-tax sides of the boundary, respectively; and ε_i is the residual. $g(\Delta\tau_i)$ controls flexibly for changes in log tax liability, τ_i . Specifically, we control for splines of $\Delta\tau_i$. Panel A shows the estimates in the subsample of properties for whom the reform meaningfully reduced inequality. Panel B shows the estimates in the remaining subsample of properties.

FIGURE 12: DYNAMIC BOUNDARY DISCONTINUITY DESIGN: REMOVAL OF INEQUITY VS NO IMPROVEMENT



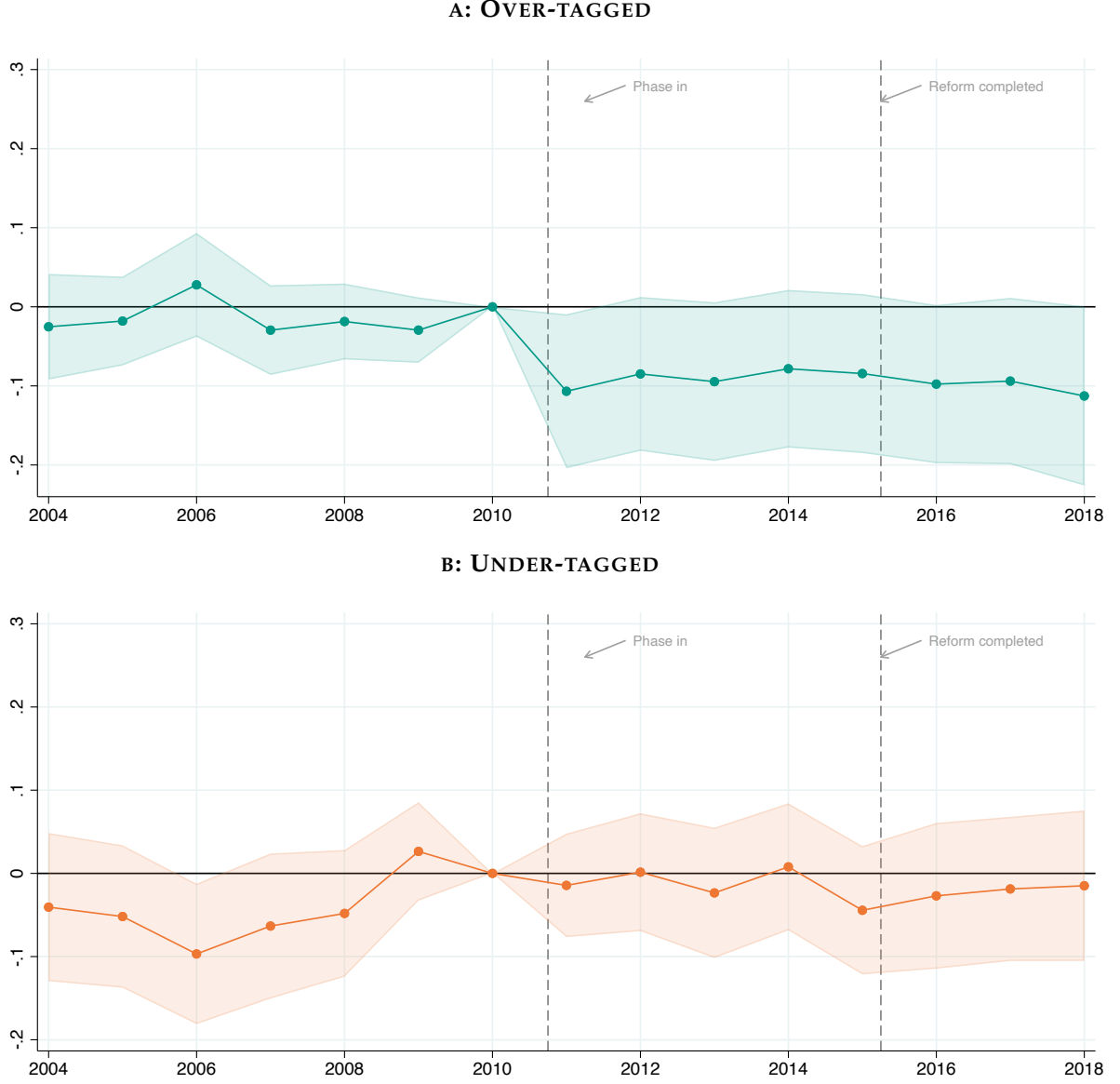
Notes: The figure shows the results of estimating equation (17) $\Delta c_i = \gamma_{s(i)} + g(\Delta \tau_i) + f_0(d_i) + HTS_i \times [\beta_0 + f_1(d_i)] + \varepsilon_i$ where the outcome variable is the change in compliance, $\gamma_{s(i)}$ are boundary-segment fixed effects, HTS_i is an indicator for being on the high-tax side of the boundary ($d_i > 0$); $f_0(d_i)$ and $f_1(d_i)$ control for distance to the boundary on the low- and high-tax sides of the boundary, respectively; and ε_i is the residual. $g(\Delta \tau_i)$ controls flexibly for changes in log tax liability, τ_i . Specifically, we control for splines of $\Delta \tau_i$. Panel A shows the estimates in the subsample of properties for whom the reform meaningfully reduced inequity. Panel B shows the estimates in the remaining subsample of properties.

FIGURE 13: DYNAMIC BOUNDARY DISCONTINUITY DESIGN: HETEROGENEITY BY IN-EQUITY REDUCTION



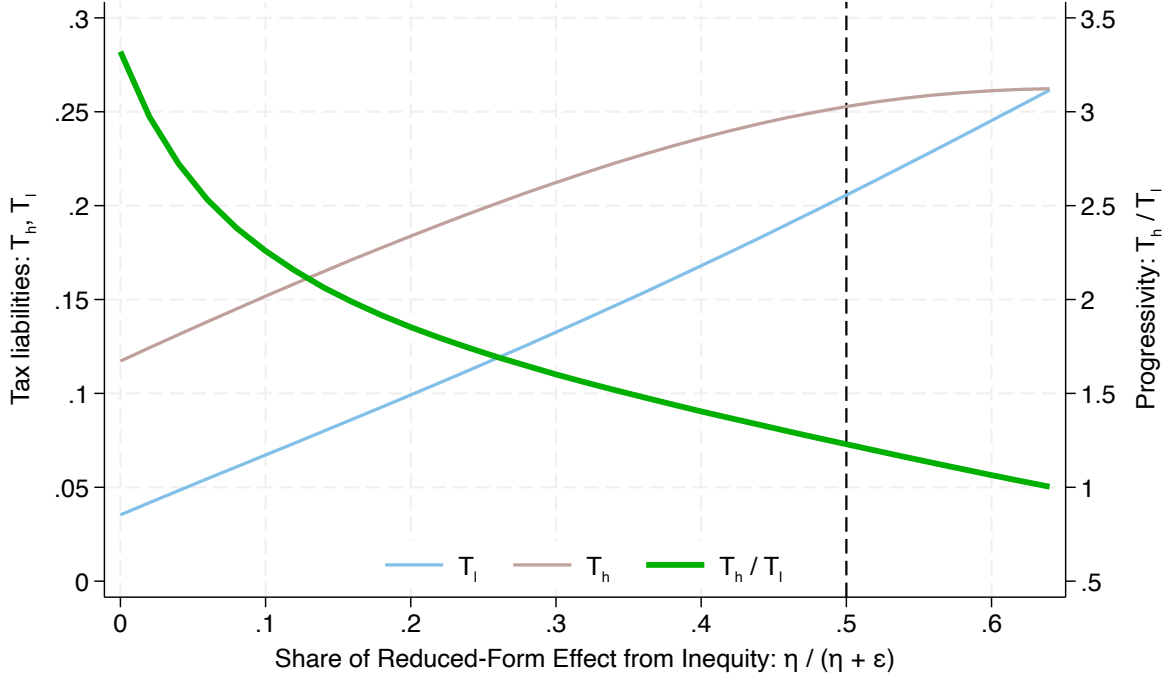
Notes: The figure shows the results of estimating equation (17) $\Delta c_i = \gamma_{s(i)} + g(\Delta \tau_i) + f_0(d_i) + HTS_i \times [\beta_0 + f_1(d_i)] + \varepsilon_i$ where $\gamma_{s(i)}$ are boundary-segment fixed effects, HTS_i is an indicator for being on the high-tax side of the boundary ($d_i > 0$); $f_0(d_i)$ and $f_1(d_i)$ control for distance to the boundary on the low- and high-tax sides of the boundary, respectively; and ε_i is the residual. $g(\Delta \tau_i)$ controls flexibly for changes in log tax liability, τ_i . Specifically, we control for splines of τ_i . We estimate (17) separately in four subsamples defined by quartiles of their change in inequity. The vertical coordinate of each dot and the vertical gray bars show the estimated impact on compliance and its 95% confidence interval. The horizontal coordinate of each dot and the horizontal gray bars show the estimated impact on inequity and its 95% confidence interval.

FIGURE 14: DIFFERENCE IN DIFFERENCE ESTIMATES OF OVERTAGGING AND UNDERTAGGING EFFECTS



Notes: The figure shows the results of the estimation of equation (20) as discussed in section 6.3: $c_{iy} = \alpha_i + \gamma_{s(i)y} + \sum_{j \neq 2010} D_{jy} \times [f_{0j}(d_i) + \beta_{0j} \Delta \tau_i + \eta_{0j} \Delta \sigma_i + HTS_i \times (\delta_j + f_{1j}(d_i) + \beta_{1j} \Delta \tau_i + \eta_{1j} \Delta \sigma_i)] + \varepsilon_{iy}$, where $\gamma_{s(i)y}$ are segment-year fixed effects, $D_{jy} \equiv 1[y = j]$ are year dummies, and we include year-specific distance controls $f_{0j}(d_i)$ and $f_{1j}(d_i)$; and year-specific controls for property i 's tax liability change due to the reform. Panel A shows the estimated η_{1j} coefficients along with their 95% confidence intervals. Panel B shows the estimated η_{0j} coefficients along with their 95% confidence intervals.

FIGURE 15: CALIBRATION OF OPTIMAL TAX SCHEDULE



Notes: The figure shows a calibration of the optimal tax schedule discussed in section 3.2. We set the parameters as follows: $\psi = 0.05$, $\rho = 2$, $y_H/y_L = 1.8$, $b(r) = 1.3$, $g_H/g_L = 1.07$. In the figure, we hold the overall response to taxation, governed by $\varepsilon + \eta$ fixed and vary the fraction of the total response that is driven by the elasticity with respect to inequity η vs the elasticity with respect to the tax liability ε . We show the two optimal tax rates and the ratio of the two: the progressivity of the tax schedule. Since the two elasticities have opposite implications for progressivity, the larger the fraction of the response that comes from inequity, the less progressive the optimal tax schedule. Our estimates in table 4 suggest that η is 0.12, implying $\varepsilon = 0.33$ placing us at the dashed vertical line, and implying that optimal progressivity is around 50% of what it would be if all responses were driven by the tax liability and none by inequity.

TABLE 1: PROPERTY TAXES AROUND THE WORLD

City	Property Tax Assessment	Does geography enter into the assessment?	Do assessment zones align with administrative divisions?
Addis Ababa (ET)	Presumptive	No	-
Amsterdam (NL)	Market value	No	-
Bangkok (TH)	Presumptive	Yes	Yes
Beijing (CN)	No property tax	-	-
Berlin (DE)	Presumptive	No	-
Bogota (CO)	Market value	-	-
Buenos Aires (AR)	Market value	No	-
Cairo (EG)	Presumptive	Yes	Yes
Chicago (US)	Market value	No	-
Delhi (IN)	Presumptive	No	-
Dhaka (BD)	Presumptive	Yes	No
Hong Kong (HK)	Market value	No	-
Istanbul (TR)	Presumptive	Yes	No
Jakarta (ID)	Market value	Yes	No
Johannesburg (ZA)	Market value	No	-
Karachi (PK)	Presumptive	Yes	No
Lagos (NG)	Market value	No	-
Lahore (PK)	Presumptive	Yes	No
Lima (PE)	Presumptive	Yes	No
London (UK)	Market value	No	-
Los Angeles (US)	Market value	No	-
Madrid (ES)	Presumptive	Yes	Yes
Manaus (BR)	Presumptive	Yes	No
Manilla (PH)	Market Value	No	-
Maputo (MZ)	Presumptive	Yes	No
Mexico City (MX)	Presumptive	Yes	Yes
Moscow (RU)	Presumptive	No	-
Mumbai (IN)	Presumptive	Yes	No
New York City (US)	Market value	No	-
Paris (FR)	Presumptive	Yes	Yes
Rio de Janeiro (BR)	Presumptive	Yes	No
Rome (IT)	Presumptive	No	-
Sao Paulo (BR)	Presumptive	Yes	No
Seoul (KR)	Presumptive	Yes	Yes
Shanghai (CN)	No property tax	-	-
Singapore (SG)	Market value	No	-
Sydney (AU)	Market value	No	-
Taipei (TW)	Presumptive	Yes	No
Tehran (IR)	Market value	No	-
Tokyo (JP)	Presumptive	No	No
Toronto (CA)	Market value	No	-

Notes: This table shows the method of property tax valuation for large urban areas across the world. Presumptive assessment uses a formula that takes observable characteristics of the property as its inputs. Market value assessment assigns a property tax based proportionally on the estimated value of the property in the real estate market. Note that China does not impose a property tax.

TABLE 2: AUGMENTED BOUNDARY DISCONTINUITY DESIGN: COMPLIANCE EFFECTS

	(1)	(2)	(3)	(4)	(5)	(6)
RD estimate	-0.10*** (0.03)	-0.09** (0.03)	-0.10*** (0.03)	-0.09*** (0.03)	-0.08** (0.03)	-0.11*** (0.03)
R^2						
Distance controls	✓	✓	✓	✓	✓	✓
Segment FEs	✓	✓	✓	✓	✓	✓
τ splines	✓	✓	✗	✓	✓	✗
exp dec FEs	✓	✗	✗	✓	✗	✓
τ decile FEs	✗	✗	✓	✗	✗	✓
exp splines	✗	✓	✗	✗	✓	✗
τ splines \times exp dec FEs	✗	✗	✗	✓	✗	✗
τ splines \times exp splines	✗	✗	✗	✗	✓	✗
τ dec FEs \times exp dec FEs	✗	✗	✗	✗	✗	✓
First-stage	0.549	0.534	0.546	0.567	0.552	0.559
Elasticity	-0.274	-0.248	-0.273	-0.264	-0.259	-0.257
N	10102	10101	10102	10102	10101	10102

Notes: The table shows the results of estimating the augmented BDD equation (12): $c_i = \gamma_{s(i)} + g(\tau_i, e_i) + f(d_i) + \beta_0 HTS_i + h(d_i) \times HTS_i + \varepsilon_i$, where $\gamma_{s(i)}$ are fixed effects for 500-meter segments along the boundaries to ensure we are comparing properties who are nearby each other; $g(\tau_i, e_i)$ are flexible controls for property i 's (log) tax liability τ_i and expansiveness e_i ; $f(d_i)$ and $h(d_i)$ control flexibly for distance to the boundary on the low- and high-tax sides of the boundary respectively; and HTS_i is an indicator for properties on the high-tax side of the boundary ($d_i > 0$). The columns use a variety of approaches to controlling flexibly for the tax liability and expansiveness. In column (1) we control for cubic splines of the tax liability and fixed effects for deciles of expansiveness. In column (2) we replace the expansiveness deciles with cubic splines of expansiveness while column (3) replaces the splines of the tax liability with deciles. Columns (4)–(6) additionally interact the tax liability controls with the expansiveness controls. The table shows remarkably consistent results: the implied elasticity of compliance with respect to inequity ranges from 0.25 to 0.27.

TABLE 3: DIFFERENCE IN BOUNDARY DISCONTINUITY DESIGN: COMPLIANCE EFFECTS

	(1)	(2)	(3)	(4)	(5)	(6)	(7)
$1(\text{high tax side}) \times \sigma $	-0.17*** (0.02)	-0.17*** (0.02)	-0.17*** (0.02)	-0.17*** (0.02)	-0.16*** (0.03)	-0.19*** (0.03)	-0.16*** (0.03)
R^2	0.116	0.116	0.116	0.116	0.120	0.118	0.124
Distance controls	✓	✓	✓	✓	✓	✓	✓
Segment fixed effects	✓	✓	✓	✓	✓	✓	✓
τ splines	✓	✓	✓	✗	✓	✓	✗
τ deciles	✗	✗	✗	✓	✗	✗	✓
Expansiveness splines	✗	✗	✓	✗	✗	✓	✗
Expansiveness deciles	✓	✓	✗	✓	✓	✗	✓
τ splines \times HTS	✗	✓	✓	✗	✓	✓	✗
τ deciles \times HTS	✗	✗	✗	✓	✗	✗	✓
τ splines \times exp deciles	✗	✗	✗	✗	✓	✗	✗
τ splines \times exp splines	✗	✗	✗	✗	✗	✓	✗
τ deciles \times exp deciles	✗	✗	✗	✗	✗	✗	✓
τ splines \times HTS \times exp deciles	✗	✗	✗	✗	✓	✗	✗
τ splines \times HTS \times exp splines	✗	✗	✗	✗	✗	✓	✗
τ deciles \times HTS \times exp deciles	✗	✗	✗	✗	✗	✗	✓
Elasticity	-0.262 (0.036)	-0.262 (0.037)	-0.274 (0.037)	-0.261 (0.036)	-0.247 (0.040)	-0.304 (0.044)	-0.247 (0.040)
N	27323	27323	27323	27323	27323	27323	27323

Notes: The table shows the results of estimation of equation (16): $c_i = \gamma_{s(i)} + g_0(\tau_i, e_i) + f(d_i) + HTS_i \times [\beta_0 + \eta \log(\sigma) + h(d_i) + g_1(\tau_i, e_i)] + \varepsilon_i$ where terms are as defined above in the notes to table 2. In column (1), we control for cubic splines of the tax liability and fixed effects for deciles of the expansiveness distribution. In column (2) we control separately for the tax liability and expansiveness on either side of the boundary. Column (3) replaces the expansiveness deciles with cubic splines in expansiveness while column (4) replaces the tax liability deciles with cubic splines. Columns (5)–(7) control for these separately on either side of the boundary.

TABLE 4: DYNAMIC DIFFERENCE IN BOUNDARY DISCONTINUITY DESIGN

	(1)	(2)	(3)	(4)
	Δ Compliance	Δ Compliance	Δ Compliance	Δ Compliance
1(high tax side)	0.010 (0.012)	-0.004 (0.030)	-0.005 (0.030)	0.004 (0.023)
1(high tax side) X change in σ	-0.095** (0.038)	-0.099** (0.040)	-0.074* (0.044)	-0.101** (0.039)
Elasticity implied	-0.149	-0.156	-0.116	-0.158
Elasticity SE	0.059	0.063	0.069	0.062
Distance controls	✓	✓	✓	✓
Segment FEs	✓	✓	✓	✓
τ splines	✓	✓	✓	✗
Expansiveness deciles	✓	✓	✗	✓
Interaction with HTS	✗	✓	✓	✓
τ splines \times expansiveness deciles	✗	✓	✗	✗
Expansiveness splines	✗	✗	✓	✗
τ splines \times expansiveness splines	✗	✗	✓	✗
τ deciles	✗	✗	✗	✓
τ deciles \times expansiveness deciles	✗	✗	✗	✓

Notes: This table shows the results of estimating equation (18) discussed in section 6.2: $\Delta c_i = \gamma_{s(u)} + g_0(\Delta \tau_i, e_i) + f_0(d_i) + HTS_i \times [\delta_0 + \eta \Delta \log(\sigma_i) + g_1(\Delta \tau_i, e_i) + f_1(d_i)] + \varepsilon_i$ where all terms are as defined above in the notes to table 2. Column (1) controls for cubic splines of the tax liability and fixed effects for deciles of the expansiveness distribution. Column (2) adds interactions between these controls and estimates them separately on either side of the boundary. Column (3) replaces the expansiveness deciles with splines, while column (4) replaces the tax liability splines with deciles of the tax liability distribution.

Appendices

A	Additional Background on IPTU in Manaus	2
B	Additional Background on the 2011 IPTU Reform	5
C	Additional Background on Distance Measure	8
D	Additional Background on Sample Selection and Robustness Checks	10
D.1	Sample including properties on neighborhood borders	10
D.2	Sample excluding properties on neighborhood borders	17
D.3	Sample with non-residential properties	21
D.4	Relaxed “large lots” drop: Drop the top 0.1% in terms of land area	32
D.5	Stringent “large CGLs” drop: Drop the top 1% in terms of land area	43
E	Additional Background on Inequity Measure (σ)	53
F	Salience of inequity	54
G	Placebo Test for Difference in Boundary Discontinuities Design	55
H	Discussion of house prices and IPTU	57
I	Proof of Proposition 1	58
J	Proof of Proposition 2	60
K	Model with Undertagging and Overtagging	62
L	Model with Location Choice and Endogenous House Prices	64
L.1	Location Choice	64
L.2	Welfare and Optimal Policy	67
M	Proof of Proposition 3	71
N	Proof of Proposition 4	73

A Additional Background on IPTU in Manaus

SEMEF calculates a property's tax bill (IPTU) as a function of a small number of easily observable characteristics of the land and any buildings on the property. Table A.1 lists the categories for each characteristic used in the calculation of the land value (VT) and building value (VE).

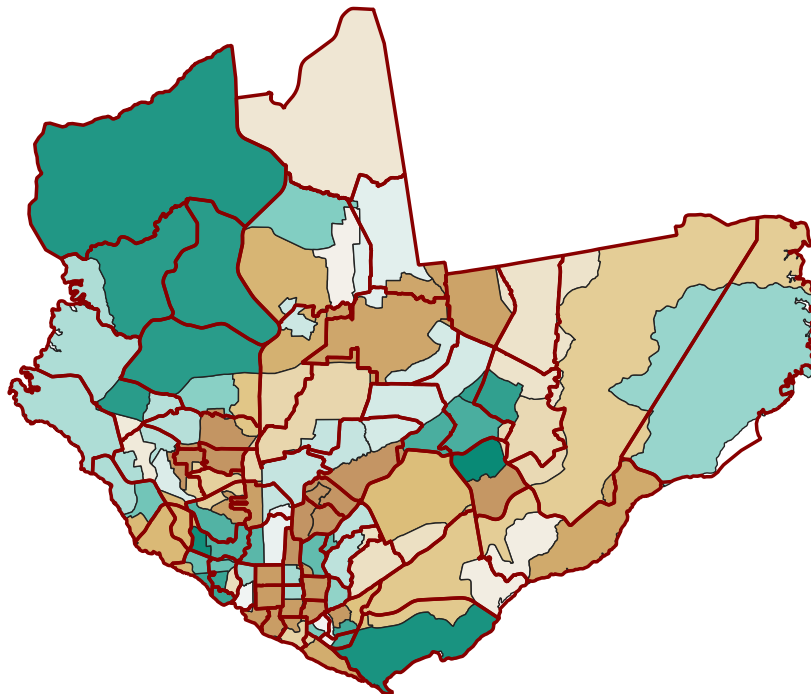
TABLE A.1: IPTU CALCULATION FACTORS

$IPTU = (VE + VT) \times aliquot$					
$VE = Value(m^2) \times Area \times (CAT/100) \times Alignment \times Construction \times Position$			$VT = Value(m^2) \times Area \times Situation \times Topography \times Pedology$		
Alignment	Construction	Position	Situation	Topography	Pedology
<ul style="list-style-type: none"> • Aligned • Backtracked 	<ul style="list-style-type: none"> • Isolated • Combined • Detached 	<ul style="list-style-type: none"> • Front • Back • Superimposed Front • Superimposed Back • Mezzanine • Gallery • Village 	<ul style="list-style-type: none"> • Corner • Middle of Block • Village • Enclave • Horizontal Condo • Favela/Stilit 	<ul style="list-style-type: none"> • Flat • Uphill • Downhill • Irregular 	<ul style="list-style-type: none"> • Floodable + 50% • Floodable - 50% • Firm

Notes: This table shows the equation used by SEMEF to calculate a household's property tax bill. CAT is defined as the sum of building components points, and factors in the construction material used in a household's roof, exterior walls, structure, and building height.

To calculate the per-square meter rate in the IPTU calculation, SEMEF divided Manaus into 65 tax sectors in 1983. Importantly, this division is only used in the IPTU calculation, as the smallest official administrative division of the city is the neighborhood (*Bairro*). As the tax sectors were created in 1983, before much of the city was built out, it is not conterminous with the bairro boundaries. Figure A.1 shows the overlay between the tax sector boundaries and the bairro boundaries (in red).


FIGURE A.1: TAX SECTOR AND NEIGHBORHOOD BOUNDARY OVERLAYS



Note: This figure shows the boundaries of tax sectors (in red) overlaid on the neighborhoods (*bairros*) in Manaus.

After a household receives its IPTU bill in January (see table A.2), it has the option to pay it in one installment by March (at a discounted rate) or to pay the bill in ten equal monthly installments. Failure to pay the complete IPTU bill by December 31 results in automatic interest and fines applied in the next billing cycle, with the property being placed on the *divida ativa* registry until the remaining balance is paid off. Despite the penalty for nonpayment, we find that compliance rates in Manaus are relatively low. Figure A.3 shows the compliance rate from 2004 through 2019. Despite a slight increase in compliance after 2008, the fraction of (nonexempt) households in the city that pay their IPTU bill in a given year is between 60 and 65 percent. However, as seen in the figure, compliance appears to be driven at the extensive margin, with the large majority of households who pay their IPTU choosing to pay the full amount owed to SEMEF that year.

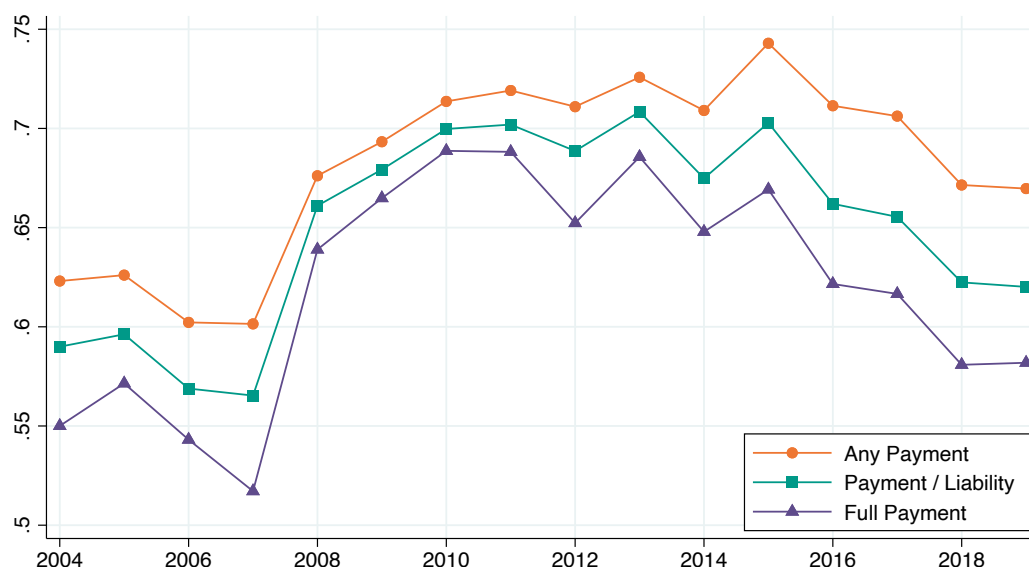
FIGURE A.2: EXAMPLE OF A 2018 IPTU BILL

 PREFEITURA DE MANAUS SEMEF DOCUMENTO DE ARRECADAÇÃO MUNICIPAL - D.A.M					
Contribuinte				D.A.M.	
[REDACTED]				21/[REDACTED]/2018	
CPF/CNPJ	Matricula/CMC	Tributos	Referência	Vencimento	Nosso Número
[REDACTED]	1/[REDACTED]	I.P.T.U. 2018	4/10	15/06/2018	11000/[REDACTED]
Endereço de Localização					
Logradouro: AV. TINTA - JARDIMAS		Número: 1		Cep: 69090295	
Bairro: CIDADE NOVA		Complemento: QD 25, CJ ETAPA I		Lote: 0200 Quadra: 0025	
Loteamento:		Quadra Lot.: 25		Lote Lot.: 0	
Imóvel: PREDIAL					
Área Terreno: 900,00		Área Total Construída: 623,55		Área Construída Unidade: 623,55	
Valor Venal Terreno: 40.304,88		Valor Venal Construção: 271.983,90			
Valor Venal Imóvel: 312.188,78		Base de Cálculo: 312.188,78		Alíquota: C,9000	
IPU PREDIAL		R\$	280,91		
TSA:		R\$	0,00		
Total:		R\$	280,91	Valor R\$ 280,91	
				Emissão: 12/06/2018 Usuário: CIDADAO	
				Autenticação:	

Note: This is an example of an IPTU bill received by a household in 2018.

Although we do not have the data necessary to compute the compliance rate in other Brazilian municipalities, we can use publicly available data on municipal finances to calculate the property tax collection rate. This rate is defined as the ratio of total revenue collected to the total amount of IPTU bills issued in a given city in a given year and can be used as a proxy for the compliance rate assuming that the distribution of property values is similar across Brazil. Figure A.4 shows the collection rates for IPTU bills in large Brazilian municipalities in 2021. Two features of the figure stand out: relative to other large cities-particularly in the south-Manaus has relatively lower collection rates. However, its low collection rate is consistent with lower collection rates in much of the northern states of Brazil.

FIGURE A.3: COMPLIANCE IS DRIVEN BY THE EXTENSIVE MARGIN



Notes: The figure shows the compliance rate by all non-exempt residential households in Manaus. The orange line depicts the fraction of households in a given year that paid at least a portion of their IPTU bill. The purple line shows the fraction of households that paid the full amount of their IPTU bill in a given year.

FIGURE A.4: IPTU COLLECTION RATE AMONG LARGE BRAZILIAN CITIES

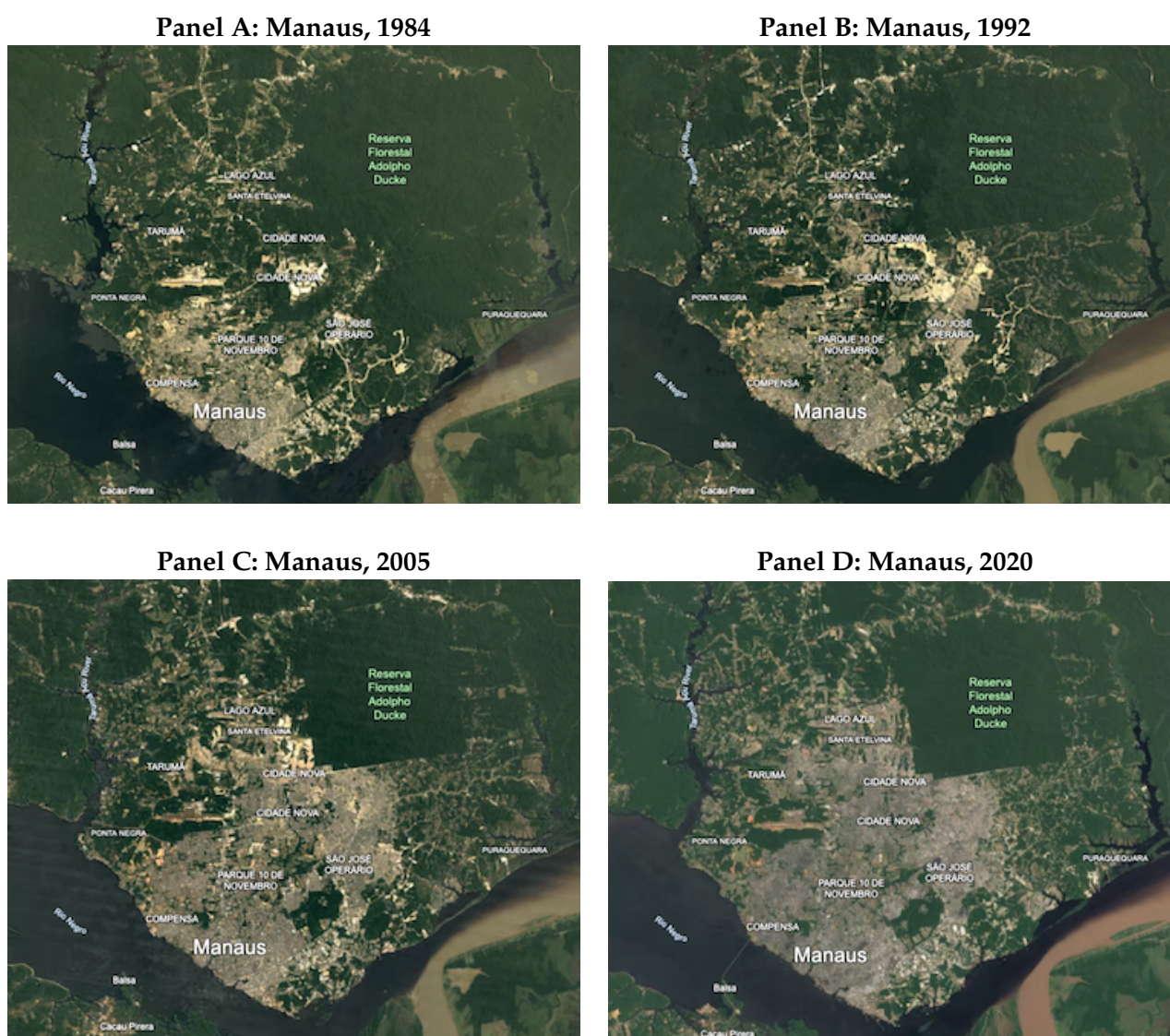


Notes: The figure shows the 2012 IPTU collection rate for cities in Brazil with more than 200,000 residents. The collection rate is defined as the ratio of collected tax revenue to total IPTU bills issued that year. Data on municipal GDP comes from the IBGE, and data on collection rates is from [Carvalho Junior \(2017\)](#).

B Additional Background on the 2011 IPTU Reform

In 2011 the government of Manaus passed Law 1.628/2011, which implemented a reform to the property tax system by altering the calculation of both the building and land value for a given property. The impetus of this reform was to better reflect the (presumptive) property values in light of the significant growth in Manaus since the IPTU was first implemented in 1983. Figure B.1 shows a timeline of satellite images of Manaus since 1984. Although the downtown core was already developed when the IPTU was created, much of the growth in the city during the past 40 years took place in the northern section of the city. Many of the tax sectors that determine the square-meter rate were sparsely populated until the late 1990s, with rates that did not reflect the increasing real estate density, activity, and value.

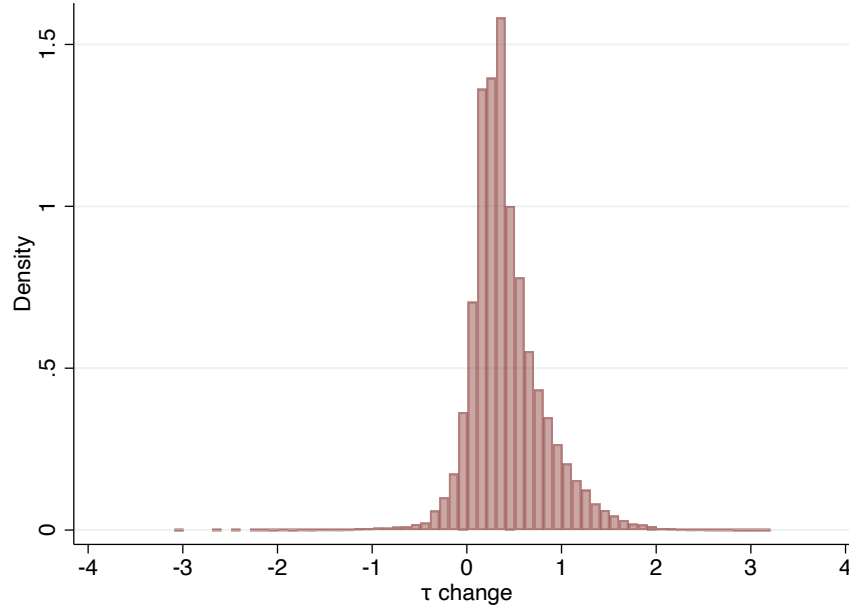
FIGURE B.1: GROWTH OF MANAUS OVER 40 YEARS THROUGH SATELLITE IMAGERY



Notes: This figure shows the growth of Manaus from 1984 to 2020 using a time lapse of satellite images. Map data: © 2023 Google / Maxar Technologies, AirbusCNES, Airbus.

The reform was not designed to be a complete overhaul of the system, but rather an update to the existing presumptive formula. The formula used to calculate the IPTU (equation 1) was unchanged, but the values for the land factors (ξ_y^A) and building factors (ξ_y^B) were changed across the different characteristics. Importantly for our identification, the reform included updates to the square-meter price ($p_{s(i)}$), with changes in the difference in rates across sector boundaries. Figure B.2 shows that for most residential properties in the city, the reform led to an increase in their tax bill.

FIGURE B.2: DISTRIBUTION OF CHANGES IN TAX BILLS DUE TO THE 2011 REFORM



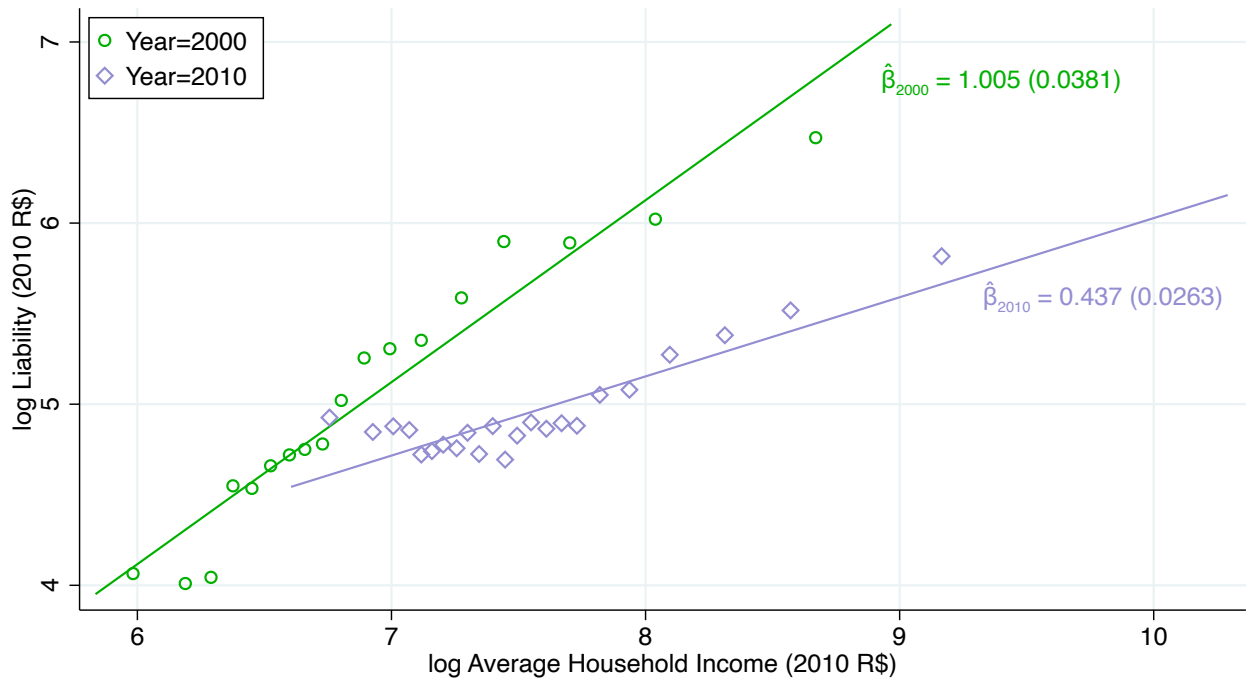
Notes: This figure shows the distribution of changes in the IPTU bill for households in our study sample.

In addition to reflecting the growth of the city since 1983, the changes implemented through the reform were meant to improve progressivity in property taxes. Without updates to the relative rates paid by households across the city, richer households would face increasingly smaller tax burdens as their property values increased, but they did not face higher IPTU bills. Figure B.3 panel A shows a weakening of tax progressivity in Manaus between the 2000 and 2010 census rounds, with a significant weakening of the relationship between the average tax bill and household income in a census tract.

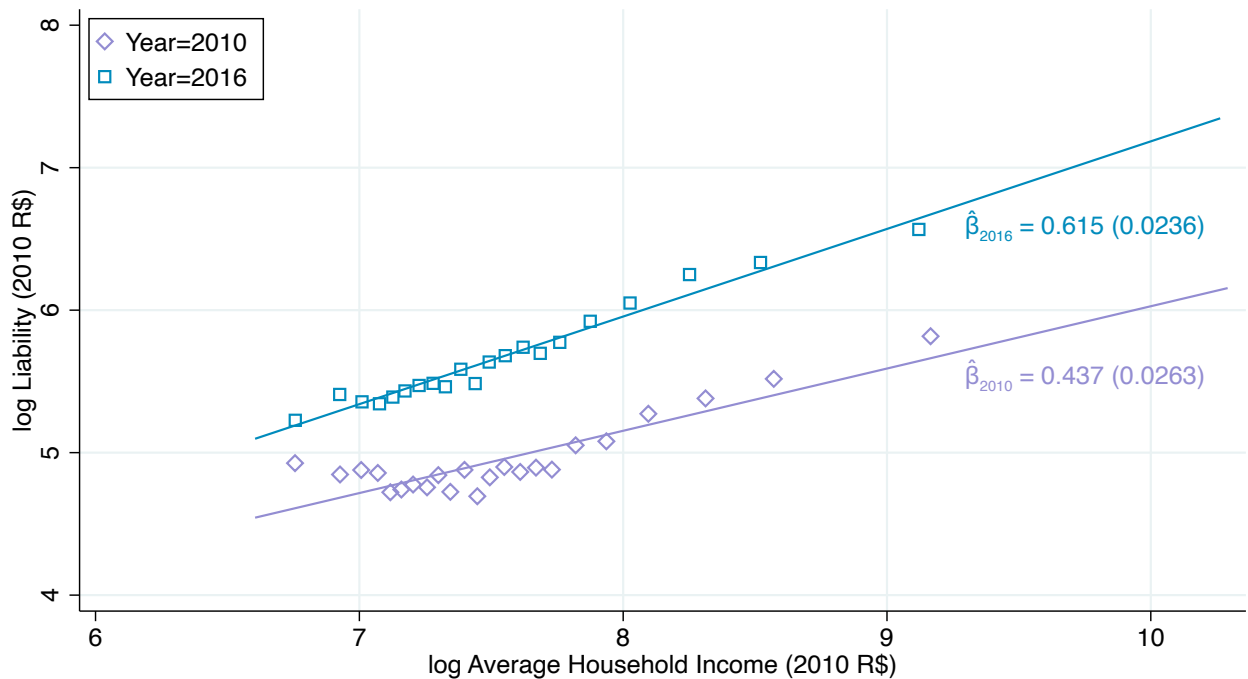
However, the 2011 reform was partially successful in strengthening the progressivity of the property tax system. Panel B of figure B.3 shows the relationship between the tax bill and average household income across census tracts in Manaus for the last pre-reform tax year (2010) and the first year when the new tax bills were fully implemented (2016). Two features are worth noting: there is an upward shift in the curves, implying that tax bills increased for almost all households in the city. However, there is also a rotation of the curve, with a steeper relationship between income and the IPTU in 2016, meaning that richer households faced a greater increase in their property taxes as a result of the reform.

FIGURE B.3: 2011 REFORM IMPROVES TARGETING OF PROPERTY TAX

Panel A: Change in Liabilities Pre-Reform



Panel B: Change in Liabilities Post-Reform



Notes: This figure plots the property tax bill against household income at the census-tract level. Data on census tracts for 2010 and 2016 comes from the 2010 census, with data on 2000 household income coming from tracts from the 2000 census. Property tax bills are shown in logs of the respective year, normalized to 2010 Reals.

C Additional Background on Distance Measure

In this section, we provide additional details on the construction of the distance measure employed in the regression discontinuity design (RDD) used in equation 10. Despite the numerous recent studies employing spatial discontinuities (Ring, 2024; Bayer *et al.*, 2007; Black, 1999; Livy, 2018; Gibbons *et al.*, 2013; Fack & Grenet, 2010; Turner *et al.*, 2014; Schönholzer, 2022; Keele & Titunik, 2015), there is no consensus on the creation of the running variable (e.g. distance), especially in an urban setting.

Several features of our setting inform our decisions about the calculation of the distance measure. First, our level of observation is the property lot, which is often quite small relative to the tax sectors and Manaus as a whole. Second, property lots vary in size and are not uniform in their orientation to the sector boundaries; some sectors have lots that are oriented so that the short side of the lot is closest to the boundary, while other sectors have the long side of the lots running parallel to the boundary. Therefore, if one were to measure the distance of the lot to the boundary by taking the distance from the centroid of the lot polygon, there would be variation in the running variable that is not caused by the “true” distance of the property to the sector boundary, but is rather an artifact of the irregular shape and orientation of the lots relative to the street grid.

In addition to issues related to lot sizes across the city, the creation of the tax sector boundary requires careful consideration in our distance calculation. SEMEF defined the sector boundaries as (almost always) running through various streets in Manaus. However, street width varies throughout the city, with some streets used in the sector boundaries being wide avenues and others quite narrow side streets or alleys. Using the full width of the street would result in borders with varying thicknesses. Moreover, the shapefiles provided by SEMEF do not place the sector boundaries in the middle of the street, which means that the distance to households on different sides of the sector will depend on how accurately the government “drew” the polygons for the tax sectors.

To address these issues, we take the approach of constructing many transects along the sector boundaries to simulate an individual “walking” into a given sector. For each of these “walks” we record both which properties we run in to, as well as its distance along the walk. Given the shapefiles identifying the property lots and tax sector polygons, we take the following steps to estimate the distance to the boundary:

1. Remove all corners where three or more tax sectors intersect (*Note: this ensures that the transects are not generated at the edge case of a boundary*)
2. Divide sector boundaries into 500 meter long segments
3. Along the entire boundary, seed “nodes” every 10 meters
4. From each node, create a transect that is perpendicular to the boundary and has a distance of 300 meters into each sector
5. Identify points where a transect intersects the polygon of a lot (*Note: this usually generates two points per lot per transect – where the transect “enters” the lot, and where it “exits” the lot*)
6. Calculate the distance of each of these intersections to the transect node

FIGURE C.4: TRANSECT CREATION ACROSS SECTOR BOUNDARIES



Notes: This figure depicts the calculation of the distance measure to the boundary used in our regression discontinuity analysis for a small section of Manaus. The red line denotes the tax sector boundary, the blue lines denote the transects generated perpendicular to the boundary, and the green polygons depict the lot lines for the properties. Transect lines are generated along the sector boundary in 10 meter intervals, with each transect extending perpendicularly into each side of the boundary for 300 meters. The yellow dots denote places where the transect intersect a lot—either through “entering” or “exiting” the lot.

Figure C.4 shows a small portion of the SEMEF shapefile after the above process is completed. It is important to note that since the transects were seeded every 10 meters along the boundary, there may be multiple transects that intersect a given property lot. Moreover, the sector boundary on the left side of the figure is drawn very close to one side of the (wide) street; without correcting this in the distance calculation, we would interpret the properties in the left sector as being farther away from the boundary, even though the properties on both sides of the boundary are on the street. To correct for this, we make the following post-calculation adjustments:

1. For each intersection point along the transect, remove the distance from the transect node to the first intersection point (*Note: this will “force” all properties nearest to the boundary to have a distance of zero to the boundary*)
2. For each lot, keep the smallest distance to the boundary

This creates a file of distances for 178,767 properties that are within 300 meters of a tax sector boundary, which we use as the base for our sample selection outlined in appendix D.

D Additional Background on Sample Selection and Robustness Checks

In this section, we provide additional details on the sampling steps to obtain the final data used, the number of properties dropped on each step, and run some robustness checks for changing some of these decisions.

There are two main samples used in the analysis: for the cross-sectional analysis, we exclude properties on neighborhood borders, but include them in the analysis using variation from the tax reform. The following table summarizes the subsampling steps we take and amount of properties dropped in each step:

TABLE D.1: SUBSAMPLING STEPS - CROSS SECTIONAL SAMPLE

Subsampling step	N left in 2010	N left 04-18
Initial data	368,824	6,595,279
Drop properties further than 300 meters from the boundary	178,767	3,011,054
Drop exempted properties	104,746	2,343,319
Drop properties on neighborhood borders	51,041	1,132,079
Drop non-residential properties	41,536	927,390
Drop lots that didn't have any property in 2010	41,536	626,076
Drop very large lots	33,500	509,486
Drop properties with no high tax side in 2010	25,097	382,229

TABLE D.2: SUBSAMPLING STEPS - TAX REFORM SAMPLE

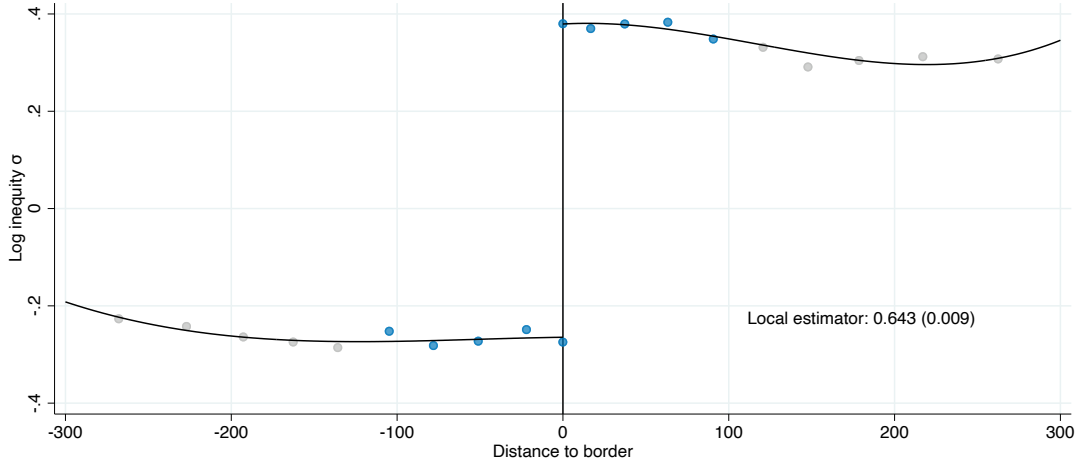
Subsampling step	N left in 2010	N left 04-18
Initial data	368,824	6,595,279
Drop properties further than 300 meters from the boundary	178,767	3,011,054
Drop exempted properties	104,746	2,343,319
Drop non-residential properties	84,869	1,915,943
Drop lots that didn't have any property in 2010	84,869	1,284,321
Drop very large CGLs	68,735	1,055,587
Drop properties with no high tax side in 2010	53,685	825,853

To test for the robustness of the results with respect to the subsampling steps, the next sub-sections show the main results from the paper using different sampling decisions.

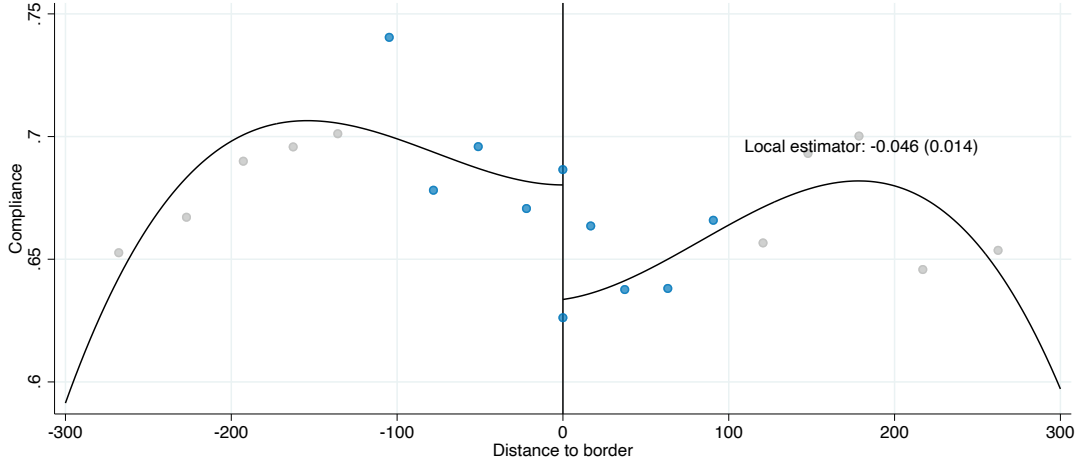
D.1 Sample including properties on neighborhood borders

In the main paper, we exclude properties on neighborhood borders for the cross-sectional analysis and include them in the analysis using variation from the tax reform. Herein, we also provide the cross-sectional analysis evidence including the properties on neighborhood borders.

FIGURE D.1: REDUCED FORM ESTIMATES



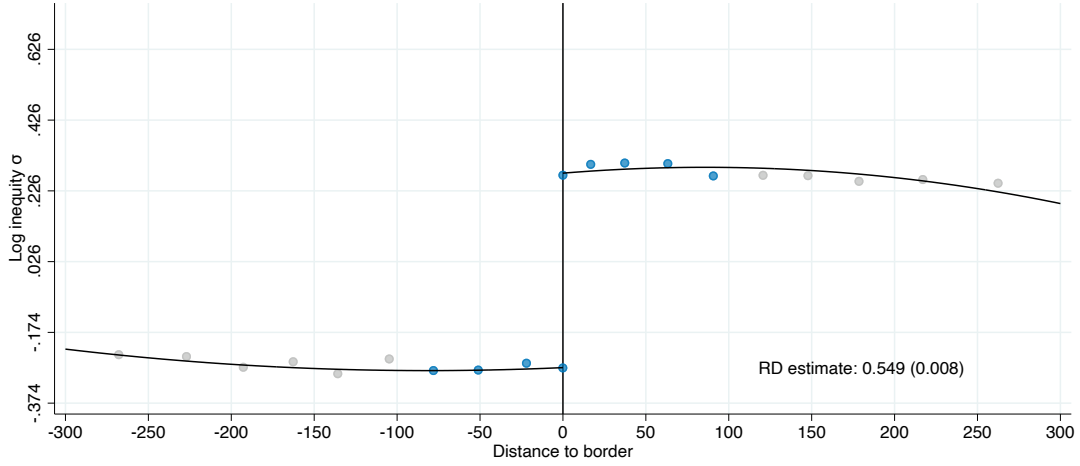
A: INEQUITY



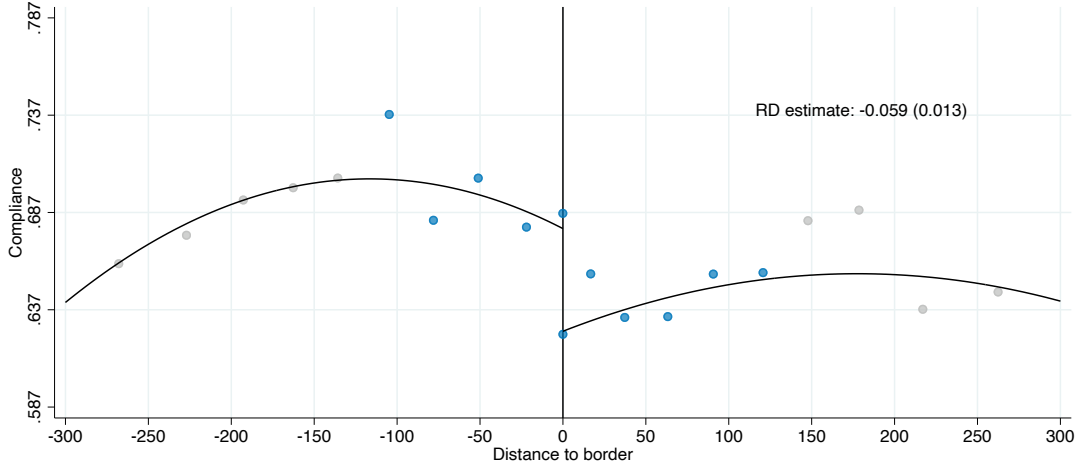
B: COMPLIANCE

Notes: The figure shows the overall change in compliance (Panel A) and inequity (Panel B) at tax sector boundaries discussed in section 4.1. Specifically, we show the results of estimating the following equation for compliance and inequity (10): y_i by taxpayer i : $c_i = \gamma_{s(i)} + f(d_i) + \beta_0 HTS_i + h(d_i) \times HTS_i + \varepsilon_i$ where $\gamma_{s(i)}$ are boundary-segment fixed effects, HTS_i is an indicator for being on the high-tax side of the boundary ($d_i > 0$); $f_0(d_i)$ and $f_1(d_i)$ control for distance to the boundary on the low- and high-tax sides of the boundary, respectively; and ε_i is the residual. Overlaid on the figure, we show the point estimate of the discontinuity in compliance estimated using local linear distance controls, the MSE-minimizing bandwidth, and triangular kernel weights in distance. The dots in the figure show the coefficients from estimating (10) with fixed effects for decile-spaced bins of distance, using the same triangular kernel weights but censoring them at their tenth percentile to give non-zero weights to distances outside the optimal bandwidth. The bins in the optimal bandwidth are shown in blue while those outside are shown in grey. The black line is a global cubic polynomial fit in the same way.

FIGURE D.2: RD CONTROLLING FOR TAU



A: SIGMA



B: COMPLIANCE

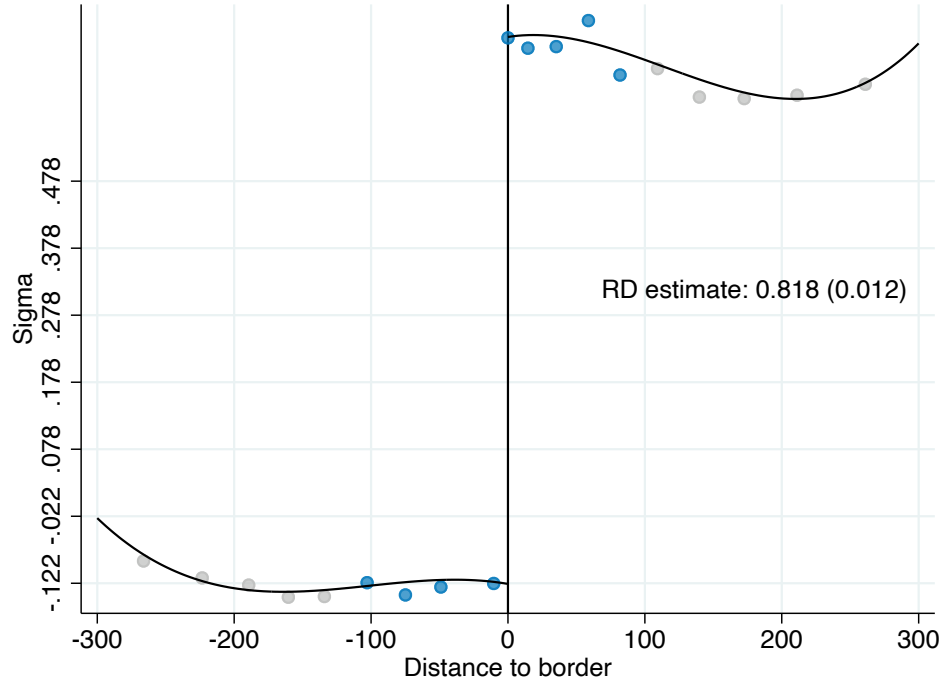
Notes: The figure shows the impact on inequity and compliance in the augmented BDD discussed in section ?? . Specifically, we show the results of estimation of equation (12): $y_i = \gamma_{s(i)} + g(\tau_i, e_i) + f(d_i) + \beta_0 HTS_i + h(d_i) \times HTS_i + \varepsilon_i$ using log-inequity σ as the outcome variable in panel A and compliance in panel B. $\gamma_{s(i)}$ are fixed effects for 500-meter segments along the boundaries to ensure we are comparing properties who are nearby each other; $g(\tau_i, e_i)$ are flexible controls for property i 's (log) tax liability τ_i and expansiveness e_i (our baseline estimates use τ splines and expansiveness deciles); $f(d_i)$ and $h(d_i)$ control flexibly for distance to the boundary on the low- and high-tax sides of the boundary respectively; and HTS_i is an indicator for properties on the high-tax side of the boundary ($d_i > 0$). Overlaid on the figure, we show the point estimate of the discontinuity in inequity estimated using local linear distance controls, the MSE-minimizing bandwidth, and triangular kernel weights in distance. The dots in the figure show the coefficients from estimating (12) with fixed effects for decile-spaced bins of distance, using the same triangular kernel weights but censoring them at their tenth percentile to give non-zero weights to distances outside the optimal bandwidth. The bins in the optimal bandwidth are shown in blue while those outside are shown in grey. The black line is a global cubic polynomial fit in the same way.

TABLE D.3: AUGMENTED BOUNDARY DISCONTINUITY DESIGN: COMPLIANCE EFFECTS

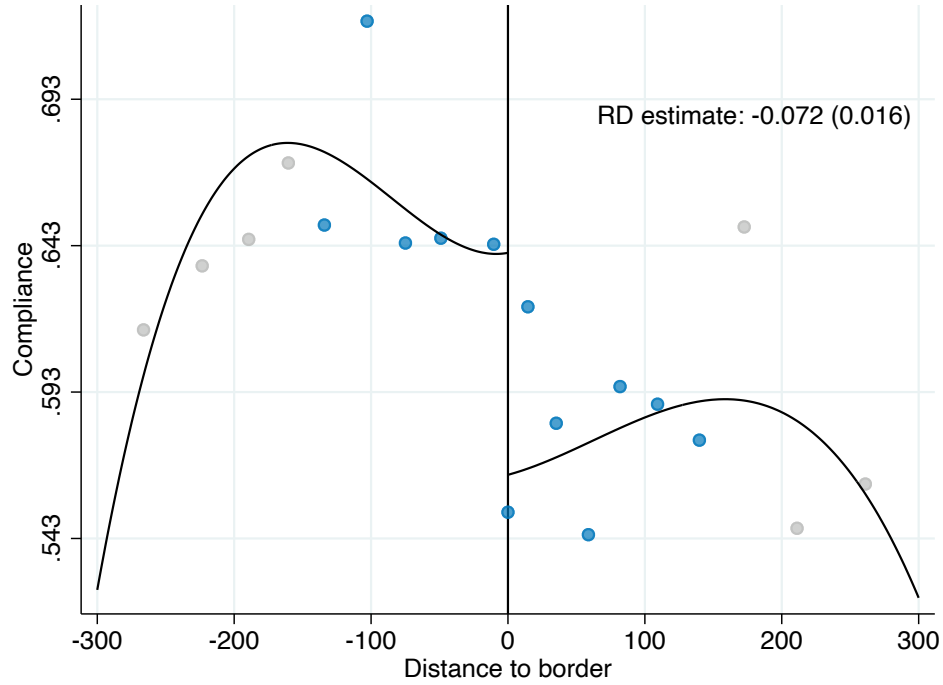
	(1)	(2)	(3)	(4)	(5)	(6)
RD_Estimate	-0.06*** (0.01)	-0.04** (0.01)	-0.06*** (0.01)	-0.06*** (0.01)	-4.56** (1.44)	-0.06*** (0.01)
R^2						
Distance controls	✓	✓	✓	✓	✓	✓
Segment FEs	✓	✓	✓	✓	✓	✓
τ splines	✓	✓	✓	✓		
exp dec FEs	✓		✓			✓
τ decile FEs					✓	✓
exp splines		✓		✓		
τ splines \times exp dec FEs			✓			
τ splines \times exp splines				✓		
τ dec FEs \times exp dec FEs						✓
First-stage	0.555	0.463	0.547	0.535	0.548	0.549
fscoef_se	(0.007)	(0.008)	(0.008)	(0.008)	(0.008)	(0.007)
Elasticity	-0.156	-0.116	-0.162	-0.156	-0.164	-0.166
elascoef_se	(0.035)	(0.044)	(0.037)	(0.041)	(0.037)	(0.037)
N	20827	20826	20827	20826	20827	20827

Notes: The table shows the results of estimating the augmented BDD equation (12): $c_i = \gamma_{s(i)} + g(\tau_i, e_i) + f(d_i) + \beta_0 HTS_i + h(d_i) \times HTS_i + \varepsilon_i$, where $\gamma_{s(i)}$ are fixed effects for 500-meter segments along the boundaries to ensure we are comparing properties who are nearby each other; $g(\tau_i, e_i)$ are flexible controls for property i 's (log) tax liability τ_i and expansiveness e_i ; $f(d_i)$ and $h(d_i)$ control flexibly for distance to the boundary on the low- and high-tax sides of the boundary respectively; and HTS_i is an indicator for properties on the high-tax side of the boundary ($d_i > 0$). The columns use a variety of approaches to controlling flexibly for the tax liability and expansiveness. In column (1) we control for cubic splines of the tax liability and fixed effects for deciles of expansiveness. In column (2) we replace the expansiveness deciles with cubic splines of expansiveness while column (3) replaces the splines of the tax liability with deciles. Columns (4)–(6) additionally interact the tax liability controls with the expansiveness controls.

FIGURE D.3: RD CONTROLLING FOR TAU - HIGH INEQUITY



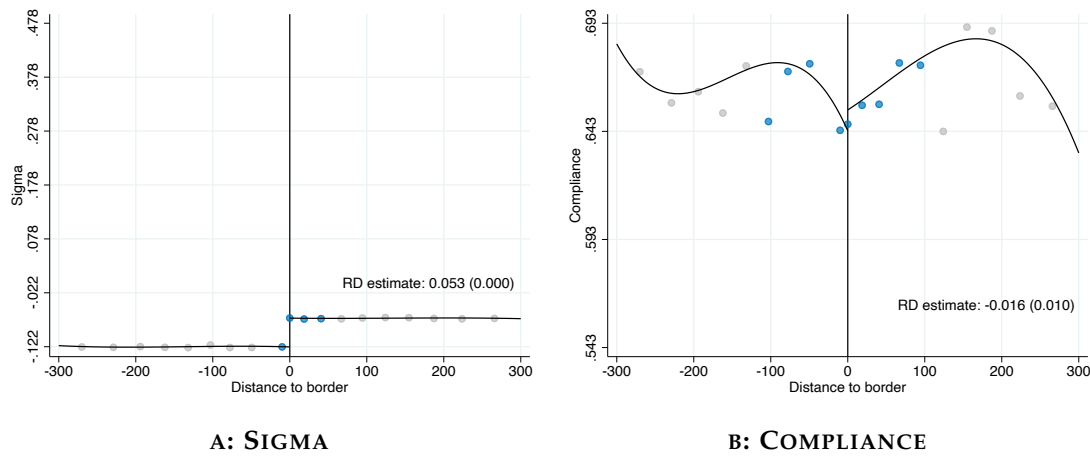
A: SIGMA



B: COMPLIANCE

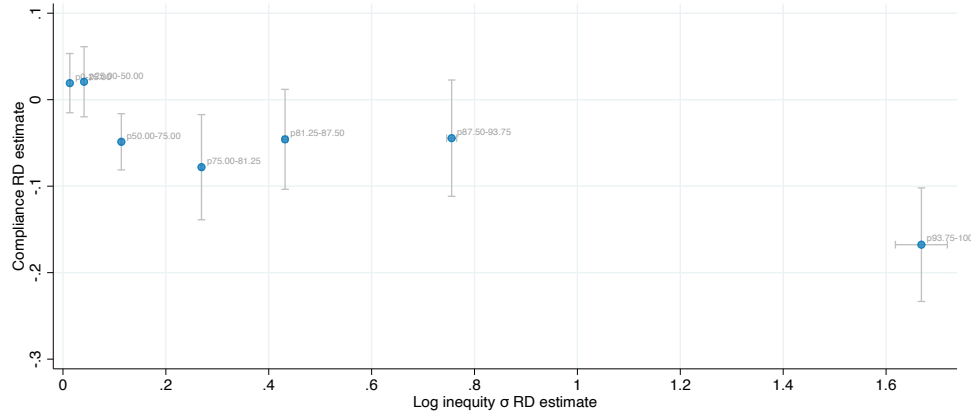
Notes: The figure shows the results of estimating equation (12): $y_i = \gamma_{s(i)} + g(\tau_i, e_i) + f(d_i) + \beta_0 HTS_i + h(d_i) \times HTS_i + \varepsilon_i$ with inequity as the outcome variable in panel A and compliance as the outcome in panel B. Terms are as defined in the notes to figure 6. Both panels show the estimates in the subsample of properties facing high inequity (defined as being in the top quartile of inequity).

FIGURE D.4: RD CONTROLLING FOR TAU - LOW INEQUITY



Notes: The figure shows the results of estimating equation (12): $y_i = \gamma_{s(i)} + g(\tau_i, e_i) + f(d_i) + \beta_0 HTS_i + h(d_i) \times HTS_i + \varepsilon_i$ with inequity as the outcome variable in panel A and compliance as the outcome in panel B. Terms are as defined in the notes to figure 6. Both panels show the estimates in the subsample of properties facing low inequity (defined as being in the bottom three quartile of inequity).

FIGURE D.5: HETEROGENEITY ANALYSIS



Notes: The figure shows the results of estimating equation (12): $c_i = \gamma_{s(i)} + g(\tau_i, e_i) + f(d_i) + \beta_0 HTS_i + h(d_i) \times HTS_i + \varepsilon_i$ where terms are as defined in the notes to figure 6. Each dot represents a different subsample. The three leftmost dots represent the three bottom quartiles of inequity. The remaining dots split the top quartile of inequity into 4 equally-sized subgroups. The vertical position and vertical grey bars of the dots display the estimated compliance effect and its 95% confidence interval. The horizontal position and horizontal grey bars of the dots display the estimated inequity change and its 95% confidence interval.

TABLE D.4: DIFFERENCE IN BOUNDARY DISCONTINUITY DESIGN: COMPLIANCE EFFECTS

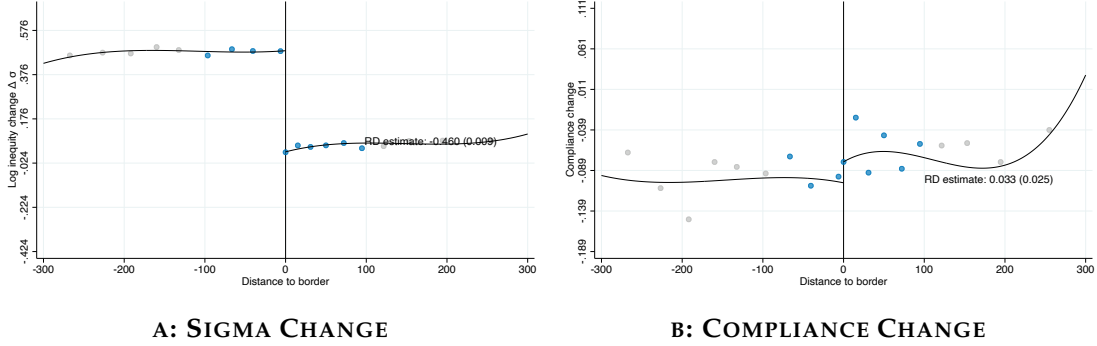
	(1)	(2)	(3)	(4)	(5)	(6)	(7)
1(high tax side)	0.00 (0.01)	0.00 (.)	0.00 (.)	0.00 (.)	0.08 (0.26)	0.07 (0.26)	0.00 (.)
1(high tax side) $\times \sigma $	-0.17*** (0.02)	-0.17*** (0.02)	-0.17*** (0.02)	-0.17*** (0.02)	-0.16*** (0.02)	-0.16*** (0.02)	-0.15*** (0.02)
R^2	0.108	0.108	0.107	0.108	0.110	0.109	0.111
Distance controls	✓	✓	✓	✓	✓	✓	✓
Segment fixed effects	✓	✓	✓	✓	✓	✓	✓
τ splines	✓	✓	✓	✗	✓	✓	✗
τ deciles	✗	✗	✗	✓	✗	✗	✓
Expansiveness splines	✗	✗	✓	✗	✗	✓	✗
Expansiveness deciles	✓	✓	✗	✓	✓	✗	✓
τ splines \times HTS	✗	✓	✓	✗	✓	✓	✗
τ deciles \times HTS	✗	✗	✗	✓	✗	✗	✓
τ splines \times exp deciles	✗	✗	✗	✗	✓	✗	✗
τ splines \times exp splines	✗	✗	✗	✗	✗	✓	✗
τ deciles \times exp deciles	✗	✗	✗	✗	✗	✗	✓
τ splines \times HTS \times exp deciles	✗	✗	✗	✗	✓	✗	✗
τ splines \times HTS \times exp splines	✗	✗	✗	✗	✗	✓	✗
τ deciles \times HTS \times exp deciles	✗	✗	✗	✗	✗	✗	✓
Elasticity	-0.263 0.025	-0.267 0.026	-0.273 0.026	-0.264 0.026	-0.245 0.028	-0.254 0.029	-0.238 0.028
N	53643	53643	53643	53643	53643	53643	53643

Notes: The table shows the results of estimation of equation (16): $c_i = \gamma_{s(i)} + g_0(\tau_i, e_i) + f(d_i) + HTS_i \times [\beta_0 + \eta \log(\sigma) + h(d_i) + g_1(\tau_i, e_i)] + \varepsilon_i$ where terms are as defined above in the notes to table 2. In column (1), we control for cubic splines of the tax liability and fixed effects for deciles of the expansiveness distribution. In column (2) we control separately for the tax liability and expansiveness on either side of the boundary. Column (3) replaces the expansiveness deciles with cubic splines in expansiveness while column (4) replaces the tax liability deciles with cubic splines. Columns (5)–(7) control for these separately on either side of the boundary.

D.2 Sample excluding properties on neighborhood borders

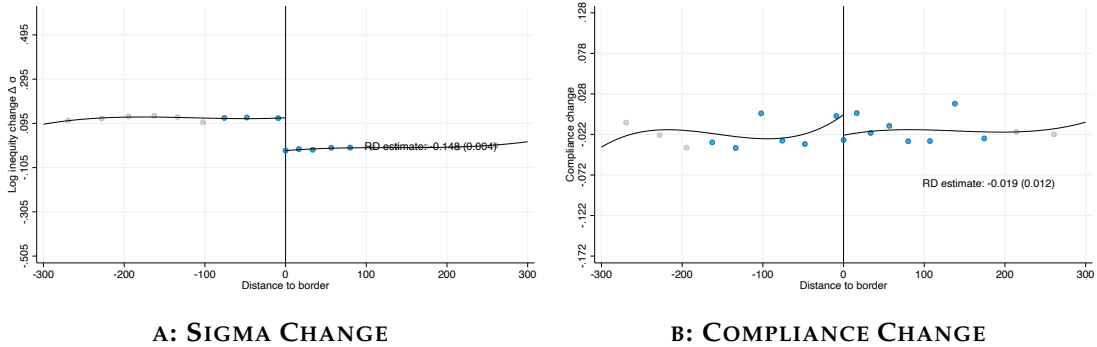
In the main paper, we exclude properties on neighborhood borders for the cross-sectional analysis, but include them in the analysis using variation from the tax reform. Herein, we also provide the evidence from the analysis using the reform for the sample that excludes properties on neighborhood borders.

FIGURE D.6: DYNAMIC BOUNDARY DISCONTINUITY DESIGN: REMOVAL OF INEQUITY



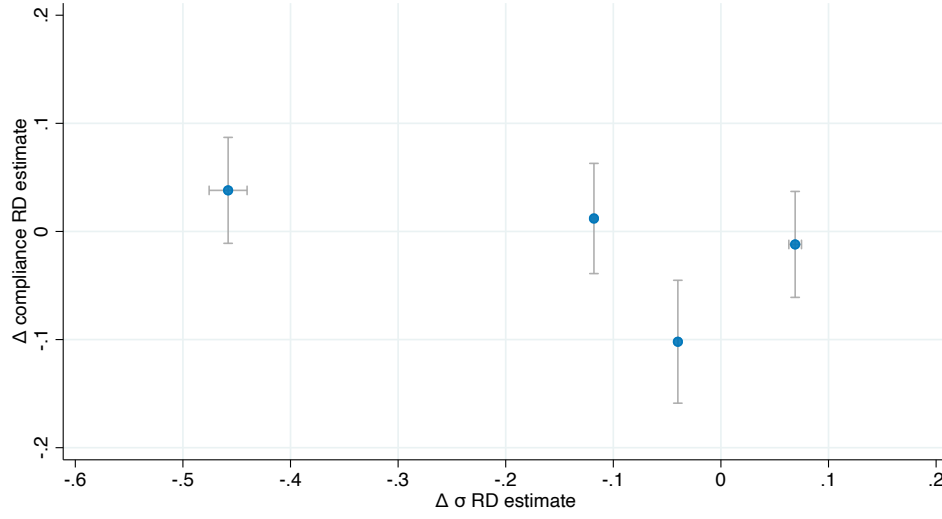
Notes: The figure shows the results of estimating equation (17) $\Delta y_i = \gamma_{s(i)} + g(\Delta \tau_i) + f_0(d_i) + HTS_i \times [\beta_0 + f_1(d_i)] + \varepsilon_i$ where the outcome variable is the change in inequity in panel A and the change in compliance in panel B; $\gamma_{s(i)}$ are boundary-segment fixed effects, HTS_i is an indicator for being on the high-tax side of the boundary ($d_i > 0$); $f_0(d_i)$ and $f_1(d_i)$ control for distance to the boundary on the low- and high-tax sides of the boundary, respectively; and ε_i is the residual. $g(\Delta \tau_i)$ controls flexibly for changes in log tax liability, τ_i . Specifically, we control for splines of $\Delta \tau_i$. Both panels shows the estimates in the subsample of properties for whom the reform meaningfully reduced inequity.

FIGURE D.7: DYNAMIC BOUNDARY DISCONTINUITY DESIGN: NO IMPROVEMENT



Notes: The figure shows the results of estimating equation (17) $\Delta y_i = \gamma_{s(i)} + g(\Delta \tau_i) + f_0(d_i) + HTS_i \times [\beta_0 + f_1(d_i)] + \varepsilon_i$ where the outcome variable is the change in inequity in panel A and the change in compliance in panel B; $\gamma_{s(i)}$ are boundary-segment fixed effects, HTS_i is an indicator for being on the high-tax side of the boundary ($d_i > 0$); $f_0(d_i)$ and $f_1(d_i)$ control for distance to the boundary on the low- and high-tax sides of the boundary, respectively; and ε_i is the residual. $g(\Delta \tau_i)$ controls flexibly for changes in log tax liability, τ_i . Specifically, we control for splines of $\Delta \tau_i$. Both panels shows the estimates in the subsample of properties for whom the reform did not meaningfully reduced inequity.

FIGURE D.8: DYNAMIC BOUNDARY DISCONTINUITY DESIGN: HETEROGENEITY BY IN-EQUITY REDUCTION



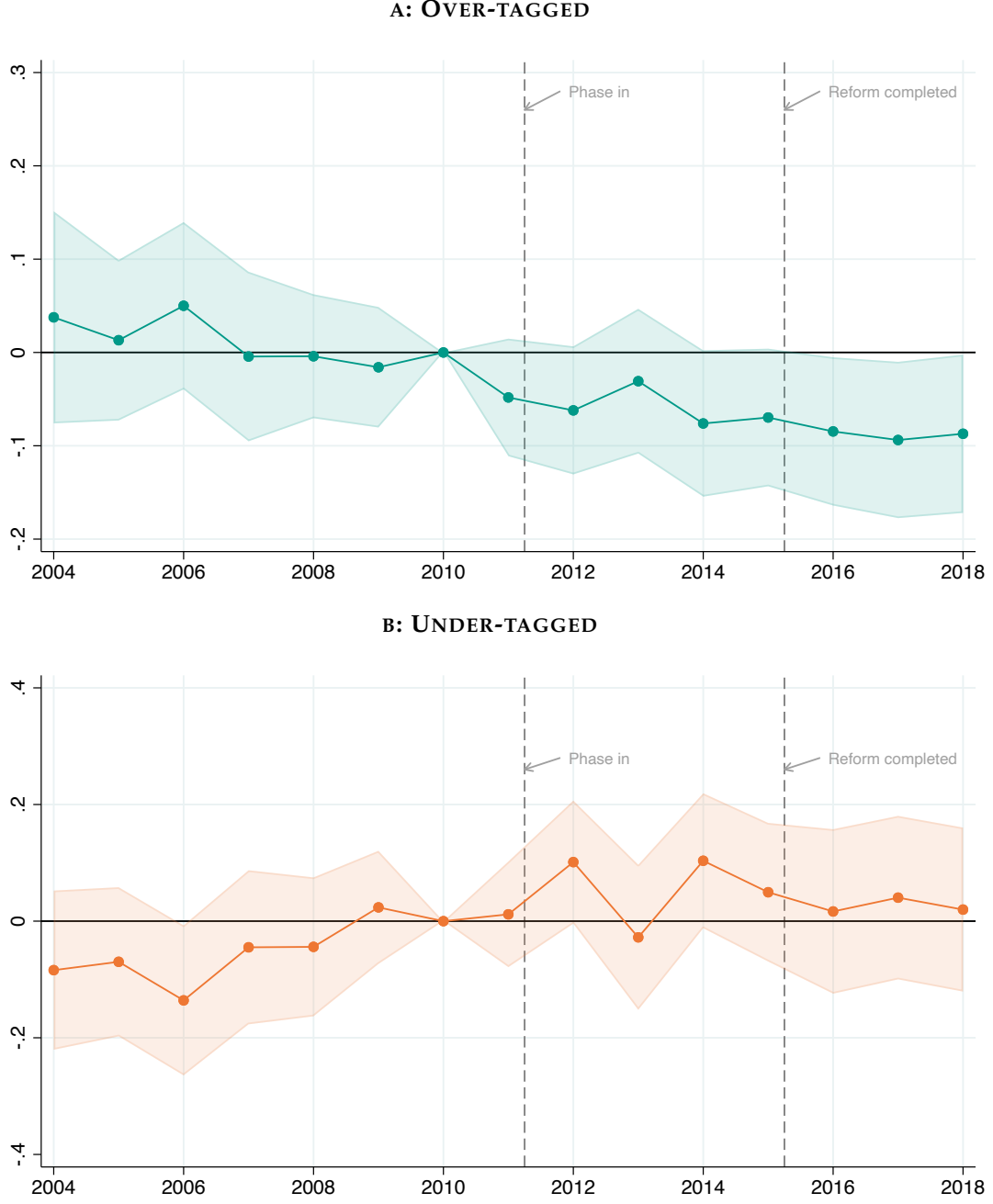
Notes: The figure shows the results of estimating equation (17) $\Delta c_i = \gamma_{s(i)} + g(\Delta \tau_i) + f_0(d_i) + HTS_i \times [\beta_0 + f_1(d_i)] + \varepsilon_i$ where $\gamma_{s(i)}$ are boundary-segment fixed effects, HTS_i is an indicator for being on the high-tax side of the boundary ($d_i > 0$); $f_0(d_i)$ and $f_1(d_i)$ control for distance to the boundary on the low- and high-tax sides of the boundary, respectively; and ε_i is the residual. $g(\Delta \tau_i)$ controls flexibly for changes in log tax liability, τ_i . Specifically, we control for splines of τ_i . We estimate (17) separately in four subsamples defined by quartiles of their change in inequity. The vertical coordinate of each dot and the vertical gray bars show the estimated impact on compliance and its 95% confidence interval. The horizontal coordinate of each dot and the horizontal gray bars show the estimated impact on inequity and its 95% confidence interval.

TABLE D.5: DYNAMIC DIFFERENCE IN BOUNDARY DISCONTINUITY DESIGN

	(1)	(2)	(3)	(4)
	Δ Compliance	Δ Compliance	Δ Compliance	Δ Compliance
1(high tax side)	-0.013 (0.012)	-0.017 (0.033)	-0.010 (0.032)	-0.010 (0.024)
1(high tax side) \times change in σ	-0.102*** (0.039)	-0.108*** (0.041)	-0.073* (0.044)	-0.112*** (0.040)
Elasticity implied	-0.159	-0.168	-0.114	-0.174
Elasticity SE	0.060	0.063	0.069	0.062
Distance controls	✓	✓	✓	✓
Segment FEs	✓	✓	✓	✓
τ splines	✓	✓	✓	✗
Expansiveness deciles	✓	✓	✗	✓
Interaction with HTS	✗	✓	✓	✓
τ splines \times expansiveness deciles	✗	✓	✗	✗
Expansiveness splines	✗	✗	✓	✗
τ splines \times expansiveness splines	✗	✗	✓	✗
τ deciles	✗	✗	✗	✓
τ deciles \times expansiveness deciles	✗	✗	✗	✓

Notes: This table shows the results of estimating equation (18) discussed in section 6.2: $\Delta c_i = \gamma_{s(u)} + g_0(\Delta \tau_i, e_i) + f_0(d_i) + HTS_i \times [\delta_0 + \eta \Delta \log(\sigma_i) + g_1(\Delta \tau_i, e_i) + f_1(d_i)] + \varepsilon_i$ where all terms are as defined above in the notes to table 2. Column (1) controls for cubic splines of the tax liability and fixed effects for deciles of the expansiveness distribution. Column (2) adds interactions between these controls and estimates them separately on either side of the boundary. Column (3) replaces the expansiveness deciles with splines, while column (4) replaces the tax liability splines with deciles of the tax liability distribution.

FIGURE D.9: DIFFERENCE IN DIFFERENCE ESTIMATES OF OVERTAGGING AND UNDERTAGGING EFFECTS

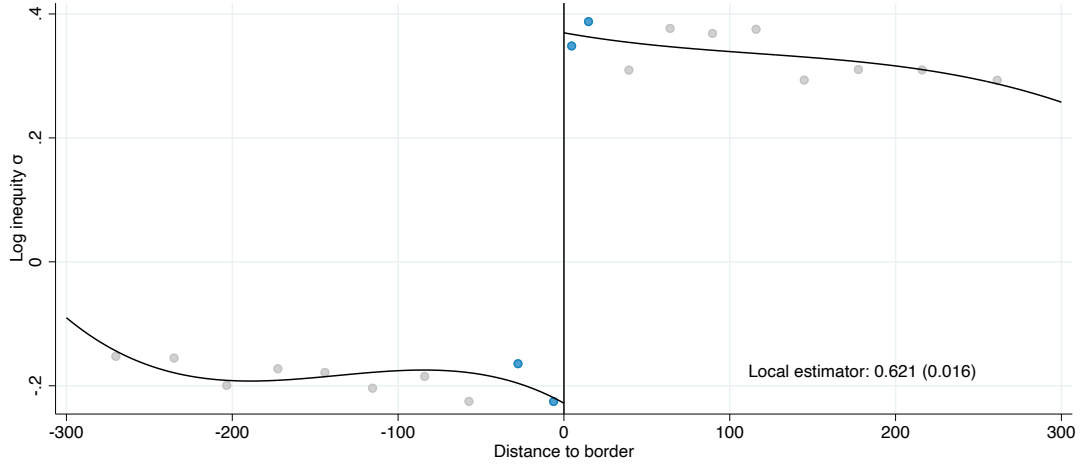


Notes: The figure shows the results of the estimation of equation (20) as discussed in section 6.3: $c_{iy} = \alpha_i + \gamma_{s(i)y} + \sum_{j \neq 2010} D_{jy} \times [f_{0j}(d_i) + \beta_{0j} \Delta \tau_i + \eta_{0j} \Delta \sigma_i + HTS_i \times (\delta_j + f_{1j}(d_i) + \beta_{1j} \Delta \tau_i + \eta_{1j} \Delta \sigma_i)] + \varepsilon_{iy}$, where $\gamma_{s(i)y}$ are segment-year fixed effects, $D_{jy} \equiv 1[y = j]$ are year dummies, and we include year-specific distance controls $f_{0j}(d_i)$ and $f_{1j}(d_i)$; and year-specific controls for property i 's tax liability change due to the reform. Panel A shows the estimated η_{1j} coefficients along with their 95% confidence intervals. Panel B shows the estimated η_{0j} coefficients along with their 95% confidence intervals.

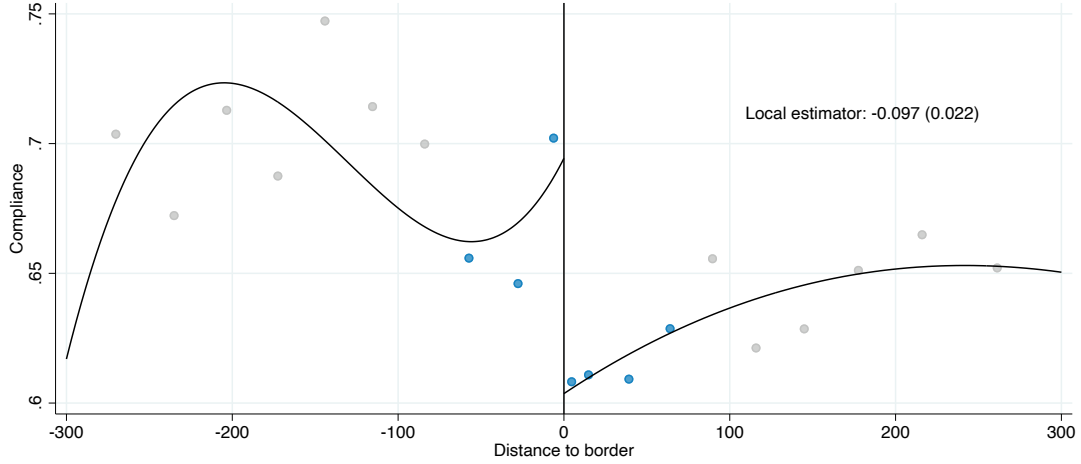
D.3 Sample with non-residential properties

In the main paper, we exclude non-residential properties. Herein, we also provide the evidence including the non-residential properties.

FIGURE D.10: REDUCED FORM ESTIMATES



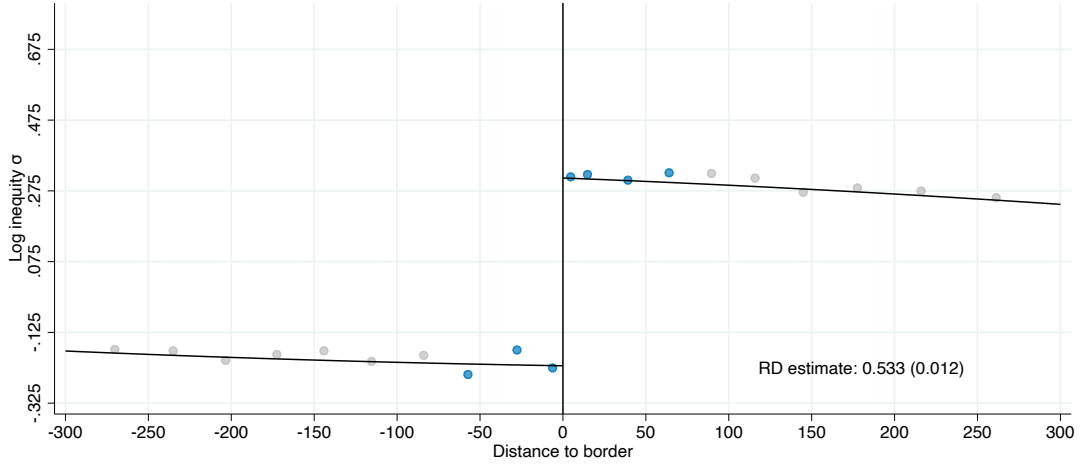
A: SIGMA



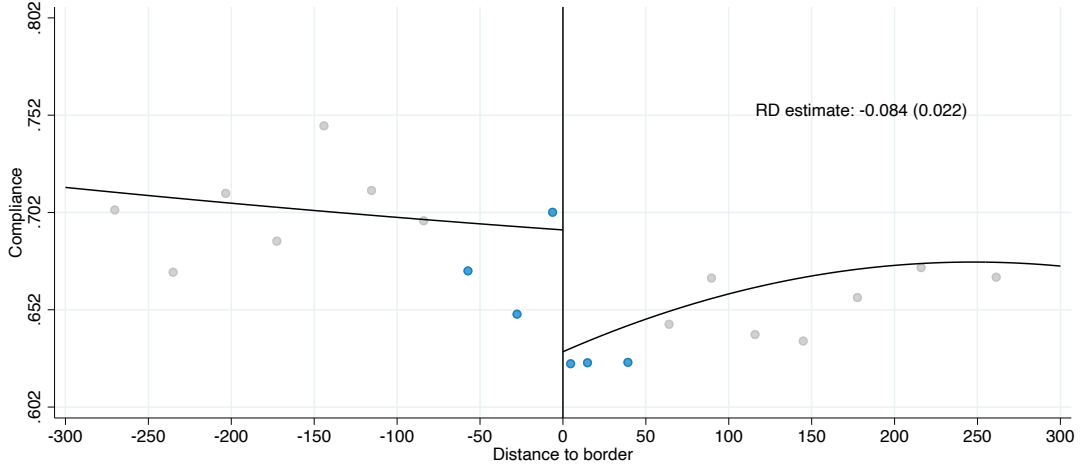
B: COMPLIANCE

Notes: The figure shows the overall change in compliance (Panel A) and inequity (Panel B) at tax sector boundaries discussed in section 4.1. Specifically, we show the results of estimating the following equation for compliance and inequity (10): y_i by taxpayer i : $c_i = \gamma_{s(i)} + f(d_i) + \beta_0 HTS_i + h(d_i) \times HTS_i + \varepsilon_i$ where $\gamma_{s(i)}$ are boundary-segment fixed effects, HTS_i is an indicator for being on the high-tax side of the boundary ($d_i > 0$); $f_0(d_i)$ and $f_1(d_i)$ control for distance to the boundary on the low- and high-tax sides of the boundary, respectively; and ε_i is the residual. Overlaid on the figure, we show the point estimate of the discontinuity in compliance estimated using local linear distance controls, the MSE-minimizing bandwidth, and triangular kernel weights in distance. The dots in the figure show the coefficients from estimating (10) with fixed effects for decile-spaced bins of distance, using the same triangular kernel weights but censoring them at their tenth percentile to give non-zero weights to distances outside the optimal bandwidth. The bins in the optimal bandwidth are shown in blue while those outside are shown in grey. The black line is a global cubic polynomial fit in the same way.

FIGURE D.11: RD CONTROLLING FOR TAU



A: SIGMA



B: COMPLIANCE

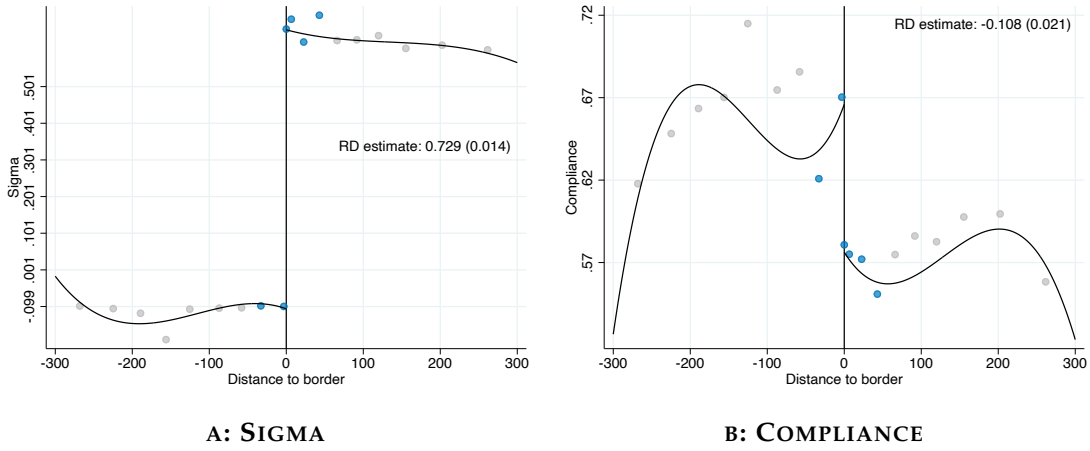
Notes: The figure shows the impact on inequity and compliance in the augmented BDD discussed in section ?? . Specifically, we show the results of estimation of equation (12): $y_i = \gamma_{s(i)} + g(\tau_i, e_i) + f(d_i) + \beta_0 HTS_i + h(d_i) \times HTS_i + \varepsilon_i$ using log-inequity σ as the outcome variable in panel A and compliance in panel B. $\gamma_{s(i)}$ are fixed effects for 500-meter segments along the boundaries to ensure we are comparing properties who are nearby each other; $g(\tau_i, e_i)$ are flexible controls for property i 's (log) tax liability τ_i and expansiveness e_i (our baseline estimates use τ splines and expansiveness deciles); $f(d_i)$ and $h(d_i)$ control flexibly for distance to the boundary on the low- and high-tax sides of the boundary respectively; and HTS_i is an indicator for properties on the high-tax side of the boundary ($d_i > 0$). Overlaid on the figure, we show the point estimate of the discontinuity in inequity estimated using local linear distance controls, the MSE-minimizing bandwidth, and triangular kernel weights in distance. The dots in the figure show the coefficients from estimating (12) with fixed effects for decile-spaced bins of distance, using the same triangular kernel weights but censoring them at their tenth percentile to give non-zero weights to distances outside the optimal bandwidth. The bins in the optimal bandwidth are shown in blue while those outside are shown in grey. The black line is a global cubic polynomial fit in the same way.

TABLE D.6: AUGMENTED BOUNDARY DISCONTINUITY DESIGN: COMPLIANCE EFFECTS

	(1)	(2)	(3)	(4)	(5)	(6)
RD_Estimate	-0.08*** (0.02)	-0.08*** (0.01)	-0.08*** (0.01)	-0.08*** (0.02)	-0.08*** (0.01)	-0.08*** (0.01)
R^2						
Distance controls	✓	✓	✓	✓	✓	✓
Segment FEs	✓	✓	✓	✓	✓	✓
τ splines	✓	✓	✓	✓		
exp dec FEs	✓		✓			✓
τ decile FEs					✓	✓
exp splines		✓		✓		
τ splines \times exp dec FEs			✓			
τ splines \times exp splines				✓		
τ dec FEs \times exp dec FEs						✓
First-stage	0.555	0.542	0.557	0.542	0.555	0.556
fscoef_se	(0.008)	(0.009)	(0.008)	(0.009)	(0.008)	(0.008)
Elasticity	-0.203	-0.199	-0.195	-0.203	-0.196	-0.185
elascoef_se	(0.037)	(0.042)	(0.037)	(0.042)	(0.036)	(0.036)
N	12055	12054	12055	12054	12055	12055

Notes: The table shows the results of estimating the augmented BDD equation (12): $c_i = \gamma_{s(i)} + g(\tau_i, e_i) + f(d_i) + \beta_0 HTS_i + h(d_i) \times HTS_i + \varepsilon_i$, where $\gamma_{s(i)}$ are fixed effects for 500-meter segments along the boundaries to ensure we are comparing properties who are nearby each other; $g(\tau_i, e_i)$ are flexible controls for property i 's (log) tax liability τ_i and expansiveness e_i ; $f(d_i)$ and $h(d_i)$ control flexibly for distance to the boundary on the low- and high-tax sides of the boundary respectively; and HTS_i is an indicator for properties on the high-tax side of the boundary ($d_i > 0$). The columns use a variety of approaches to controlling flexibly for the tax liability and expansiveness. In column (1) we control for cubic splines of the tax liability and fixed effects for deciles of expansiveness. In column (2) we replace the expansiveness deciles with cubic splines of expansiveness while column (3) replaces the splines of the tax liability with deciles. Columns (4)–(6) additionally interact the tax liability controls with the expansiveness controls.

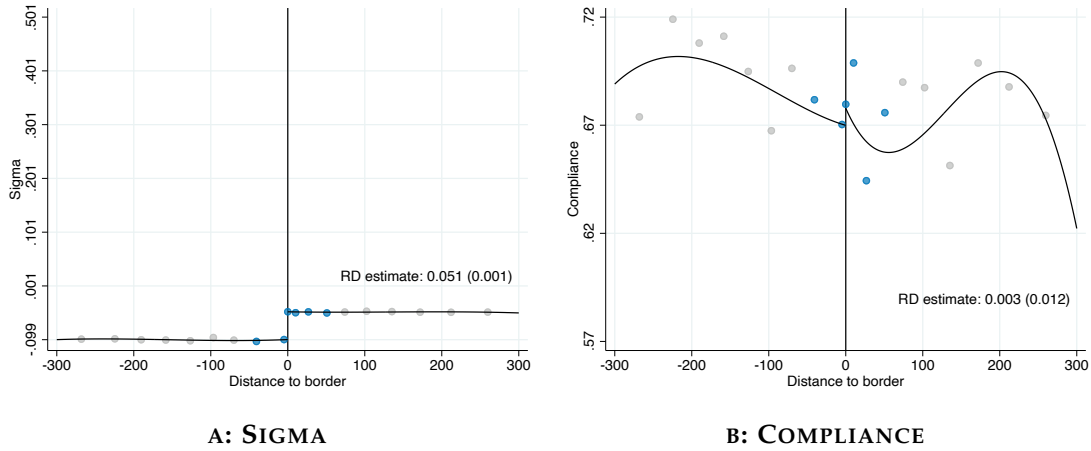
FIGURE D.12: RD CONTROLLING FOR TAU - HIGH INEQUITY



Notes:

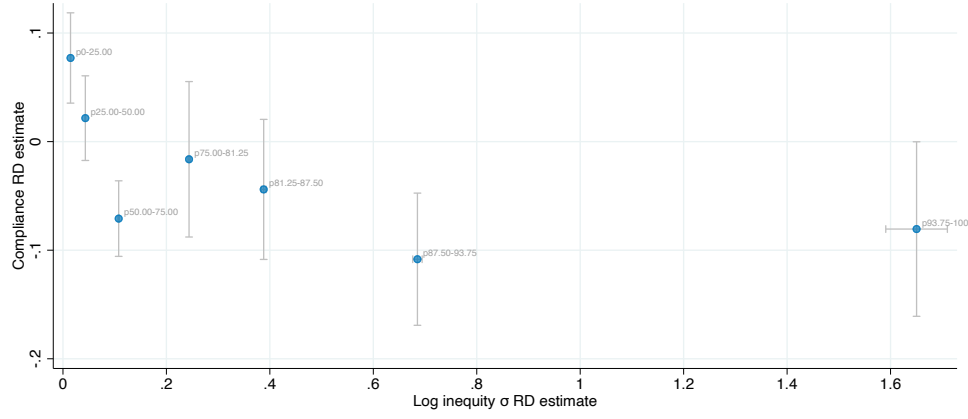
The figure shows the results of estimating equation (12): $y_i = \gamma_{s(i)} + g(\tau_i, e_i) + f(d_i) + \beta_0 HTS_i + h(d_i) \times HTS_i + \varepsilon_i$ with inequity as the outcome variable in panel A and compliance as the outcome in panel B. Terms are as defined in the notes to figure 6. Both panels show the estimates in the subsample of properties facing high inequity (defined as being in the top quartile of inequity).

FIGURE D.13: RD CONTROLLING FOR TAU - LOW INEQUITY



Notes: The figure shows the results of estimating equation (12): $y_i = \gamma_{s(i)} + g(\tau_i, e_i) + f(d_i) + \beta_0 HTS_i + h(d_i) \times HTS_i + \varepsilon_i$ with inequity as the outcome variable in panel A and compliance as the outcome in panel B. Terms are as defined in the notes to figure 6. Both panels show the estimates in the subsample of properties facing low inequity (defined as being in the bottom three quartile of inequity).

FIGURE D.14: HETEROGENEITY ANALYSIS



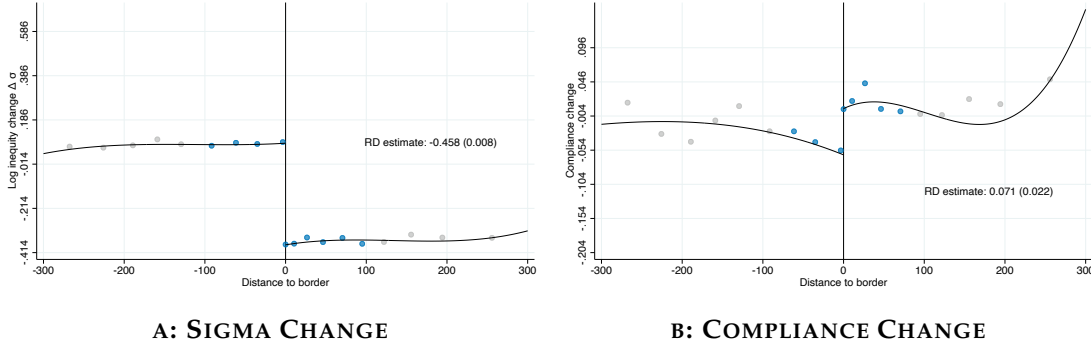
Notes: The figure shows the results of estimating equation (12): $c_i = \gamma_{s(i)} + g(\tau_i, e_i) + f(d_i) + \beta_0 HTS_i + h(d_i) \times HTS_i + \varepsilon_i$ where terms are as defined in the notes to figure 6. Each dot represents a different subsample. The three leftmost dots represent the three bottom quartiles of inequity. The remaining dots split the top quartile of inequity into 4 equally-sized subgroups. The vertical position and vertical grey bars of the dots display the estimated compliance effect and its 95% confidence interval. The horizontal position and horizontal grey bars of the dots display the estimated inequity change and its 95% confidence interval.

TABLE D.7: DIFFERENCE IN BOUNDARY DISCONTINUITY DESIGN: COMPLIANCE EFFECTS

	(1)	(2)	(3)	(4)	(5)	(6)	(7)
1(high tax side)	-0.01 (0.01)	0.00 (.)	0.00 (.)	0.00 (.)	0.49 (0.30)	0.42 (0.30)	0.00 (.)
1(high tax side) $\times \sigma $	-0.16*** (0.02)	-0.16*** (0.02)	-0.17*** (0.02)	-0.16*** (0.02)	-0.14*** (0.02)	-0.15*** (0.02)	-0.14*** (0.02)
R^2	0.134	0.134	0.134	0.134	0.137	0.136	0.141
Distance controls	✓	✓	✓	✓	✓	✓	✓
Segment fixed effects	✓	✓	✓	✓	✓	✓	✓
τ splines	✓	✓	✓	✗	✓	✓	✗
τ deciles	✗	✗	✗	✓	✗	✗	✓
Expansiveness splines	✗	✗	✓	✗	✗	✓	✗
Expansiveness deciles	✓	✓	✗	✓	✓	✗	✓
τ splines \times HTS	✗	✓	✓	✗	✓	✓	✗
τ deciles \times HTS	✗	✗	✗	✓	✗	✗	✓
τ splines \times exp deciles	✗	✗	✗	✗	✓	✗	✗
τ splines \times exp splines	✗	✗	✗	✗	✗	✓	✗
τ deciles \times exp deciles	✗	✗	✗	✗	✗	✗	✓
τ splines \times HTS \times exp deciles	✗	✗	✗	✗	✓	✗	✗
τ splines \times HTS \times exp splines	✗	✗	✗	✗	✗	✓	✗
τ deciles \times HTS \times exp deciles	✗	✗	✗	✗	✗	✗	✓
Elasticity	-0.244 0.031	-0.243 0.031	-0.252 0.031	-0.242 0.031	-0.214 0.034	-0.232 0.035	-0.211 0.034
N	31587	31587	31587	31587	31587	31587	31587

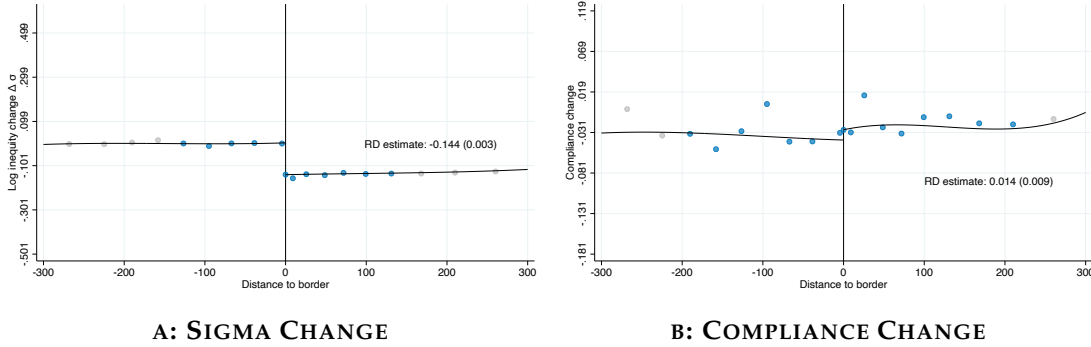
Notes: The table shows the results of estimation of equation (16): $c_i = \gamma_{s(i)} + g_0(\tau_i, e_i) + f(d_i) + HTS_i \times [\beta_0 + \eta \log(\sigma) + h(d_i) + g_1(\tau_i, e_i)] + \varepsilon_i$ where terms are as defined above in the notes to table 2. In column (1), we control for cubic splines of the tax liability and fixed effects for deciles of the expansiveness distribution. In column (2) we control separately for the tax liability and expansiveness on either side of the boundary. Column (3) replaces the expansiveness deciles with cubic splines in expansiveness while column (4) replaces the tax liability deciles with cubic splines. Columns (5)–(7) control for these separately on either side of the boundary.

FIGURE D.15: DYNAMIC BOUNDARY DISCONTINUITY DESIGN: REMOVAL OF INEQUITY



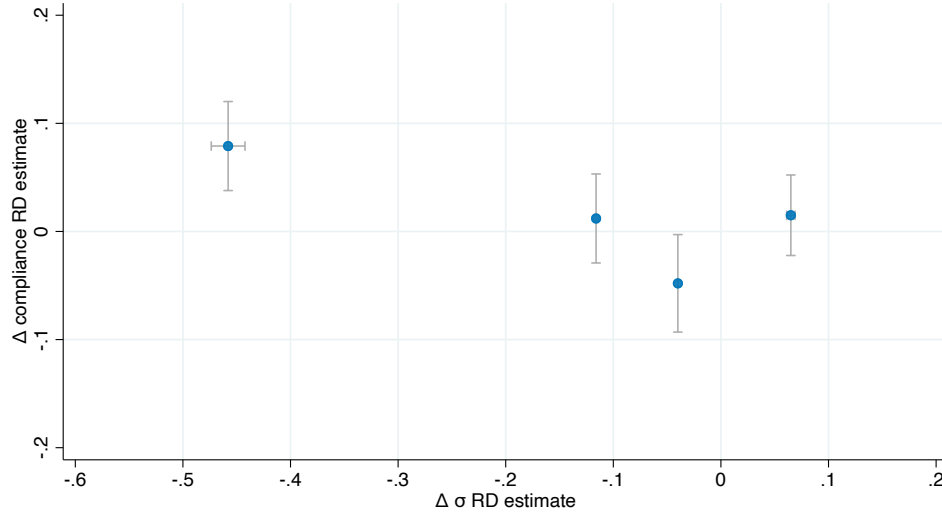
Notes: The figure shows the results of estimating equation (17) $\Delta y_i = \gamma_{s(i)} + g(\Delta \tau_i) + f_0(d_i) + HTS_i \times [\beta_0 + f_1(d_i)] + \varepsilon_i$ where the outcome variable is the change in inequity in panel A and the change in compliance in panel B; $\gamma_{s(i)}$ are boundary-segment fixed effects, HTS_i is an indicator for being on the high-tax side of the boundary ($d_i > 0$); $f_0(d_i)$ and $f_1(d_i)$ control for distance to the boundary on the low- and high-tax sides of the boundary, respectively; and ε_i is the residual. $g(\Delta \tau_i)$ controls flexibly for changes in log tax liability, τ_i . Specifically, we control for splines of $\Delta \tau_i$. Both panels shows the estimates in the subsample of properties for whom the reform meaningfully reduced inequity.

FIGURE D.16: DYNAMIC BOUNDARY DISCONTINUITY DESIGN: NO IMPROVEMENT



Notes: The figure shows the results of estimating equation (17) $\Delta y_i = \gamma_{s(i)} + g(\Delta \tau_i) + f_0(d_i) + HTS_i \times [\beta_0 + f_1(d_i)] + \varepsilon_i$ where the outcome variable is the change in inequity in panel A and the change in compliance in panel B; $\gamma_{s(i)}$ are boundary-segment fixed effects, HTS_i is an indicator for being on the high-tax side of the boundary ($d_i > 0$); $f_0(d_i)$ and $f_1(d_i)$ control for distance to the boundary on the low- and high-tax sides of the boundary, respectively; and ε_i is the residual. $g(\Delta \tau_i)$ controls flexibly for changes in log tax liability, τ_i . Specifically, we control for splines of $\Delta \tau_i$. Both panels shows the estimates in the subsample of properties for whom the reform did not meaningfully reduced inequity.

FIGURE D.17: DYNAMIC BOUNDARY DISCONTINUITY DESIGN: HETEROGENEITY BY IN-EQUITY REDUCTION



Notes: The figure shows the results of estimating equation (17) $\Delta c_i = \gamma_{s(i)} + g(\Delta \tau_i) + f_0(d_i) + HTS_i \times [\beta_0 + f_1(d_i)] + \varepsilon_i$ where $\gamma_{s(i)}$ are boundary-segment fixed effects, HTS_i is an indicator for being on the high-tax side of the boundary ($d_i > 0$); $f_0(d_i)$ and $f_1(d_i)$ control for distance to the boundary on the low- and high-tax sides of the boundary, respectively; and ε_i is the residual. $g(\Delta \tau_i)$ controls flexibly for changes in log tax liability, τ_i . Specifically, we control for splines of τ_i . We estimate (17) separately in four subsamples defined by quartiles of their change in inequity. The vertical coordinate of each dot and the vertical gray bars show the estimated impact on compliance and its 95% confidence interval. The horizontal coordinate of each dot and the horizontal gray bars show the estimated impact on inequity and its 95% confidence interval.

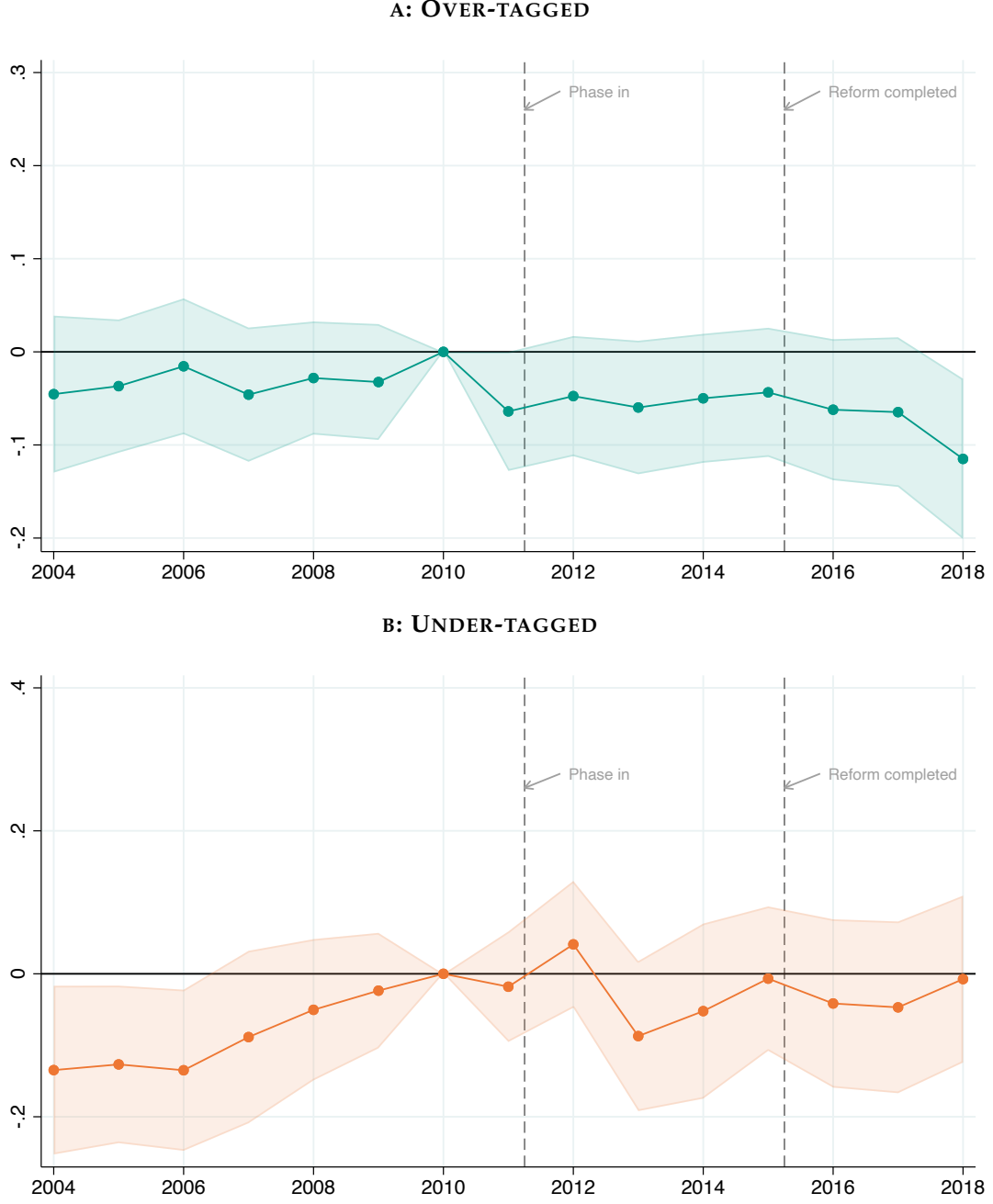
TABLE D.8: DYNAMIC DIFFERENCE IN BOUNDARY DISCONTINUITY DESIGN

	(1)	(2)	(3)	(4)
	Δ Compliance	Δ Compliance	Δ Compliance	Δ Compliance
1(high tax side)	0.006 (0.010)	0.007 (0.027)	0.009 (0.027)	-0.001 (0.021)
1(high tax side) X change in σ	-0.086*** (0.033)	-0.088** (0.035)	-0.083** (0.038)	-0.092*** (0.034)
Elasticity implied	-0.129	-0.132	-0.125	-0.138
Elasticity SE	0.050	0.053	0.056	0.052
Distance controls	✓	✓	✓	✓
Segment FEs	✓	✓	✓	✓
τ splines	✓	✓	✓	✗
Expansiveness deciles	✓	✓	✗	✓
Interaction with HTS	✗	✓	✓	✓
τ splines \times expansiveness deciles	✗	✓	✗	✗
Expansiveness splines	✗	✗	✓	✗
τ splines \times expansiveness splines	✗	✗	✓	✗
τ deciles	✗	✗	✗	✓
τ deciles \times expansiveness deciles	✗	✗	✗	✓

Notes: This table shows the results of estimating equation (18) discussed in section 6.2:

$\Delta c_i = \gamma_{s(u)} + g_0(\Delta \tau_i, e_i) + f_0(d_i) + HTS_i \times [\delta_0 + \eta \Delta \log(\sigma_i) + g_1(\Delta \tau_i, e_i) + f_1(d_i)] + \varepsilon_i$ where all terms are as defined above in the notes to table 2. Column (1) controls for cubic splines of the tax liability and fixed effects for deciles of the expansiveness distribution. Column (2) adds interactions between these controls and estimates them separately on either side of the boundary. Column (3) replaces the expansiveness deciles with splines, while column (4) replaces the tax liability splines with deciles of the tax liability distribution.

FIGURE D.18: DIFFERENCE IN DIFFERENCE ESTIMATES OF OVERTAGGING AND UNDERTAGGING EFFECTS

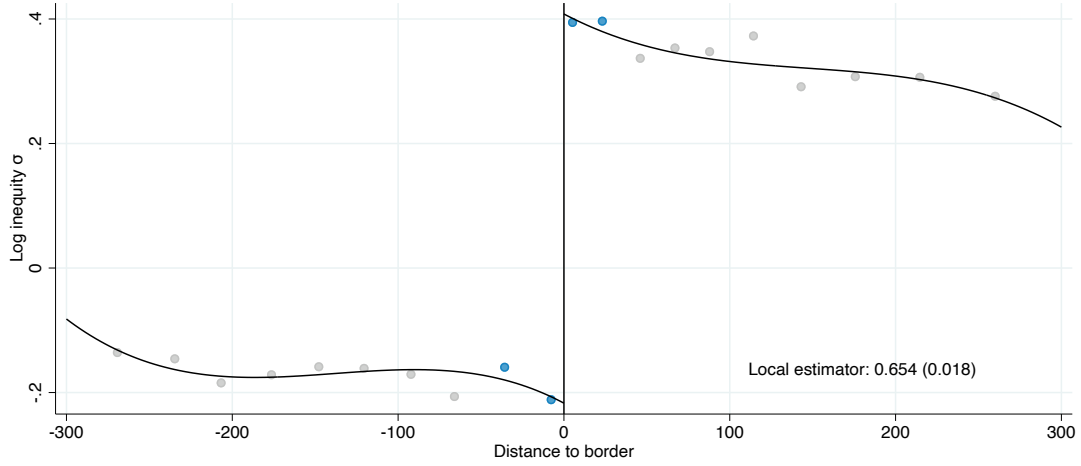


Notes: The figure shows the results of the estimation of equation (20) as discussed in section 6.3: $c_{iy} = \alpha_i + \gamma_{s(i)y} + \sum_{j \neq 2010} D_{jy} \times [f_{0j}(d_i) + \beta_{0j} \Delta \tau_i + \eta_{0j} \Delta \sigma_i + HTS_i \times (\delta_j + f_{1j}(d_i) + \beta_{1j} \Delta \tau_i + \eta_{1j} \Delta \sigma_i)] + \varepsilon_{iy}$, where $\gamma_{s(i)y}$ are segment-year fixed effects, $D_{jy} \equiv 1[y = j]$ are year dummies, and we include year-specific distance controls $f_{0j}(d_i)$ and $f_{1j}(d_i)$; and year-specific controls for property i 's tax liability change due to the reform. Panel A shows the estimated η_{1j} coefficients along with their 95% confidence intervals. Panel B shows the estimated η_{0j} coefficients along with their 95% confidence intervals.

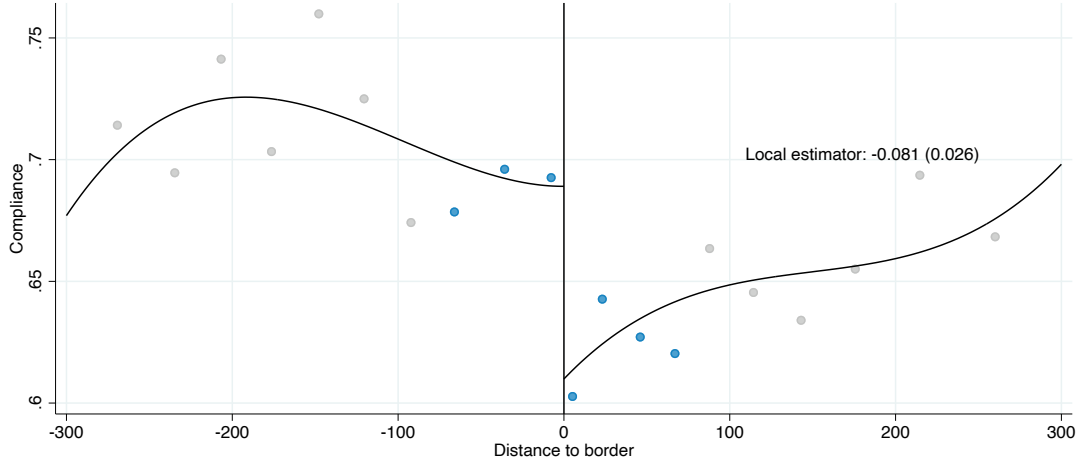
D.4 Relaxed “large lots” drop: Drop the top 0.1% in terms of land area

In the main paper, we exclude “very large” lots because they introduce measurement error. We define “very large” lots as the top 0.5% in terms of land area. Here, we provide evidence with a sample that excludes only the top 0.1% of lots in terms of land area.

FIGURE D.19: REDUCED FORM ESTIMATES



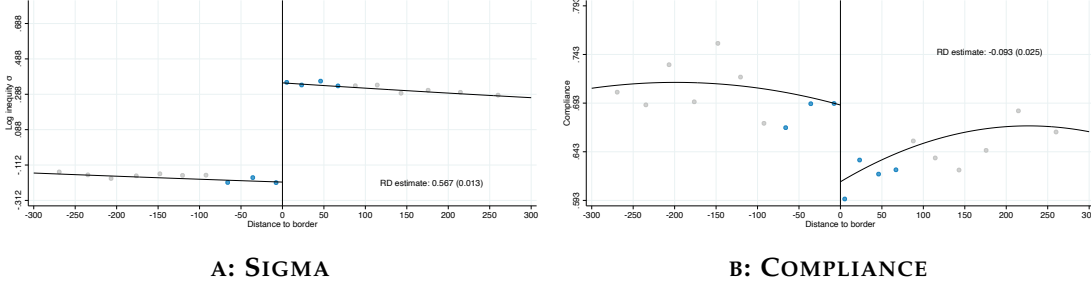
A: SIGMA



B: COMPLIANCE

Notes: The figure shows the overall change in compliance (Panel A) and inequity (Panel B) at tax sector boundaries discussed in section 4.1. Specifically, we show the results of estimating the following equation for compliance and inequity (10): y_i by taxpayer i : $c_i = \gamma_{s(i)} + f(d_i) + \beta_0 HTS_i + h(d_i) \times HTS_i + \varepsilon_i$ where $\gamma_{s(i)}$ are boundary-segment fixed effects, HTS_i is an indicator for being on the high-tax side of the boundary ($d_i > 0$); $f_0(d_i)$ and $f_1(d_i)$ control for distance to the boundary on the low- and high-tax sides of the boundary, respectively; and ε_i is the residual. Overlaid on the figure, we show the point estimate of the discontinuity in compliance estimated using local linear distance controls, the MSE-minimizing bandwidth, and triangular kernel weights in distance. The dots in the figure show the coefficients from estimating (10) with fixed effects for decile-spaced bins of distance, using the same triangular kernel weights but censoring them at their tenth percentile to give non-zero weights to distances outside the optimal bandwidth. The bins in the optimal bandwidth are shown in blue while those outside are shown in grey. The black line is a global cubic polynomial fit in the same way.

FIGURE D.20: RD CONTROLLING FOR TAU



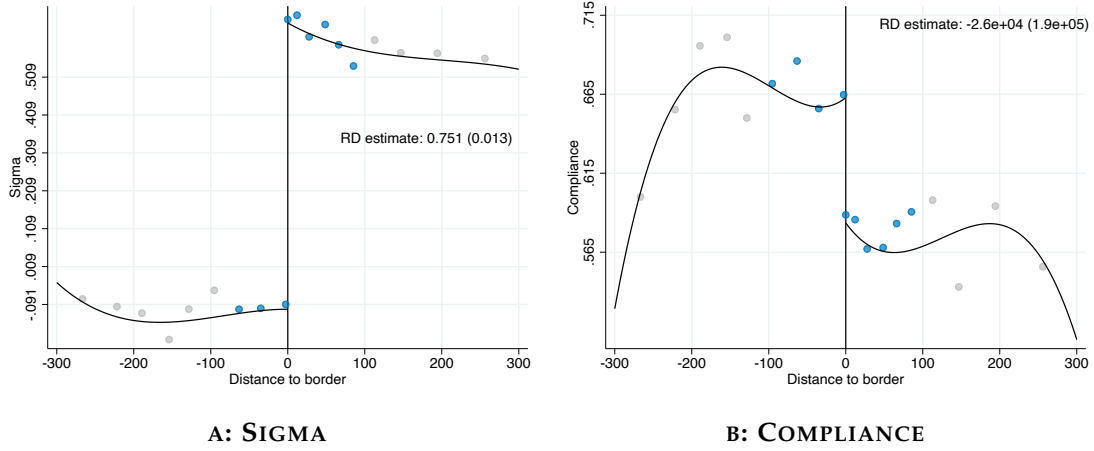
Notes: The figure shows the impact on inequity and compliance in the augmented BDD discussed in section ?? . Specifically, we show the results of estimation of equation (12): $y_i = \gamma_{s(i)} + g(\tau_i, e_i) + f(d_i) + \beta_0 HTS_i + h(d_i) \times HTS_i + \varepsilon_i$ using log-inequity σ as the outcome variable in panel A and compliance in panel B. $\gamma_{s(i)}$ are fixed effects for 500-meter segments along the boundaries to ensure we are comparing properties who are nearby each other; $g(\tau_i, e_i)$ are flexible controls for property i 's (log) tax liability τ_i and expansiveness e_i (our baseline estimates use τ splines and expansiveness deciles); $f(d_i)$ and $h(d_i)$ control flexibly for distance to the boundary on the low- and high-tax sides of the boundary respectively; and HTS_i is an indicator for properties on the high-tax side of the boundary ($d_i > 0$). Overlaid on the figure, we show the point estimate of the discontinuity in inequity estimated using local linear distance controls, the MSE-minimizing bandwidth, and triangular kernel weights in distance. The dots in the figure show the coefficients from estimating (12) with fixed effects for decile-spaced bins of distance, using the same triangular kernel weights but censoring them at their tenth percentile to give non-zero weights to distances outside the optimal bandwidth. The bins in the optimal bandwidth are shown in blue while those outside are shown in grey. The black line is a global cubic polynomial fit in the same way.

TABLE D.9: AUGMENTED BOUNDARY DISCONTINUITY DESIGN: COMPLIANCE EFFECTS

	(1)	(2)	(3)	(4)	(5)	(6)
RD_Estimate	-0.08*** (0.02)	-0.06*** (0.02)	-0.08*** (0.02)	-0.06*** (0.02)	-0.08*** (0.02)	-0.08*** (0.02)
R^2						
Distance controls	✓	✓	✓	✓	✓	✓
Segment FEs	✓	✓	✓	✓	✓	✓
τ splines	✓	✓	✓	✓		
exp dec FEs	✓		✓			✓
τ decile FEs					✓	✓
exp splines		✓		✓		
τ splines \times exp dec FEs			✓			
τ splines \times exp splines				✓		
τ dec FEs \times exp dec FEs						✓
First-stage	0.553	0.497	0.564	0.526	0.552	0.566
fscoef_se	(0.009)	(0.009)	(0.009)	(0.009)	(0.009)	(0.009)
Elasticity	-0.211	-0.171	-0.216	-0.162	-0.208	-0.223
elascoef_se	(0.045)	(0.054)	(0.044)	(0.052)	(0.045)	(0.045)
N	9966	9965	9966	9965	9966	9966

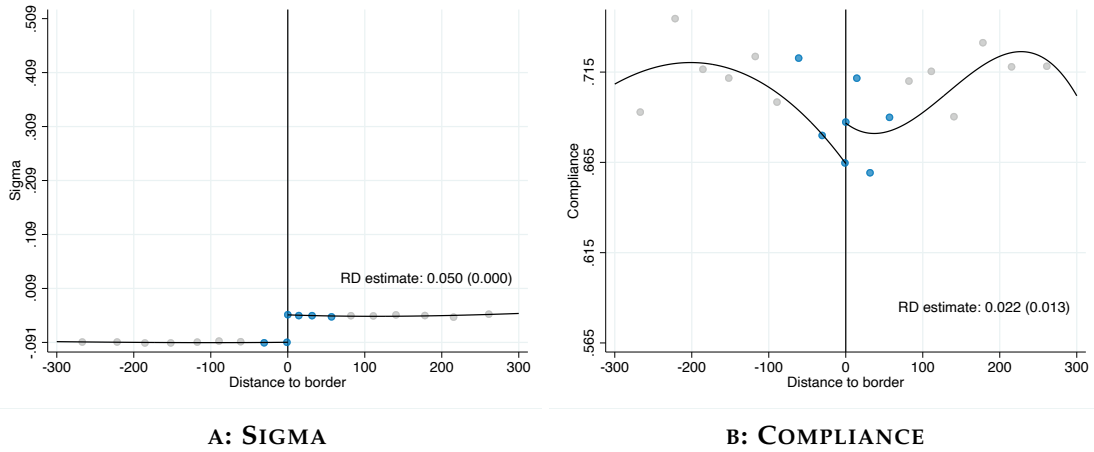
Notes: The table shows the results of estimating the augmented BDD equation (12): $c_i = \gamma_{s(i)} + g(\tau_i, e_i) + f(d_i) + \beta_0 HTS_i + h(d_i) \times HTS_i + \varepsilon_i$, where $\gamma_{s(i)}$ are fixed effects for 500-meter segments along the boundaries to ensure we are comparing properties who are nearby each other; $g(\tau_i, e_i)$ are flexible controls for property i 's (log) tax liability τ_i and expansiveness e_i ; $f(d_i)$ and $h(d_i)$ control flexibly for distance to the boundary on the low- and high-tax sides of the boundary respectively; and HTS_i is an indicator for properties on the high-tax side of the boundary ($d_i > 0$). The columns use a variety of approaches to controlling flexibly for the tax liability and expansiveness. In column (1) we control for cubic splines of the tax liability and fixed effects for deciles of expansiveness. In column (2) we replace the expansiveness deciles with cubic splines of expansiveness while column (3) replaces the splines of the tax liability with deciles. Columns (4)–(6) additionally interact the tax liability controls with the expansiveness controls.

FIGURE D.21: RD CONTROLLING FOR TAU - HIGH INEQUITY



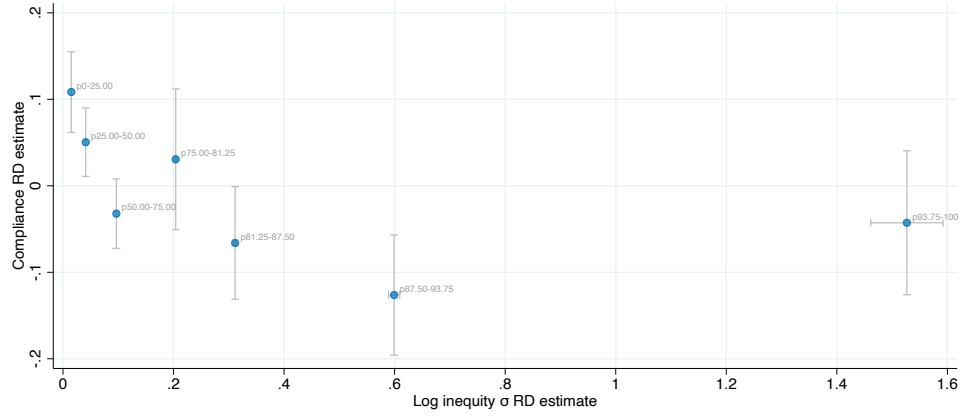
Notes: The figure shows the results of estimating equation (12): $y_i = \gamma_{s(i)} + g(\tau_i, e_i) + f(d_i) + \beta_0 HTS_i + h(d_i) \times HTS_i + \varepsilon_i$ with inequality as the outcome variable in panel A and compliance as the outcome in panel B. Terms are as defined in the notes to figure 6. Both panels show the estimates in the subsample of properties facing high inequality (defined as being in the top quartile of inequality).

FIGURE D.22: RD CONTROLLING FOR TAU - LOW INEQUITY



Notes: The figure shows the results of estimating equation (12): $y_i = \gamma_{s(i)} + g(\tau_i, e_i) + f(d_i) + \beta_0 HTS_i + h(d_i) \times HTS_i + \varepsilon_i$ with inequality as the outcome variable in panel A and compliance as the outcome in panel B. Terms are as defined in the notes to figure 6. Both panels show the estimates in the subsample of properties facing low inequality (defined as being in the bottom three quartile of inequality).

FIGURE D.23: HETEROGENEITY ANALYSIS



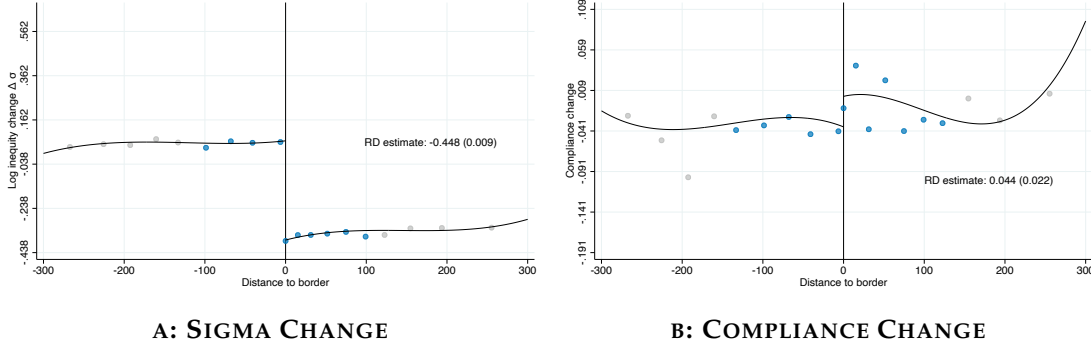
Notes: The figure shows the results of estimating equation (12): $c_i = \gamma_{s(i)} + g(\tau_i, e_i) + f(d_i) + \beta_0 HTS_i + h(d_i) \times HTS_i + \varepsilon_i$ where terms are as defined in the notes to figure 6. Each dot represents a different subsample. The three leftmost dots represent the three bottom quartiles of inequity. The remaining dots split the top quartile of inequity into 4 equally-sized subgroups. The vertical position and vertical grey bars of the dots display the estimated compliance effect and its 95% confidence interval. The horizontal position and horizontal grey bars of the dots display the estimated inequity change and its 95% confidence interval.

TABLE D.10: DIFFERENCE IN BOUNDARY DISCONTINUITY DESIGN: COMPLIANCE EFFECTS

	(1)	(2)	(3)	(4)	(5)	(6)	(7)
1(high tax side)	0.02 (0.01)	0.00 (.)	0.00 (.)	0.00 (.)	0.13 (0.34)	0.08 (0.33)	0.00 (.)
1(high tax side) $\times \sigma $	-0.17*** (0.02)	-0.17*** (0.02)	-0.17*** (0.02)	-0.17*** (0.02)	-0.15*** (0.03)	-0.16*** (0.03)	-0.15*** (0.03)
R^2	0.137	0.137	0.137	0.137	0.141	0.140	0.145
Distance controls	✓	✓	✓	✓	✓	✓	✓
Segment fixed effects	✓	✓	✓	✓	✓	✓	✓
τ splines	✓	✓	✓	✗	✓	✓	✗
τ deciles	✗	✗	✗	✓	✗	✗	✓
Expansiveness splines	✗	✗	✓	✗	✗	✓	✗
Expansiveness deciles	✓	✓	✗	✓	✓	✗	✓
τ splines \times HTS	✗	✓	✓	✗	✓	✓	✗
τ deciles \times HTS	✗	✗	✗	✓	✗	✗	✓
τ splines \times exp deciles	✗	✗	✗	✗	✓	✗	✗
τ splines \times exp splines	✗	✗	✗	✗	✗	✓	✗
τ deciles \times exp deciles	✗	✗	✗	✗	✗	✗	✓
τ splines \times HTS \times exp deciles	✗	✗	✗	✗	✓	✗	✗
τ splines \times HTS \times exp splines	✗	✗	✗	✗	✗	✓	✗
τ deciles \times HTS \times exp deciles	✗	✗	✗	✗	✗	✗	✓
Elasticity	-0.252 0.035	-0.253 0.035	-0.259 0.036	-0.254 0.035	-0.223 0.039	-0.242 0.040	-0.224 0.039
N	27968	27968	27968	27968	27968	27968	27968

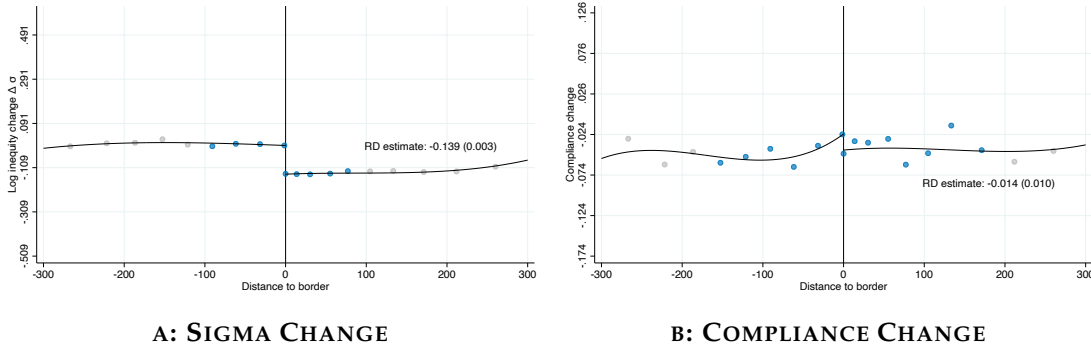
Notes: The table shows the results of estimation of equation (16): $c_i = \gamma_{s(i)} + g_0(\tau_i, e_i) + f(d_i) + HTS_i \times [\beta_0 + \eta \log(\sigma) + h(d_i) + g_1(\tau_i, e_i)] + \varepsilon_i$ where terms are as defined above in the notes to table 2. In column (1), we control for cubic splines of the tax liability and fixed effects for deciles of the expansiveness distribution. In column (2) we control separately for the tax liability and expansiveness on either side of the boundary. Column (3) replaces the expansiveness deciles with cubic splines in expansiveness while column (4) replaces the tax liability deciles with cubic splines. Columns (5)–(7) control for these separately on either side of the boundary.

FIGURE D.24: DYNAMIC BOUNDARY DISCONTINUITY DESIGN: REMOVAL OF INEQUITY



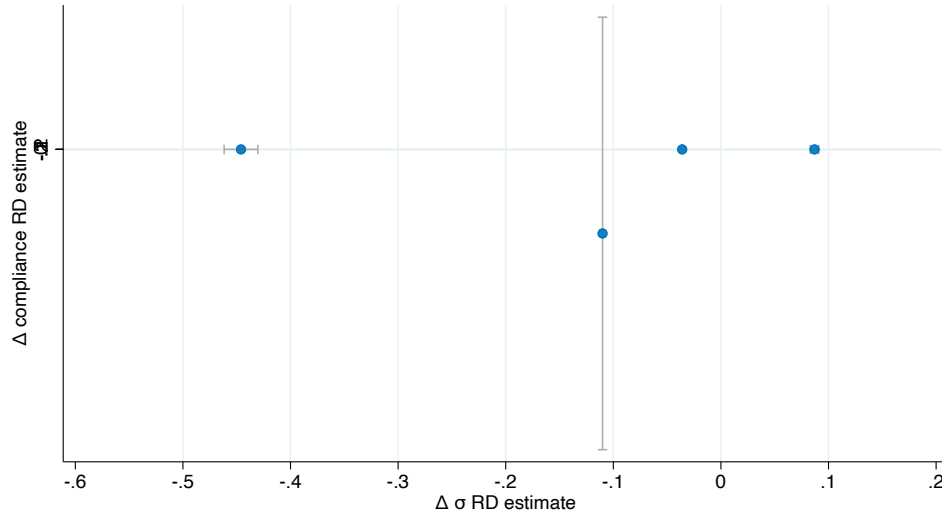
Notes: The figure shows the results of estimating equation (17) $\Delta y_i = \gamma_{s(i)} + g(\Delta \tau_i) + f_0(d_i) + HTS_i \times [\beta_0 + f_1(d_i)] + \varepsilon_i$ where the outcome variable is the change in inequity in panel A and the change in compliance in panel B; $\gamma_{s(i)}$ are boundary-segment fixed effects, HTS_i is an indicator for being on the high-tax side of the boundary ($d_i > 0$); $f_0(d_i)$ and $f_1(d_i)$ control for distance to the boundary on the low- and high-tax sides of the boundary, respectively; and ε_i is the residual. $g(\Delta \tau_i)$ controls flexibly for changes in log tax liability, τ_i . Specifically, we control for splines of $\Delta \tau_i$. Both panels shows the estimates in the subsample of properties for whom the reform meaningfully reduced inequity.

FIGURE D.25: DYNAMIC BOUNDARY DISCONTINUITY DESIGN: NO IMPROVEMENT



Notes: The figure shows the results of estimating equation (17) $\Delta y_i = \gamma_{s(i)} + g(\Delta \tau_i) + f_0(d_i) + HTS_i \times [\beta_0 + f_1(d_i)] + \varepsilon_i$ where the outcome variable is the change in inequity in panel A and the change in compliance in panel B; $\gamma_{s(i)}$ are boundary-segment fixed effects, HTS_i is an indicator for being on the high-tax side of the boundary ($d_i > 0$); $f_0(d_i)$ and $f_1(d_i)$ control for distance to the boundary on the low- and high-tax sides of the boundary, respectively; and ε_i is the residual. $g(\Delta \tau_i)$ controls flexibly for changes in log tax liability, τ_i . Specifically, we control for splines of $\Delta \tau_i$. Both panels shows the estimates in the subsample of properties for whom the reform did not meaningfully reduced inequity.

FIGURE D.26: DYNAMIC BOUNDARY DISCONTINUITY DESIGN: HETEROGENEITY BY IN-EQUITY REDUCTION



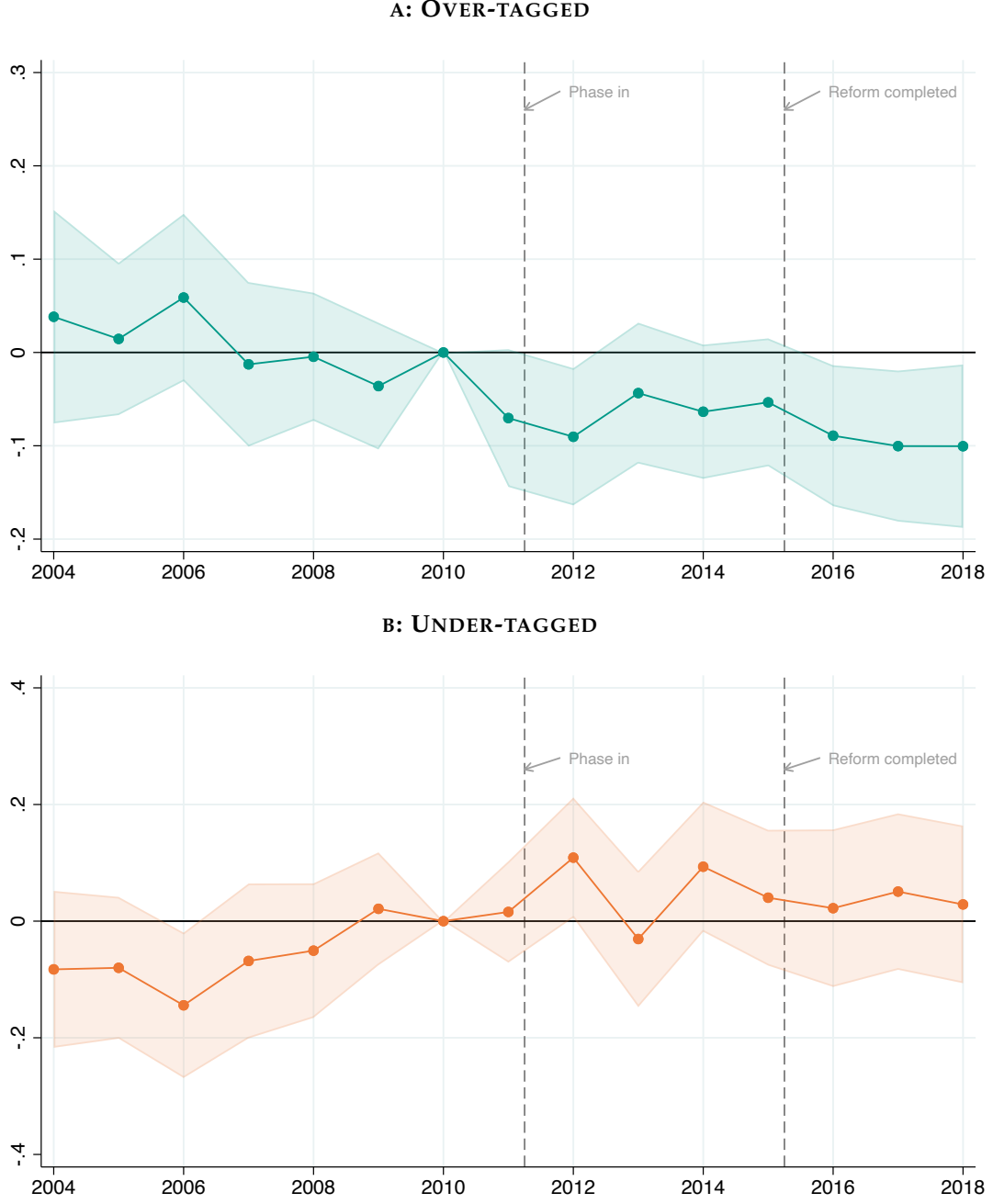
Notes: The figure shows the results of estimating equation (17) $\Delta c_i = \gamma_{s(i)} + g(\Delta \tau_i) + f_0(d_i) + HTS_i \times [\beta_0 + f_1(d_i)] + \varepsilon_i$ where $\gamma_{s(i)}$ are boundary-segment fixed effects, HTS_i is an indicator for being on the high-tax side of the boundary ($d_i > 0$); $f_0(d_i)$ and $f_1(d_i)$ control for distance to the boundary on the low- and high-tax sides of the boundary, respectively; and ε_i is the residual. $g(\Delta \tau_i)$ controls flexibly for changes in log tax liability, τ_i . Specifically, we control for splines of τ_i . We estimate (17) separately in four subsamples defined by quartiles of their change in inequity. The vertical coordinate of each dot and the vertical gray bars show the estimated impact on compliance and its 95% confidence interval. The horizontal coordinate of each dot and the horizontal gray bars show the estimated impact on inequity and its 95% confidence interval.

TABLE D.11: DYNAMIC DIFFERENCE IN BOUNDARY DISCONTINUITY DESIGN

	(1)	(2)	(3)	(4)
	Δ Compliance	Δ Compliance	Δ Compliance	Δ Compliance
1(high tax side)	-0.008 (0.011)	-0.009 (0.032)	-0.010 (0.031)	-0.008 (0.022)
1(high tax side) \times change in σ	-0.091** (0.037)	-0.094** (0.040)	-0.088** (0.043)	-0.098** (0.039)
Elasticity implied	-0.138	-0.143	-0.133	-0.149
Elasticity SE	0.057	0.060	0.065	0.059
Distance controls	✓	✓	✓	✓
Segment FEs	✓	✓	✓	✓
τ splines	✓	✓	✓	✗
Expansiveness deciles	✓	✓	✗	✓
Interaction with HTS	✗	✓	✓	✓
τ splines \times expansiveness deciles	✗	✓	✗	✗
Expansiveness splines	✗	✗	✓	✗
τ splines \times expansiveness splines	✗	✗	✓	✗
τ deciles	✗	✗	✗	✓
τ deciles \times expansiveness deciles	✗	✗	✗	✓

Notes: This table shows the results of estimating equation (18) discussed in section 6.2: $\Delta c_i = \gamma_{s(u)} + g_0(\Delta \tau_i, e_i) + f_0(d_i) + HTS_i \times [\delta_0 + \eta \Delta \log(\sigma_i) + g_1(\Delta \tau_i, e_i) + f_1(d_i)] + \varepsilon_i$ where all terms are as defined above in the notes to table 2. Column (1) controls for cubic splines of the tax liability and fixed effects for deciles of the expansiveness distribution. Column (2) adds interactions between these controls and estimates them separately on either side of the boundary. Column (3) replaces the expansiveness deciles with splines, while column (4) replaces the tax liability splines with deciles of the tax liability distribution.

FIGURE D.27: DIFFERENCE IN DIFFERENCE ESTIMATES OF OVERTAGGING AND UNDERTAGGING EFFECTS

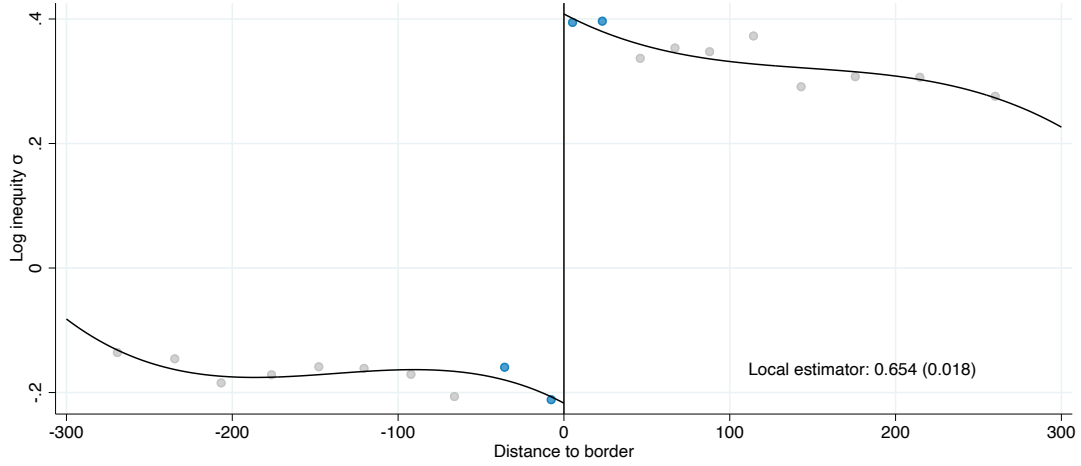


Notes: The figure shows the results of the estimation of equation (20) as discussed in section 6.3: $c_{iy} = \alpha_i + \gamma_{s(i)y} + \sum_{j \neq 2010} D_{jy} \times [f_{0j}(d_i) + \beta_{0j} \Delta \tau_i + \eta_{0j} \Delta \sigma_i + HTS_i \times (\delta_j + f_{1j}(d_i) + \beta_{1j} \Delta \tau_i + \eta_{1j} \Delta \sigma_i)] + \varepsilon_{iy}$, where $\gamma_{s(i)y}$ are segment-year fixed effects, $D_{jy} \equiv 1[y = j]$ are year dummies, and we include year-specific distance controls $f_{0j}(d_i)$ and $f_{1j}(d_i)$; and year-specific controls for property i 's tax liability change due to the reform. Panel A shows the estimated η_{1j} coefficients along with their 95% confidence intervals. Panel B shows the estimated η_{0j} coefficients along with their 95% confidence intervals.

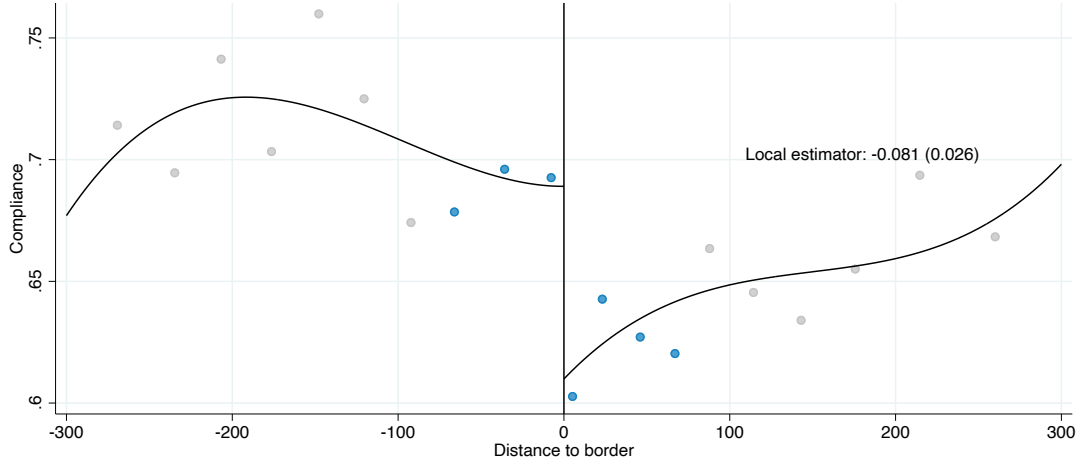
D.5 Stringent “large CGLs” drop: Drop the top 1% in terms of land area

In the main paper, we exclude “very large” lots because they introduce measurement error. We define “very large” lots as the top 0.5% in terms of land area. Here, we provide evidence with a sample that excludes the top 1% of lots in terms of land area.

FIGURE D.28: REDUCED FORM ESTIMATES



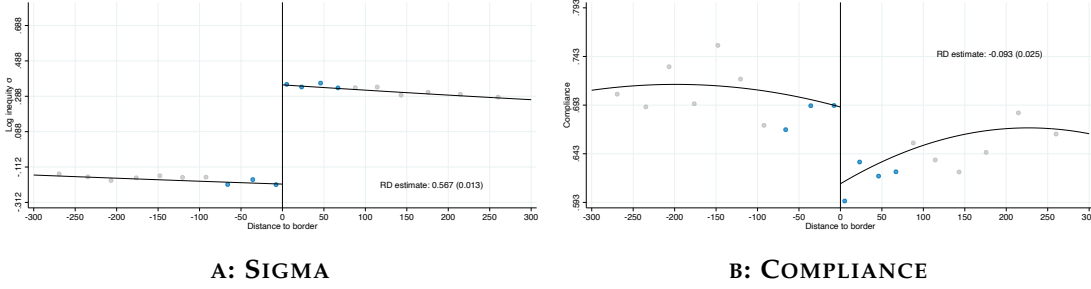
A: SIGMA



B: COMPLIANCE

Notes: The figure shows the overall change in compliance (Panel A) and inequity (Panel B) at tax sector boundaries discussed in section 4.1. Specifically, we show the results of estimating the following equation for compliance and inequity (10): y_i by taxpayer i : $c_i = \gamma_{s(i)} + f(d_i) + \beta_0 HTS_i + h(d_i) \times HTS_i + \varepsilon_i$ where $\gamma_{s(i)}$ are boundary-segment fixed effects, HTS_i is an indicator for being on the high-tax side of the boundary ($d_i > 0$); $f_0(d_i)$ and $f_1(d_i)$ control for distance to the boundary on the low- and high-tax sides of the boundary, respectively; and ε_i is the residual. Overlaid on the figure, we show the point estimate of the discontinuity in compliance estimated using local linear distance controls, the MSE-minimizing bandwidth, and triangular kernel weights in distance. The dots in the figure show the coefficients from estimating (10) with fixed effects for decile-spaced bins of distance, using the same triangular kernel weights but censoring them at their tenth percentile to give non-zero weights to distances outside the optimal bandwidth. The bins in the optimal bandwidth are shown in blue while those outside are shown in grey. The black line is a global cubic polynomial fit in the same way.

FIGURE D.29: RD CONTROLLING FOR TAU



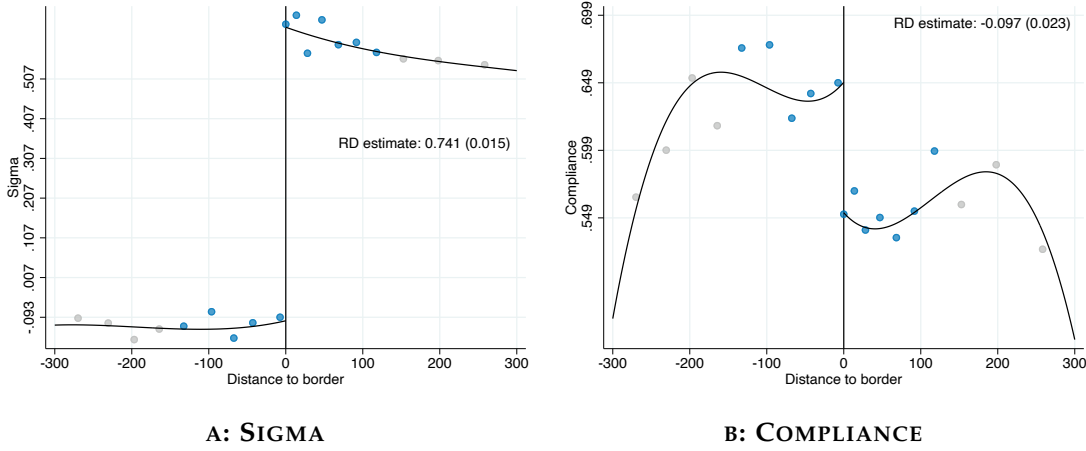
Notes: The figure shows the results of estimating equation (12): $y_i = \gamma_{s(i)} + g(\tau_i, e_i) + f(d_i) + \beta_0 HTS_i + h(d_i) \times HTS_i + \varepsilon_i$ with inequality as the outcome variable in panel A and compliance as the outcome in panel B. Terms are as defined in the notes to figure 6. Both panels show the estimates in the subsample of properties facing low inequality (defined as being in the bottom three quartile of inequality).

TABLE D.12: AUGMENTED BOUNDARY DISCONTINUITY DESIGN: COMPLIANCE EFFECTS

	(1)	(2)	(3)	(4)	(5)	(6)
RD_Estimate	-0.09*** (0.02)	-0.08*** (0.02)	-0.10*** (0.02)	-0.08*** (0.02)	-0.09*** (0.02)	-0.10*** (0.02)
R^2						
Distance controls	✓	✓	✓	✓	✓	✓
Segment FEs	✓	✓	✓	✓	✓	✓
τ splines	✓	✓	✓	✓		
exp dec FEs	✓		✓			✓
τ decile FEs					✓	✓
exp splines		✓		✓		
τ splines \times exp dec FEs			✓			
τ splines \times exp splines				✓		
τ dec FEs \times exp dec FEs						✓
First-stage	0.519	0.499	0.531	0.513	0.518	0.535
fscoef_se	(0.011)	(0.011)	(0.011)	(0.010)	(0.011)	(0.011)
Elasticity	-0.252	-0.228	-0.264	-0.238	-0.253	-0.260
elascoef_se	(0.059)	(0.067)	(0.056)	(0.065)	(0.059)	(0.056)
N	8800	8799	8800	8799	8800	8800

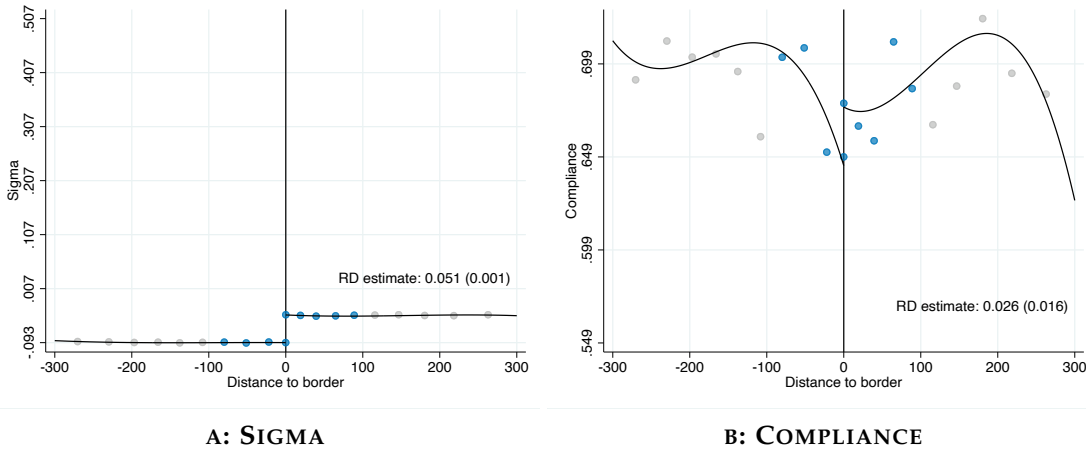
Notes: The table shows the results of estimating the augmented BDD equation (12): $c_i = \gamma_{s(i)} + g(\tau_i, e_i) + f(d_i) + \beta_0 HTS_i + h(d_i) \times HTS_i + \varepsilon_i$, where $\gamma_{s(i)}$ are fixed effects for 500-meter segments along the boundaries to ensure we are comparing properties who are nearby each other; $g(\tau_i, e_i)$ are flexible controls for property i 's (log) tax liability τ_i and expansiveness e_i ; $f(d_i)$ and $h(d_i)$ control flexibly for distance to the boundary on the low- and high-tax sides of the boundary respectively; and HTS_i is an indicator for properties on the high-tax side of the boundary ($d_i > 0$). The columns use a variety of approaches to controlling flexibly for the tax liability and expansiveness. In column (1) we control for cubic splines of the tax liability and fixed effects for deciles of expansiveness. In column (2) we replace the expansiveness deciles with cubic splines of expansiveness while column (3) replaces the splines of the tax liability with deciles. Columns (4)–(6) additionally interact the tax liability controls with the expansiveness controls.

FIGURE D.30: RD CONTROLLING FOR TAU - HIGH INEQUITY



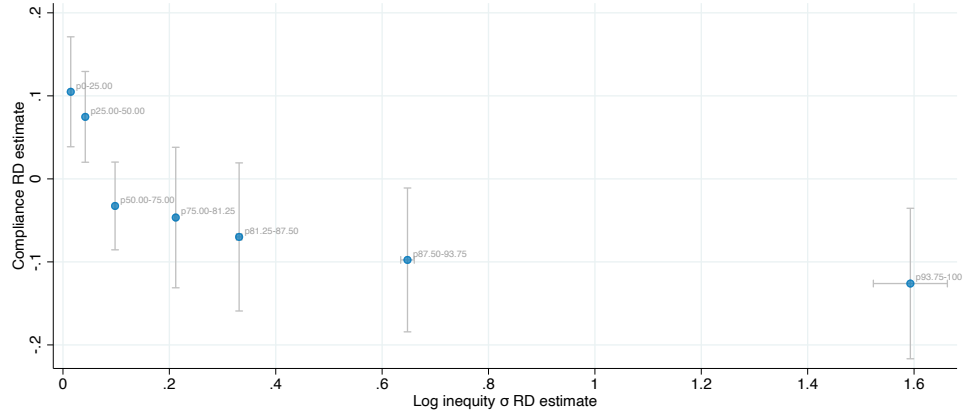
Notes: The figure shows the results of estimating equation (12): $y_i = \gamma_{s(i)} + g(\tau_i, e_i) + f(d_i) + \beta_0 HTS_i + h(d_i) \times HTS_i + \varepsilon_i$ with inequality as the outcome variable in panel A and compliance as the outcome in panel B. Terms are as defined in the notes to figure 6. Both panels show the estimates in the subsample of properties facing high inequality (defined as being in the top quartile of inequality).

FIGURE D.31: RD CONTROLLING FOR TAU - LOW INEQUITY



Notes: The figure shows the results of estimating equation (12): $y_i = \gamma_{s(i)} + g(\tau_i, e_i) + f(d_i) + \beta_0 HTS_i + h(d_i) \times HTS_i + \varepsilon_i$ with inequality as the outcome variable in panel A and compliance as the outcome in panel B. Terms are as defined in the notes to figure 6. Both panels show the estimates in the subsample of properties facing low inequality (defined as being in the bottom three quartile of inequality).

FIGURE D.32: HETEROGENEITY ANALYSIS



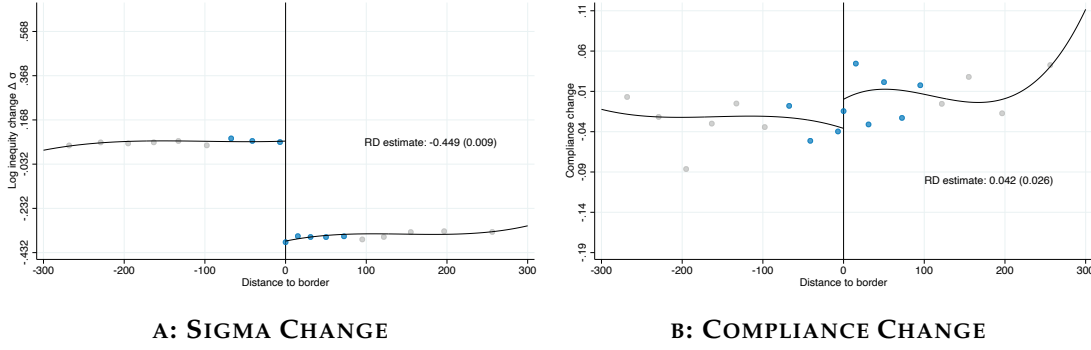
Notes: The figure shows the results of estimating equation (12): $c_i = \gamma_{s(i)} + g(\tau_i, e_i) + f(d_i) + \beta_0 HTS_i + h(d_i) \times HTS_i + \varepsilon_i$ where terms are as defined in the notes to figure 6. Each dot represents a different subsample. The three leftmost dots represent the three bottom quartiles of inequity. The remaining dots split the top quartile of inequity into 4 equally-sized subgroups. The vertical position and vertical grey bars of the dots display the estimated compliance effect and its 95% confidence interval. The horizontal position and horizontal grey bars of the dots display the estimated inequity change and its 95% confidence interval.

TABLE D.13: DIFFERENCE IN BOUNDARY DISCONTINUITY DESIGN: COMPLIANCE EFFECTS

	(1)	(2)	(3)	(4)	(5)	(6)	(7)
1(high tax side)	0.00 (0.02)	0.00 (.)	0.00 (.)	0.00 (.)	0.23 (0.38)	0.21 (0.37)	0.00 (.)
1(high tax side) $\times \sigma $	-0.17*** (0.02)	-0.17*** (0.03)	-0.18*** (0.03)	-0.17*** (0.02)	-0.15*** (0.03)	-0.19*** (0.03)	-0.15*** (0.03)
R^2	0.124	0.124	0.124	0.124	0.127	0.126	0.131
Distance controls	✓	✓	✓	✓	✓	✓	✓
Segment fixed effects	✓	✓	✓	✓	✓	✓	✓
τ splines	✓	✓	✓	✗	✓	✓	✗
τ deciles	✗	✗	✗	✓	✗	✗	✓
Expansiveness splines	✗	✗	✓	✗	✗	✓	✗
Expansiveness deciles	✓	✓	✗	✓	✓	✗	✓
τ splines \times HTS	✗	✓	✓	✗	✓	✓	✗
τ deciles \times HTS	✗	✗	✗	✓	✗	✗	✓
τ splines \times exp deciles	✗	✗	✗	✗	✓	✗	✗
τ splines \times exp splines	✗	✗	✗	✗	✗	✓	✗
τ deciles \times exp deciles	✗	✗	✗	✗	✗	✗	✓
τ splines \times HTS \times exp deciles	✗	✗	✗	✗	✓	✗	✗
τ splines \times HTS \times exp splines	✗	✗	✗	✗	✗	✓	✗
τ deciles \times HTS \times exp deciles	✗	✗	✗	✗	✗	✗	✓
Elasticity	-0.261 0.039	-0.262 0.039	-0.282 0.040	-0.263 0.039	-0.229 0.043	-0.300 0.050	-0.235 0.043
N	23868	23868	23868	23868	23868	23868	23868

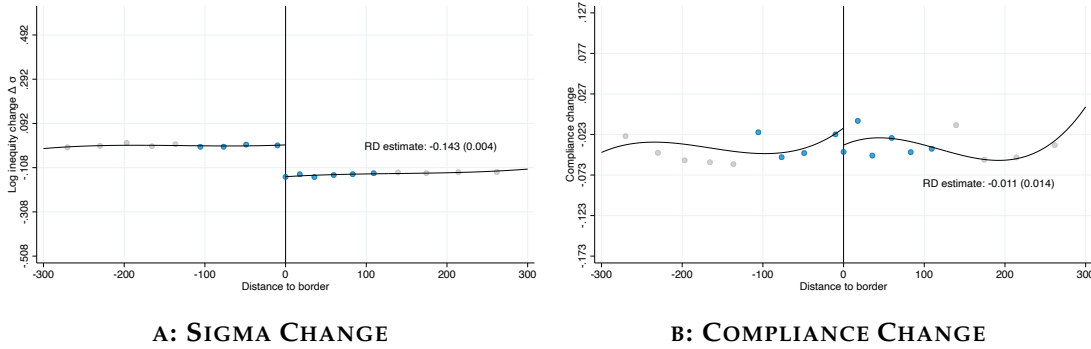
Notes: The table shows the results of estimation of equation (16): $c_i = \gamma_{s(i)} + g_0(\tau_i, e_i) + f(d_i) + HTS_i \times [\beta_0 + \eta \log(\sigma) + h(d_i) + g_1(\tau_i, e_i)] + \varepsilon_i$ where terms are as defined above in the notes to table 2. In column (1), we control for cubic splines of the tax liability and fixed effects for deciles of the expansiveness distribution. In column (2) we control separately for the tax liability and expansiveness on either side of the boundary. Column (3) replaces the expansiveness deciles with cubic splines in expansiveness while column (4) replaces the tax liability deciles with cubic splines. Columns (5)–(7) control for these separately on either side of the boundary.

FIGURE D.33: DYNAMIC BOUNDARY DISCONTINUITY DESIGN: REMOVAL OF INEQUITY



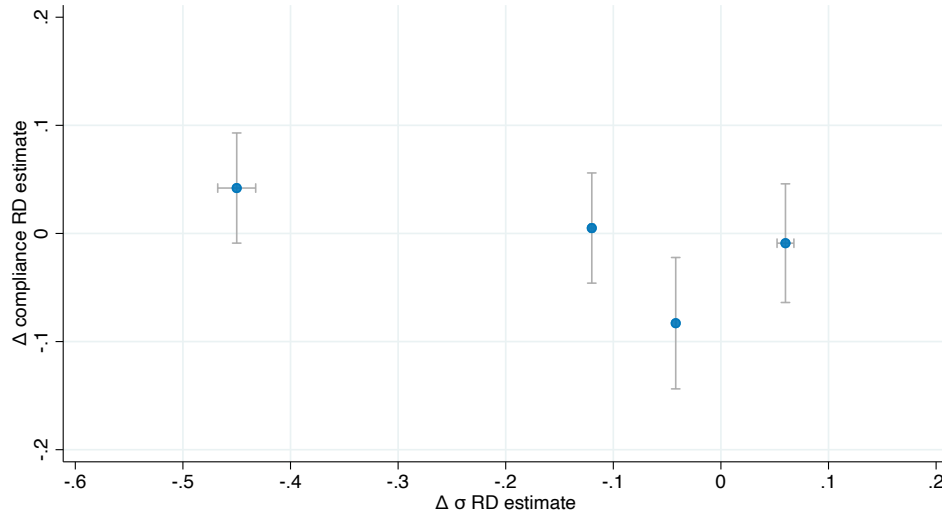
Notes: The figure shows the results of estimating equation (17) $\Delta y_i = \gamma_{s(i)} + g(\Delta \tau_i) + f_0(d_i) + HTS_i \times [\beta_0 + f_1(d_i)] + \varepsilon_i$ where the outcome variable is the change in inequity in panel A and the change in compliance in panel B; $\gamma_{s(i)}$ are boundary-segment fixed effects, HTS_i is an indicator for being on the high-tax side of the boundary ($d_i > 0$); $f_0(d_i)$ and $f_1(d_i)$ control for distance to the boundary on the low- and high-tax sides of the boundary, respectively; and ε_i is the residual. $g(\Delta \tau_i)$ controls flexibly for changes in log tax liability, τ_i . Specifically, we control for splines of $\Delta \tau_i$. Both panels shows the estimates in the subsample of properties for whom the reform meaningfully reduced inequity.

FIGURE D.34: DYNAMIC BOUNDARY DISCONTINUITY DESIGN: NO IMPROVEMENT



Notes: The figure shows the results of estimating equation (17) $\Delta y_i = \gamma_{s(i)} + g(\Delta \tau_i) + f_0(d_i) + HTS_i \times [\beta_0 + f_1(d_i)] + \varepsilon_i$ where the outcome variable is the change in inequity in panel A and the change in compliance in panel B; $\gamma_{s(i)}$ are boundary-segment fixed effects, HTS_i is an indicator for being on the high-tax side of the boundary ($d_i > 0$); $f_0(d_i)$ and $f_1(d_i)$ control for distance to the boundary on the low- and high-tax sides of the boundary, respectively; and ε_i is the residual. $g(\Delta \tau_i)$ controls flexibly for changes in log tax liability, τ_i . Specifically, we control for splines of $\Delta \tau_i$. Both panels shows the estimates in the subsample of properties for whom the reform did not meaningfully reduced inequity.

FIGURE D.35: DYNAMIC BOUNDARY DISCONTINUITY DESIGN: HETEROGENEITY BY IN-EQUITY REDUCTION



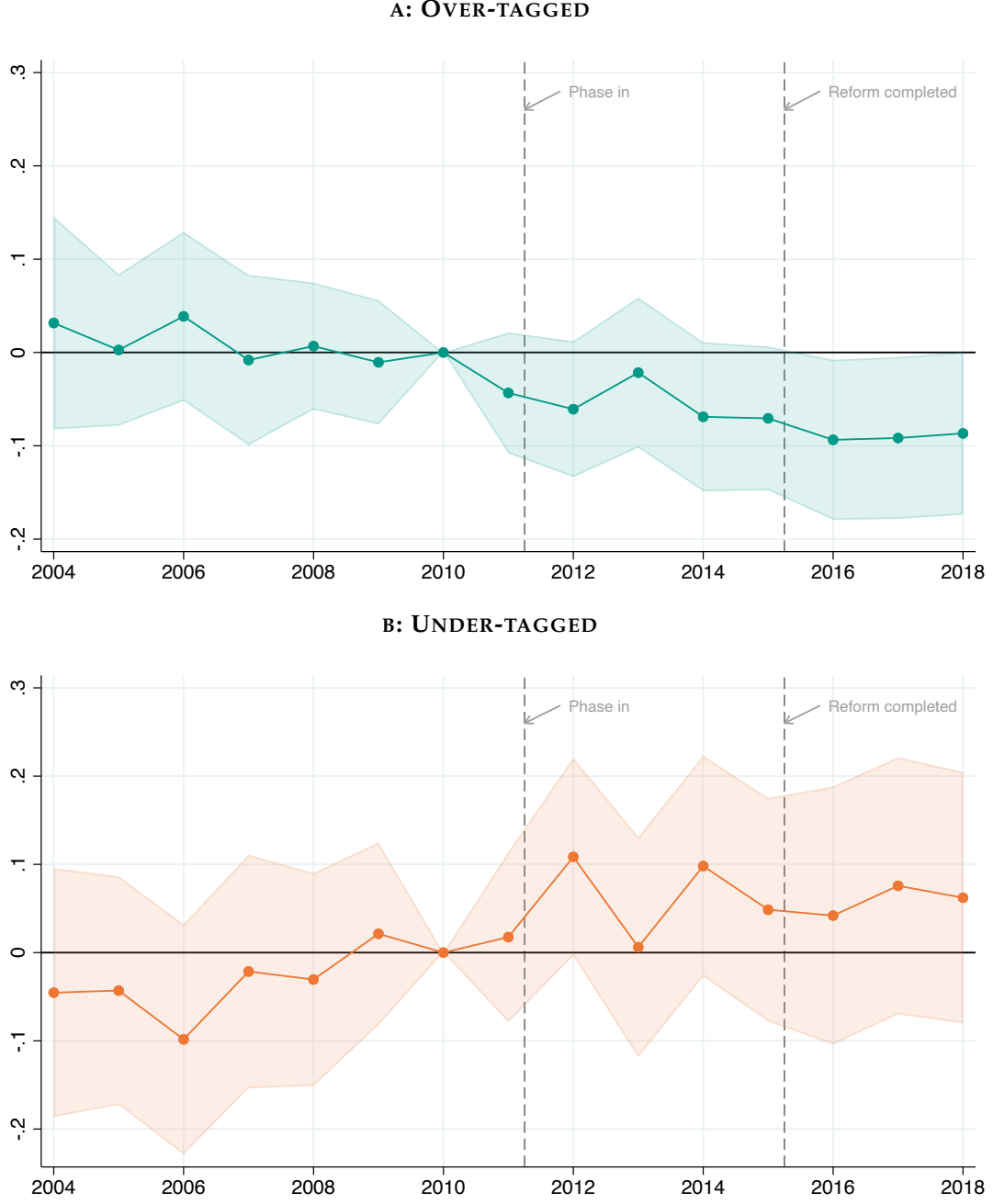
Notes: The figure shows the results of estimating equation (17) $\Delta c_i = \gamma_{s(i)} + g(\Delta \tau_i) + f_0(d_i) + HTS_i \times [\beta_0 + f_1(d_i)] + \varepsilon_i$ where $\gamma_{s(i)}$ are boundary-segment fixed effects, HTS_i is an indicator for being on the high-tax side of the boundary ($d_i > 0$); $f_0(d_i)$ and $f_1(d_i)$ control for distance to the boundary on the low- and high-tax sides of the boundary, respectively; and ε_i is the residual. $g(\Delta \tau_i)$ controls flexibly for changes in log tax liability, τ_i . Specifically, we control for splines of τ_i . We estimate (17) separately in four subsamples defined by quartiles of their change in inequity. The vertical coordinate of each dot and the vertical gray bars show the estimated impact on compliance and its 95% confidence interval. The horizontal coordinate of each dot and the horizontal gray bars show the estimated impact on inequity and its 95% confidence interval.

TABLE D.14: DYNAMIC DIFFERENCE IN BOUNDARY DISCONTINUITY DESIGN

	(1)	(2)	(3)	(4)
	Δ Compliance	Δ Compliance	Δ Compliance	Δ Compliance
1(high tax side)	-0.005 (0.012)	-0.012 (0.033)	-0.009 (0.032)	-0.005 (0.025)
1(high tax side) \times change in σ	-0.088** (0.040)	-0.097** (0.042)	-0.086* (0.047)	-0.104** (0.041)
Elasticity implied	-0.139	-0.153	-0.135	-0.163
Elasticity SE	0.062	0.066	0.074	0.065
Distance controls	✓	✓	✓	✓
Segment FEs	✓	✓	✓	✓
τ splines	✓	✓	✓	✗
Expansiveness deciles	✓	✓	✗	✓
Interaction with HTS	✗	✓	✓	✓
τ splines \times expansiveness deciles	✗	✓	✗	✗
Expansiveness splines	✗	✗	✓	✗
τ splines \times expansiveness splines	✗	✗	✓	✗
τ deciles	✗	✗	✗	✓
τ deciles \times expansiveness deciles	✗	✗	✗	✓

Notes: This table shows the results of estimating equation (18) discussed in section 6.2: $\Delta c_i = \gamma_{s(u)} + g_0(\Delta \tau_i, e_i) + f_0(d_i) + HTS_i \times [\delta_0 + \eta \Delta \log(\sigma_i) + g_1(\Delta \tau_i, e_i) + f_1(d_i)] + \varepsilon_i$ where all terms are as defined above in the notes to table 2. Column (1) controls for cubic splines of the tax liability and fixed effects for deciles of the expansiveness distribution. Column (2) adds interactions between these controls and estimates them separately on either side of the boundary. Column (3) replaces the expansiveness deciles with splines, while column (4) replaces the tax liability splines with deciles of the tax liability distribution.

FIGURE D.36: DIFFERENCE IN DIFFERENCE ESTIMATES OF OVERTAGGING AND UNDERTAGGING EFFECTS

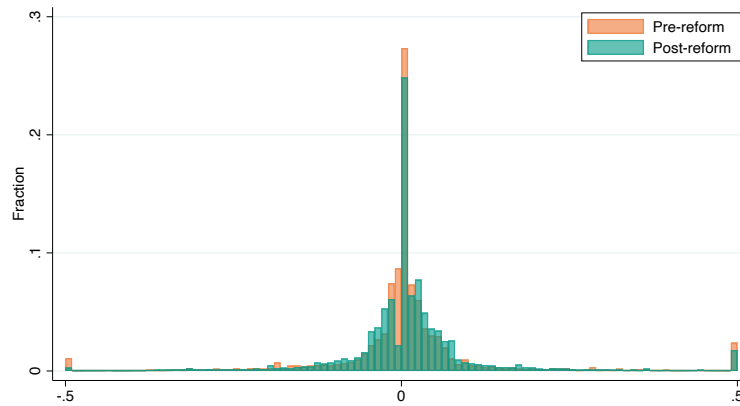


Notes: The figure shows the results of the estimation of equation (20) as discussed in section 6.3: $c_{iy} = \alpha_i + \gamma_{s(i)y} + \sum_{j \neq 2010} D_{jy} \times [f_{0j}(d_i) + \beta_{0j} \Delta \tau_i + \eta_{0j} \Delta \sigma_i + HTS_i \times (\delta_j + f_{1j}(d_i) + \beta_{1j} \Delta \tau_i + \eta_{1j} \Delta \sigma_i)] + \varepsilon_{iy}$, where $\gamma_{s(i)y}$ are segment-year fixed effects, $D_{jy} \equiv 1[y = j]$ are year dummies, and we include year-specific distance controls $f_{0j}(d_i)$ and $f_{1j}(d_i)$; and year-specific controls for property i 's tax liability change due to the reform. Panel A shows the estimated η_{1j} coefficients along with their 95% confidence intervals. Panel B shows the estimated η_{0j} coefficients along with their 95% confidence intervals.

E Additional Background on Inequity Measure (σ)

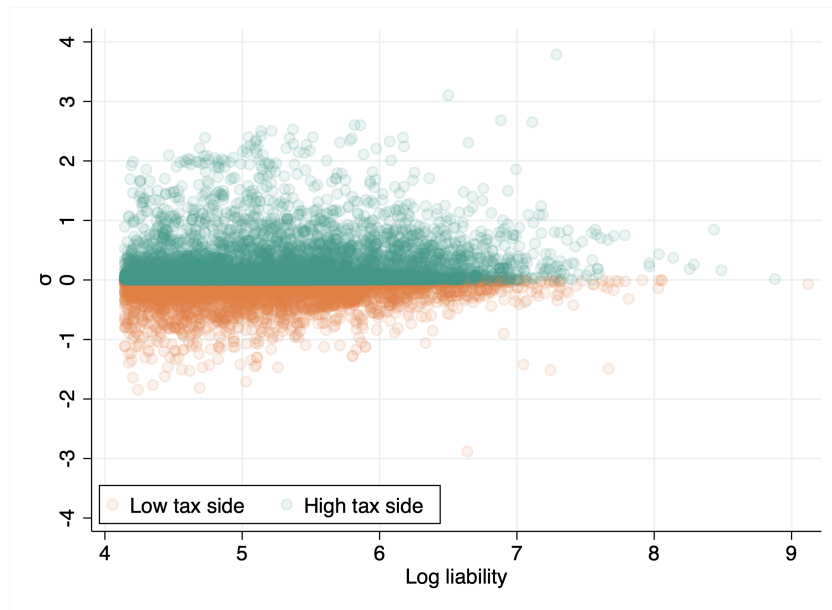
In this appendix, we provide additional evidence for our measurement of inequity (σ) and its relationship to the direct tax paid by the household (τ). Figure E.37 shows the distribution of the inequity measure for households in our sample. The histogram shows a large amount of variation in the level of inequity faced by households of different sides of the tax sectors.

FIGURE E.37: DISTRIBUTION OF σ_i



Although our measure of inequity is relative to a household's own tax liability, it is not collinear with it (figure E.38). The fact that households with the same tax liability face different levels of inequity allows us to disentangle the effect on compliance separately in section 5.

FIGURE E.38: τ_i AND σ_i ARE NOT COLLINEAR



Note: This figure plots a household's (log) tax liability against its inequity value (σ). Properties in a sector with a higher square-meter price than the neighboring sector are defined as being on the "high tax side".

F Salience of inequity

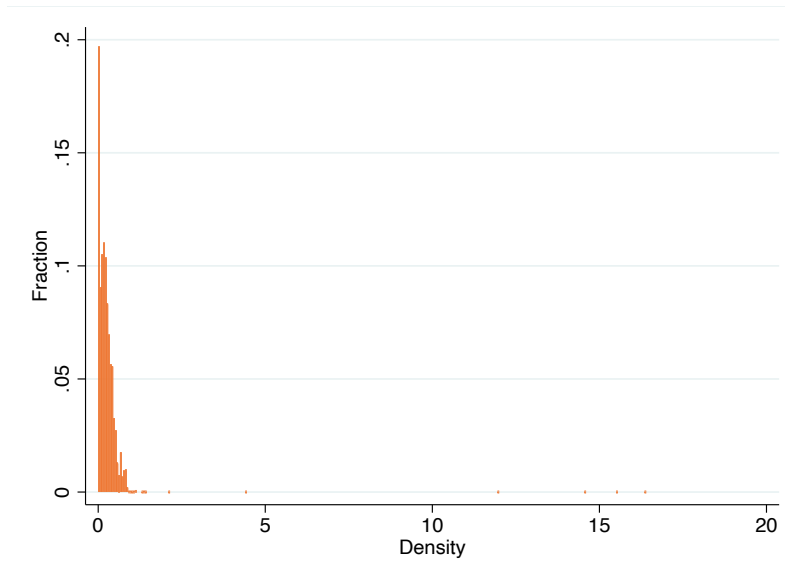
We measure the salience of inequity for each property i as how similar the properties on the same sector border, but on the other side, are to property i . Specifically, we first measure for each property what their counterfactual tax liability, $\hat{\tau}_i$. Then, we define our measure of salience as the density of $\hat{\tau}_i$ on the tax liability distribution of the other side of the boundary for each property i .

We take the following steps to estimate the density:

1. Calculate \hat{T}_i for all observations in 2010.
2. For each street segment $s \in S$ and tax sides $h \in \{0, 1\}$:
 - If there are zero or only one observation on the other side of the boundary in the same street segment, store the density as 0 for all properties on s and h .
 - Store the values \hat{T}_i of all properties in s and h . Call that set V .
 - Estimate the density of each point from V using the distribution of T_i on the other side of the boundary in the same street segment. Use the epanechnikov kernel.
 - Store the density estimator of each value from V for the properties in s and h .

The distribution of this salience measure is as follows:

FIGURE F.1: DISTRIBUTION OF OUR MEASURE OF SALIENCE



We then split our sample into disjoint groups using the quintiles of our salience measure and estimate the BDD controlling for τ_i in each group:

$$c_i = \gamma_{seg} + g(\tau_i, E_i) + f(d_i) + \beta_0 HTS_i + h(d_i) \times HTS_i + \varepsilon_i$$

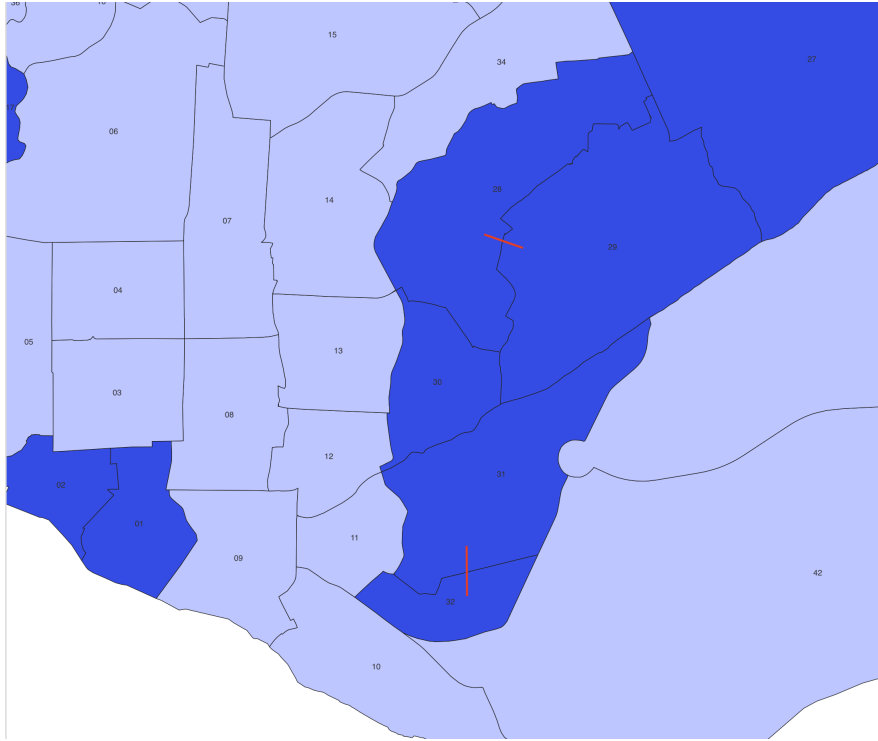
where we use splines of tau and deciles of expansiveness. The results are displayed in figure 7.

G Placebo Test for Difference in Boundary Discontinuities Design

In the Difference in Boundary Discontinuities Design, Section 5.2, we allow for discontinuities in the untreated potential outcomes G_0 at the boundaries, and for the distribution of ν_0 to be discontinuous at the boundary. This implies that we allow for selection at the boundary in the untreated potential outcomes such that the right- and left limits of $\mathbb{E}[G_0(t, d, \nu_0) | \tau = t, D = d]$ at $D = 0$ need not be the same. However, we require that the gap be constant across potential treatment levels σ_z .

To test this assumption, we constructed a placebo test using sector boundaries where there is no high tax side and therefore for all properties $\sigma_i = 0$. We then construct a dataset in which we stack the properties of each sector boundary with the properties of the closest sector boundary with a different sector rate. For instance, in figure G.1 the border from sectors 31-32 is linked to the border from sectors 28-29.³⁶ We define each boundary as “high tax boundary” or “low tax boundary” depending on the sector rates applied. For instance, the border 31-32 is defined as “low tax boundary” since the sector rate is 0.02 and the border 28-29 is defined as “high tax side” because the sector rate is 0.03.

FIGURE G.1: DISTRIBUTION OF OUR MEASURE OF SALIENCE



This allows us to construct simulated σ s that measure the difference in what each property would be if they were in the other sector boundary:

$$\tilde{\sigma}_i = \frac{T_h}{T_l} = \frac{1 + p_{d(i)} \frac{a_i}{b_i}}{1 + \hat{p}_{d(i)} \frac{a_i}{b_i}} \quad (\text{G.1})$$

³⁶We don't link 31-32 to the sectors 30-31 because they have the same sector rate as 31-32

where $d(i)$ is the boundary that i is in, $p_{d(i)}$ is the sector rate in the boundary $d(i)$ and $\hat{p}_{d(i)}$ is the sector rate in the boundary linked to $d(i)$. Nonetheless, not that the true σ_i is still 0 for all properties. This allows us to estimate the following placebo Difference in Boundary Discontinuities Design:

$$c_i = \gamma_{s(i)} + g_0(\tau_i, e_i) + f(d_i) + HTS_i \times [\beta_0 + \eta \log(\tilde{\sigma}) + h(d_i) + g_1(\tau_i, e_i)] + \varepsilon_i \quad (\text{G.2})$$

The results are displayed below.

TABLE G.1: DIFFERENCE IN BOUNDARY DISCONTINUITY DESIGN: COMPLIANCE EFFECTS AND PLACEBO INEQUITY

	(1)	(2)	(3)	(4)	(5)	(6)	(7)
1(high tax side)	-0.03 (0.02)	0.00 (.)	0.00 (.)	0.00 (.)	-2.56** (0.95)	-1.64* (0.82)	0.00 (.)
1(high tax side) $\times \sigma $	-0.05 (0.07)	-0.04 (0.07)	0.10 (0.12)	-0.05 (0.07)	0.03 (0.08)	-0.04 (0.16)	0.03 (0.08)
R^2	0.044	0.045	0.045	0.046	0.056	0.048	0.071
Distance controls	✓	✓	✓	✓	✓	✓	✓
Segment fixed effects	✓	✓	✓	✓	✓	✓	✓
τ splines	✓	✓	✓	✗	✓	✓	✗
τ deciles	✗	✗	✗	✓	✗	✗	✓
Expansiveness splines	✗	✗	✓	✗	✗	✓	✗
Expansiveness deciles	✓	✓	✗	✓	✓	✗	✓
τ splines \times HTS	✗	✓	✓	✗	✓	✓	✗
τ deciles \times HTS	✗	✗	✗	✓	✗	✗	✓
τ splines \times exp deciles	✗	✗	✗	✗	✓	✗	✗
τ splines \times exp splines	✗	✗	✗	✗	✗	✓	✗
τ deciles \times exp deciles	✗	✗	✗	✗	✗	✗	✓
τ splines \times HTS \times exp deciles	✗	✗	✗	✗	✓	✗	✗
τ splines \times HTS \times exp splines	✗	✗	✗	✗	✗	✓	✗
τ deciles \times HTS \times exp deciles	✗	✗	✗	✗	✗	✗	✓
Elasticity	-0.080 0.125	-0.076 0.126	0.184 0.210	-0.089 0.124	0.046 0.136	-0.067 0.284	0.046 0.135
N	12304	12304	12304	12304	12304	12304	12304

Notes: This table shows ...

H Discussion of house prices and IPTU

I Proof of Proposition 1

Proof. To see that the optimal property tax satisfies (2) and (3), note that without mistagging, social welfare is

$$W = \omega_L V_{Ll} + \omega_H V_{Hh} + B(r) \quad (\text{I.1})$$

The government chooses T_l and T_h to maximize W subject to its constraint that $r = c_L T_l + c_H T_h$. Without inequity, household compliance decisions depend only on the tax that they face and so the (normalized) social marginal welfare effects of changes in the two taxes are

$$\begin{aligned} \frac{dW}{dT_l} \frac{1}{b(r)} &= \frac{\omega_L}{b(r)} \frac{\partial V_{Ll}}{\partial T_l} + \frac{dr}{dT_l} = 0 \\ \frac{dW}{dT_h} \frac{1}{b(r)} &= \frac{\omega_H}{b(r)} \frac{\partial V_{Hh}}{\partial T_h} + \frac{dr}{dT_h} = 0 \end{aligned}$$

with marginal revenue effects

$$\begin{aligned} \frac{dr}{dT_l} &= c_{Ll} + \frac{dc_{Ll}}{dT_l} T_l = c_{Ll} (1 - \varepsilon) \\ \frac{dr}{dT_h} &= c_{Hh} + \frac{dc_{Hh}}{dT_h} T_h = c_{Hh} (1 - \varepsilon) \end{aligned}$$

The marginal private welfare effects are

$$\frac{\partial V_{\theta\phi}}{\partial T_\phi} = -c_{\theta\phi} u'(y_\theta - T_\phi) \simeq -c_{\theta\phi} u'(y_\theta) \left(1 + \rho \frac{T_\phi}{y_\theta} \right) \quad (\text{I.2})$$

where we approximate marginal utility using $u'(y_\theta - T_\phi) \simeq u'(y_\theta) (1 + \rho T_\phi / y_\theta)$, where $\rho \equiv -u''(x)x/u'(x)$ is the coefficient of relative risk aversion (Chetty, 2006). Combining these elements, the optimal property taxes satisfy the first order conditions

$$\frac{dW}{dT_l} \frac{1}{b(r)} = -g_L \left(1 + \rho \frac{T_l}{y_L} \right) c_L + c_L (1 - \varepsilon) = 0 \quad (\text{I.3})$$

$$\frac{dW}{dT_h} \frac{1}{b(r)} = -g_H \left(1 + \rho \frac{T_h}{y_H} \right) c_H + c_H (1 - \varepsilon) = 0 \quad (\text{I.4})$$

Solving equations (I.3) and (I.4) yields expressions (2) and (3) in Lemma 1.

To see that the level of taxation is lower the stronger are behavioral responses, note that differentiation of (2) and (3) shows that both taxes are lower when ε is higher. Since the private marginal welfare effects are strictly negative, the optimum is on the increasing side of the Laffer curve and so tax revenues also decrease.

To see that the progressivity of the tax is increasing in the relative welfare weights, combine (2) and (3) and rearrange so that we can relate the progressivity of the tax schedule to the ratio of the welfare weights:

$$\frac{g_L}{g_H} = \frac{1 + \rho T_h / y_H}{1 + \rho T_l / y_L}$$

Similarly, we can combine (2) and (3) to relate the progressivity of the tax schedule to the com-

pliance elasticity:

$$\frac{T_h/y_H}{T_l/y_L} = 1 + \frac{\left(\frac{g_L}{g_H} - 1\right)(1 - \varepsilon)}{1 - \varepsilon - g_L}$$

Differentiating with respect to ε shows that the progressivity of the optimal tax schedule is increasing in the compliance elasticity. \square

J Proof of Proposition 2

Proof. Social welfare with mistagging is

$$W = \psi \omega_L V_{Lh} + (1 - \psi) \omega_L V_{Ll} + \omega_H V_{Hh} + B(r) \quad (\text{J.1})$$

where the private welfare of the θ -types with the ϕ tag is

$$V_{\theta\phi} = \int_{-\infty}^{\gamma_{\theta\phi}^*} (u(y_\theta) - \gamma) dF(\gamma) + \int_{\gamma_{\theta\phi}^*}^{\infty} (u(y_\theta - T_\phi) - d(\sigma)) dF(\gamma) \quad (\text{J.2})$$

The optimal tax schedule satisfies $dW/dT_l = dW/dT_h = 0$.

Starting with the government's budget, total revenue is

$$r = \psi c_{L,h} T_h + (1 - \psi) c_{L,l} T_l + c_{H,h} T_h$$

and the effects of changes in taxes on tax revenue are:

$$\begin{aligned} \frac{dr}{dT_h} &= \psi \left(c_{L,h} + \frac{dc_{L,h}}{dT_h} T_h \right) + c_{H,h} + \frac{dc_{H,h}}{dT_h} T_h \\ &= \psi c_{L,h} (1 - \varepsilon - \eta) + c_{H,h} (1 - \varepsilon) \\ \frac{dr}{dT_l} &= \psi \frac{dc_{L,h}}{dT_l} T_h + (1 - \psi) \left(c_{L,l} + \frac{dc_{L,l}}{dT_l} T_l \right) \\ &= \psi c_{L,h} \eta \sigma + (1 - \psi) c_{L,l} (1 - \varepsilon) \end{aligned}$$

For the $\{Ll\}$ and the $\{Hh\}$ types, the marginal private welfare effects of a small change in the tax liability are as in equation (I.2) in the the proof of lemma 1 in appendix I. However, for the $\{Lh\}$ types we now have marginal welfare effects

$$\begin{aligned} \frac{dV_{Lh}}{dT_l} &= \int_{\gamma_{Lh}^*}^{\infty} -d'(\sigma) \frac{\partial \sigma}{\partial T_l} dF = c_{L,h} d'(\sigma) \frac{T_h}{T_l^2} \\ &\simeq c_{L,h} u'(y_L - T_h) \frac{\eta T_h}{\varepsilon T_l} \simeq c_{L,h} u'(y_L) \left[1 + \rho \frac{T_l}{y_L} \right] \frac{\eta}{\varepsilon} \sigma \\ \frac{dV_{Lh}}{dT_h} &= \int_{\gamma_{Lh}^*}^{\infty} \left[-u'(y_L - T_h) - d'(\sigma) \frac{\partial \sigma}{\partial T_h} \right] = -c_{Lh} \left[u'(y_L - T_h) + d'(\sigma) \frac{\partial \sigma}{\partial T_h} \right] \\ &\simeq -c_{Lh} u'(y_L - T_h) \left(1 + \frac{\eta}{\varepsilon} \right) \simeq -c_{L,h} u'(y_L) \left[1 + \rho \frac{T_l}{y_L} \right] \left(1 + \frac{\eta}{\varepsilon} \right) \end{aligned}$$

where we have approximated marginal utility around y_L using $u'(y) \simeq u'(y_L) \left(1 - \rho \frac{y - y_L}{y_L} \right)$. We also follow Allcott & Taubinsky (2015) and Brockmeyer *et al.* (2023) to express the marginal

disutility of inequity in money-metric terms. To see this, note that

$$\begin{aligned}\varepsilon &\equiv -\frac{\partial c_{Lh}}{\partial T_h} \frac{T_h}{c_{Lh}} = \frac{f(\gamma_{L,h}^*)}{1-F(\gamma_{Lh}^*)} \frac{\partial \gamma_{Lh}^*}{\partial T_h} T_h = \frac{f(\gamma_{Lh}^*)}{1-F(\gamma_{Lh}^*)} u'(y_L - T_h) T_h \\ \eta &\equiv -\frac{\partial c_{Lh}}{\partial \sigma} \frac{\sigma}{c_{Lh}} = \frac{f(\gamma_{Lh}^*)}{1-F(\gamma_{Lh}^*)} \frac{\partial \gamma_{Lh}^*}{\partial \sigma} \sigma = \frac{f(\gamma_{Lh}^*)}{1-F(\gamma_{Lh}^*)} d'(\sigma) \sigma \\ &\Leftrightarrow d'(\sigma) = \frac{\eta}{\varepsilon} u'(y_L - T_h) T_l\end{aligned}$$

Mistagged households have higher marginal utility for two reasons. First, they face higher taxes, reducing consumption and raising marginal utility T_h/y_L (the $\rho \frac{T_l}{y_L} \sigma$ term in the square brackets). Second, they experience disutility from inequity, with money-metric equivalent $(\eta/\varepsilon) u' T_l$. Increases in T_h aggravate both of these forces, so $dV_{Lh}/dT_h < 0$. However, even though mistagged households don't face the tax T_l , increases in T_l reduce inequity σ , improving their welfare: $dV_{Lh}/dT_l > 0$.

Combining these elements, we can see that the (normalized) marginal social welfare effects are:

$$\begin{aligned}\frac{dW}{dT_l} \frac{1}{b(r)} &= \frac{\omega_L}{b(r)} \psi \frac{dV_{L,h}}{dT_l} + \frac{\omega_L}{b(r)} (1-\psi) \frac{dV_{L,l}}{dT_l} + \frac{dr}{dT_l} \\ &\simeq g_L \psi c_{L,h} \left[1 + \rho \frac{T_l}{y_L} \sigma \right] \frac{\eta}{\varepsilon} \sigma - g_L (1-\psi) c_{L,l} \left[1 + \rho \frac{T_l}{y_L} \right] + [\psi c_{L,h} \eta \sigma + (1-\psi) c_{L,l} (1-\varepsilon)]\end{aligned}\quad (\text{J.3})$$

$$\begin{aligned}\frac{dW}{dT_h} \frac{1}{b(r)} &= \frac{\omega_L}{b(r)} \psi \frac{dV_{L,h}}{dT_h} + \frac{\omega_H}{b(r)} \frac{dV_{H,h}}{dT_h} + \frac{dr}{dT_h} \\ &\simeq -g_L \psi c_{L,h} \left[1 + \rho \frac{T_h}{y_L} \right] \left(1 + \frac{\eta}{\varepsilon} \right) - g_H c_{H,h} \left[1 + \rho \frac{T_h}{y_H} \right] + [\psi c_{L,h} (1-\varepsilon-\eta) + c_{H,h} (1-\varepsilon)]\end{aligned}\quad (\text{J.4})$$

Dividing (J.3) and (J.4) by the number of taxpayers of each tax, these can be written as

$$\frac{dW}{dT_l} \frac{1}{b(r)} \frac{1}{(1-\psi) c_{Ll}} \simeq g_L \varphi_l \left[1 + \rho \frac{T_l}{y_L} \sigma \right] \frac{\eta}{\varepsilon} \sigma - g_L \left[1 + \rho \frac{T_l}{y_L} \right] + \varphi_l \eta \sigma + (1-\varepsilon) = 0 \quad (\text{J.5})$$

$$\begin{aligned}\frac{dW}{dT_h} \frac{1}{b(r)} \frac{1}{\psi c_{Lh} + c_{Hh}} &\simeq -g_L \varphi_h \left[1 + \rho \frac{T_h}{y_L} \right] \left(1 + \frac{\eta}{\varepsilon} \right) - g_H (1-\varphi_h) \left[1 + \rho \frac{T_h}{y_H} \right] \\ &\quad + \varphi_h (1-\varepsilon-\eta) + (1-\varphi_h) (1-\varepsilon) = 0\end{aligned}\quad (\text{J.6})$$

where $\varphi_l = \psi c_{Lh}/(1-\psi) c_{Ll}$ is the number of mistagged L households relative to the number of l -tax taxpayers; and $\varphi_h = \psi c_{Lh}/(\psi c_{Lh} + c_{Hh})$ is the number of mistagged L households relative to the number of h -tax taxpayers.

Rearranging (J.5) and (J.6) yields the expressions (6) and (7) for the optimal tax schedule in proposition 2. Applying the implicit function theorem to the system of equations (J.5) and (J.6) yields the comparative static statements in proposition 2. \square

K Model with Undertagging and Overtagging

This appendix presents the details of the model briefly discussed in section 3.3.1. We generalize the model in section 3.2 in two ways. First, we allow for a fraction $\psi_{Hl} \geq 0$ of H -type households to be undertagged with the l tag (in addition to the fraction ψ_{Lh} of overtagged L -types). This creates a fourth group of households whose compliance and marginal welfare effects we need to incorporate into the analysis. Second, we allow undertagged and overtagged households to have different elasticities of compliance with respect to inequity. Undertagged households' elasticity is η_{Hl} while overtagged households' elasticity is η_{Lh} . This is important since our empirical evidence in section 6.3 suggests that undertagged households do not respond to inequity, only overtagged households do.

Undertagged households' compliance responds to both the high-tag tax T_h and the low-tag tax T_l . Specifically,

$$\begin{aligned}\frac{dc_{Hl}}{dT_h} &= \frac{\partial c_{Hl}}{\partial \sigma_{Hl}} \frac{\partial \sigma_{Hl}}{\partial T_h} = \frac{c_{Hl}}{\sigma_{Hl}} \eta_{Hl} \frac{T_l}{T_h^2} = \frac{c_{Hl}}{T_h} \eta_{Hl} \\ \frac{dc_{Hl}}{dT_l} &= \frac{\partial c_{Hl}}{\partial T_l} + \frac{\partial c_{Hl}}{\partial \sigma_{Hl}} \frac{\partial \sigma_{Hl}}{\partial T_l} = -\varepsilon \frac{c_{Hl}}{T_l} - \eta_{Hl} \frac{c_{Hl}}{\sigma_{Hl}} \frac{1}{T_h} = -\frac{c_{Hl}}{T_l} (\varepsilon + \eta_{Hl})\end{aligned}$$

We can also connect the marginal disutility of inequity and the marginal utility of consumption for this fourth group:

$$\begin{aligned}\gamma_{Hl}^* &= u(y_H) - u(y_H - T_l) + d(\sigma_{Hl}) & \frac{\partial \gamma_{Hl}^*}{\partial T_l} &= u'(y_H - T_l) & \frac{\partial \gamma_{Hl}^*}{\partial \sigma_{Hl}} &= d'(\sigma_{Hl}) \\ \varepsilon &\equiv -\frac{\partial c_{Hl}}{\partial T_l} \frac{T_l}{c_{Hl}} = \frac{f(\gamma_{Hl}^*)}{1 - F(\gamma_{Hl}^*)} \frac{\partial \gamma_{Hl}^*}{\partial T_l} T_l & \eta_{Hl} &\equiv -\frac{\partial c_{Hl}}{\partial \sigma_{Hl}} \frac{\sigma_{Hl}}{c_{Hl}} \frac{f(\gamma_{Hl}^*)}{1 - F(\gamma_{Hl}^*)} \frac{\partial \gamma_{Hl}^*}{\partial \sigma_{Hl}} \sigma_{Hl} \\ &\leftrightarrow d'(\sigma_{Hl}) = \frac{\eta_{Hl}}{\varepsilon} u'(y_H - T_l) T_h\end{aligned}$$

Incorporating the undertagged households, the revenue from taxation now becomes:

$$r = \psi_{Lh} c_{Lh} T_h + (1 - \psi_{Lh}) c_{Ll} T_l + \psi_{Hl} c_{Hl} T_l + (1 - \psi_{Hl}) c_{Hh} T_h$$

the effects of tax changes are:

$$\begin{aligned}\frac{dr}{dT_h} &= \psi_{Lh} \left(c_{Lh} + \frac{dc_{Lh}}{dT_h} T_h \right) + \psi_{Hl} \frac{dc_{Hl}}{dT_h} T_l + (1 - \psi_{Hl}) \left(c_{Hh} + \frac{dc_{Hh}}{dT_h} T_h \right) \\ &= \psi_{Lh} c_{Lh} (1 - \varepsilon - \eta_{Lh}) + \psi_{Hl} c_{Hl} \eta_{Hl} \frac{1}{\sigma} + (1 - \psi_{Hl}) c_{Hh} (1 - \varepsilon) \\ \frac{dr}{dT_l} &= \psi_{Lh} \frac{dc_{Lh}}{dT_l} T_h + (1 - \psi_{Lh}) \left(c_{Lh} + \frac{dc_{Ll}}{dT_l} T_l \right) + \psi_{Hl} \left(c_{Hl} + \frac{dc_{Hl}}{dT_l} T_l \right) \\ &= \psi_{Lh} c_{Lh} \eta \sigma + (1 - \psi_{Lh}) c_{Ll} (1 - \varepsilon) + \psi_{Hl} c_{Hl} (1 - \varepsilon - \eta_{Hl})\end{aligned}$$

where $\sigma = T_h/T_l$ is the extent of inequity (but note that $\sigma_{Hl} = 1/\sigma$ while $\sigma_{Lh} = \sigma$).

The undertagged H -type households have private welfare

$$V_{Hl} = \int_{-\infty}^{\gamma_{Hl}^*} [u(y_H) - \gamma] dF(\gamma) + \int_{\gamma_{Hl}^*}^{\infty} [u(y_H - T_l) - d(\sigma_{Hl})] dF(\gamma)$$

with marginal welfare effects

$$\begin{aligned}
\frac{dV_{Hl}}{dT_l} &= \int_{\gamma_{Hl}^*}^{\infty} \left[-u'(y_H - T_l) - d'(\sigma_{Hl}) \frac{\partial \sigma_{Hl}}{\partial T_l} \right] dF(\gamma) = -c_{Hl} \left[u'(y_H - T_l) + d'(\sigma_{Hl}) \frac{1}{T_h} \right] \\
&\simeq -c_{Lh} u'(y_H - T_l) \left(1 + \frac{\eta_{Hl}}{\varepsilon} \right) \simeq -c_{Lh} u'(y_H) \left[1 + \rho \frac{T_l}{y_H} \right] \left(1 + \frac{\eta_{Hl}}{\varepsilon} \right) \\
\frac{dV_{Hl}}{dT_h} &= \int_{\gamma_{Hl}^*}^{\infty} -d'(\sigma_{Hl}) \frac{\partial \sigma_{Hl}}{\partial T_h} dF(\gamma) = c_{Hl} d'(\sigma_{Hl}) \frac{T_l}{T_h^2} \\
&\simeq c_{Hl} u'(y_H - T_l) \frac{\eta_{Hl}}{\varepsilon} \frac{T_l}{T_h} \simeq c_{Hl} u'(y_H) \left[1 + \rho \frac{T_l}{y_H} \right] \frac{\eta_{Hl}}{\varepsilon} \frac{1}{\sigma}
\end{aligned}$$

Combining these elements, we can see that the marginal social welfare effects are:

$$\begin{aligned}
W &= \omega_L \psi_{Lh} V_{Lh} + \omega_L (1 - \psi_{Lh}) V_{Ll} + \omega_H \psi_{Hl} V_{Hl} + \omega_H (1 - \psi_{Hl}) V_{Hh} + B(r) \\
\frac{dW}{dT_l} \frac{1}{b(r)} &= \omega_L \psi_{Lh} \frac{dV_{Lh}}{dT_l} + \omega_L (1 - \psi_{Lh}) \frac{dV_{Ll}}{dT_l} + \omega_H \psi_{Hl} \frac{dV_{Hl}}{dT_l} + b(r) \frac{dr}{dT_l} \\
&\simeq g_L \psi_{Lh} c_{Lh} \left[1 + \rho \frac{T_h}{y_L} \right] \frac{\eta_{Lh}}{\varepsilon} \sigma - g_L (1 - \psi_{Lh}) c_{Ll} \left(1 + \rho \frac{T_l}{y_L} \right) \\
&\quad - g_H \psi_{Hl} c_{Hl} \left[1 + \rho \frac{T_l}{y_H} \right] \left(1 + \frac{\eta_{Hl}}{\varepsilon} \right) \\
&\quad + [\psi_{Lh} c_{Lh} \eta_{Lh} \sigma + (1 - \psi_{Lh}) c_{Ll} (1 - \varepsilon) + \psi_{Hl} c_{Hl} (1 - \varepsilon - \eta_{Hl})] \\
\frac{dW}{dT_h} \frac{1}{b(r)} &= \omega_L \psi_{Lh} \frac{dV_{Lh}}{dT_h} + \omega_H \psi_{Hl} \frac{dV_{Hl}}{dT_h} + \omega_H (1 - \psi_{Hl}) \frac{dV_{Hh}}{dT_h} + b(r) \frac{dr}{dT_h} \\
&\simeq -g_L \psi_{Lh} c_{Lh} \left[1 + \rho \frac{T_h}{y_L} \right] \left(1 + \frac{\eta_{Lh}}{\varepsilon} \right) + g_H \psi_{Hl} c_{Hl} \left[1 + \rho \frac{T_l}{y_H} \right] \frac{\eta_{Hl}}{\varepsilon} \frac{1}{\sigma} \\
&\quad - g_H (1 - \psi_{Hl}) c_{Hh} \left(1 + \rho \frac{T_h}{y_H} \right) \\
&\quad + [\psi_{Lh} c_{Lh} (1 - \varepsilon - \eta_{Lh}) + \psi_{Hl} c_{Hl} \eta_{Hl} \frac{1}{\sigma} + (1 - \psi_{Hl}) c_{Hh} (1 - \varepsilon)]
\end{aligned}$$

Rearranging these yields the expressions for the optimal tax schedule in section 3.3.1:

$$\begin{aligned}
\frac{T_l}{y_L} &= \frac{1 - \varepsilon - \bar{g}_l + \varphi_{Ll} \frac{\eta_{Lh}}{\varepsilon} \sigma (g_L + \varepsilon) - \varphi_{Hl} \frac{\eta_{Hl}}{\varepsilon} (g_H + \varepsilon)}{\rho \left(\bar{g}_l + g_H \varphi_{Hl} \left[\left(1 + \frac{\eta_{Hl}}{\varepsilon} \right) \frac{y_L}{y_H} - 1 \right] - g_L \varphi_{Ll} \frac{\eta_{Lh}}{\varepsilon} \sigma^2 \right)} \\
\frac{T_h}{y_H} &= \frac{1 - \varepsilon - \bar{g}_h + \varphi_{Hh} \frac{\eta_{Hl}}{\varepsilon} \frac{1}{\sigma} (g_H + \varepsilon) - \varphi_{Lh} \frac{\eta_{Lh}}{\varepsilon} (g_L + \varepsilon)}{\rho \left(\bar{g}_h + g_L \varphi_{Lh} \left[\left(1 + \frac{\eta_{Lh}}{\varepsilon} \right) \frac{y_H}{y_L} - 1 \right] - g_H \varphi_{Hh} \frac{\eta_{Hl}}{\varepsilon} \frac{1}{\sigma^2} \right)}
\end{aligned}$$

L Model with Location Choice and Endogenous House Prices

This appendix presents the details of the model briefly discussed in section 3.3.2. In section L.1 we present a micro-founded model of residential location choice, while in section L.2 we study the welfare implications and optimal policy.

L.1 Location Choice

We consider an extension of the model presented in section 3.2 in which households first choose where to live and then whether to pay the corresponding property tax. Households are characterized by three traits: First, they have an evasion cost γ that governs how much utility they lose from evading the tax, as in section 3.2. Second, they have idiosyncratic preferences for the houses on the high side of the boundary ξ_h and the low side ξ_l . Third, they are either high or low-income $y_H \gg y_L$. For simplicity, we will assume that H -type houses are sufficiently expensive that high-income households are never willing to live in an L -type house, so that we can focus only on the choice of low-income households between L -type houses in the low-tax sector and L -type houses in the high-tax sector.

A household living in a house tagged ϕ that pays its property tax receives utility

$$u_{L\phi}^{\text{pay}} = u(v_L - p_{L\phi} - T_\phi) - d(\tilde{\sigma}) + \xi_\phi \quad (\text{L.1})$$

where v_L is the value of the housing services the house provides and $p_{L\phi}$ is the (annualized) market price of a house of type L with a tag of ϕ . Note that this price does not depend on whether taxes are paid, it is a market price for that type of house. Of course, households who anticipate not paying their property taxes would have a higher willingness to pay for the house than those who plan to evade. The disutility from inequity now reflects only the portion of inequity that is not capitalized into house prices: $\tilde{\sigma} = \left(1 + \frac{p_{Lh} - p_{Ll}}{T_h - T_l}\right) \frac{T_h}{T_l}$. At the extreme, when tax differences are fully capitalized into house prices, $p_{Ll} - p_{Lh} = T_h - T_l$ and $\tilde{\sigma} = 0$, and so households no longer experience inequity. However, whenever tax differences are less than fully capitalized into house prices, mistagging still generates inequity and shapes optimal policy schedules.

If, on the other hand, households don't pay their property tax, they receive utility

$$u_{L\phi}^{\text{evade}} = u(v_L - p_{L\phi}) - \gamma + \xi_\phi \quad (\text{L.2})$$

Households pay their property tax whenever this makes them better off:

$$\begin{aligned} u_{Ll}^{\text{pay}} > u_{Ll}^{\text{evade}} &\leftrightarrow \gamma > \gamma_l^* = u(v_L - p_{Ll}) - u(v_L - p_{Ll} - T_l) \\ u_{Lh}^{\text{pay}} > u_{Lh}^{\text{evade}} &\leftrightarrow \gamma > \gamma_h^* = u(v_L - p_{Lh}) - u(v_L - p_{Lh} - T_h) + d(\tilde{\sigma}) \end{aligned}$$

Assuming there is no over-capitalization of taxes into house prices (i.e. that $p_{Ll} - p_{Lh} \leq T_h - T_l$), we can also see that this means that $\gamma_h^* > \gamma_l^*$.

The thresholds γ_l^*, γ_h^* define three types of households, and we can characterize the location choice of each type in turn.

First, for households with $\gamma > \gamma_h^*$, who pay their taxes regardless of which location they

choose, they prefer the high-tax side to the low-tax side whenever

$$\begin{aligned} u(v_L - p_{Lh} - T_h) - d(\tilde{\sigma}) + \xi_h &> u(v_L - p_{Ll} - T_l) + \xi_l \\ \Delta\xi = \xi_h - \xi_l &> u(v_L - p_{Ll} - T_l) - u(v_L - p_{Lh} - T_h) + d(\tilde{\sigma}) = \xi_{hh}^* \geq 0 \end{aligned} \quad (\text{L.3})$$

Second, for households with $\gamma < \gamma_l^*$, who evade the tax regardless of which location they choose, they prefer the high-tax side whenever

$$\begin{aligned} u(v_L - p_{Lh}) + \xi_h &> u(v_L - p_{Ll}) + \xi_l \\ \Delta\xi = \xi_h - \xi_l &> u(v_L - p_{Ll}) - u(v_L - p_{Lh}) = \xi_{hl}^* \leq 0 \end{aligned} \quad (\text{L.4})$$

Finally, the third, intermediate group has $\gamma_l^* < \gamma \leq \gamma_h^*$. These households evade on the high-tax side, but pay property tax on the low-tax side. They prefer to live on the high-tax side (and evade the property tax) whenever

$$\begin{aligned} u(v_L - p_{Lh}) - \gamma + \xi_h &> u(v_L - p_{Ll} - T_l) + \xi_l \\ \gamma &< u(v_L - p_{Lh}) - u(v_L - p_{Ll} - T_l) + \xi_h - \xi_l = \bar{\gamma}(\Delta\xi) \end{aligned} \quad (\text{L.5})$$

Combining conditions (L.3), (L.4), and (L.5), we can characterize all households' location and evasion decisions. Household i chooses location ϕ and compliance $\in \{\text{pay}, \text{evade}\}$ according to:

$$\{\phi^i, \text{compliance}^i\} = \begin{cases} \{l, \text{evade}\}, & \text{if } \gamma^i \leq \gamma_l^* \text{ \& } \Delta\xi^i \leq \xi_{hl}^*; \\ \{l, \text{pay}\}, & \text{if } (\gamma^i > \gamma_l^* \text{ \& } \Delta\xi^i \leq \xi_{hl}^*) \text{ or } (\gamma^i > \bar{\gamma}(\Delta\xi^i) \text{ \& } \xi_{hl}^* < \Delta\xi^i \leq \xi_{hh}^*); \\ \{h, \text{evade}\}, & \text{if } (\gamma^i \leq \bar{\gamma}(\Delta\xi^i) \text{ \& } \xi_{hl}^* < \Delta\xi^i \leq \xi_{hh}^*) \text{ or } (\gamma^i > \gamma_h^* \text{ \& } \Delta\xi^i > \xi_{hh}^*); \\ \{h, \text{pay}\}, & \text{if } \gamma^i > \gamma_h^* \text{ \& } \Delta\xi^i > \xi_{hh}^*. \end{cases} \quad (\text{L.6})$$

Figure L.1 illustrates the four types of households and the boundaries dividing them.

Equation L.6 characterizes households' decisions taking taxes T_ϕ and house prices $p_{L\phi}$ as given. To pin down prices, we need the demand for each type of house to equal the supply. If the joint distribution of $\gamma, \Delta\xi$ is given by $J(\gamma, \Delta\xi)$, then the demand for houses on the low-tax side is

$$Q_l^D = \int_{-\infty}^{\xi_{hl}^*} \int_{-\infty}^{\infty} j(\gamma, \Delta\xi) d\gamma d\Delta\xi + \int_{\xi_{hl}^*}^{\xi_{hh}^*} \int_{\bar{\gamma}(\Delta\xi)}^{\infty} j(\gamma, \Delta\xi) d\gamma d\Delta\xi$$

Similarly demand for houses on the high-tax side is

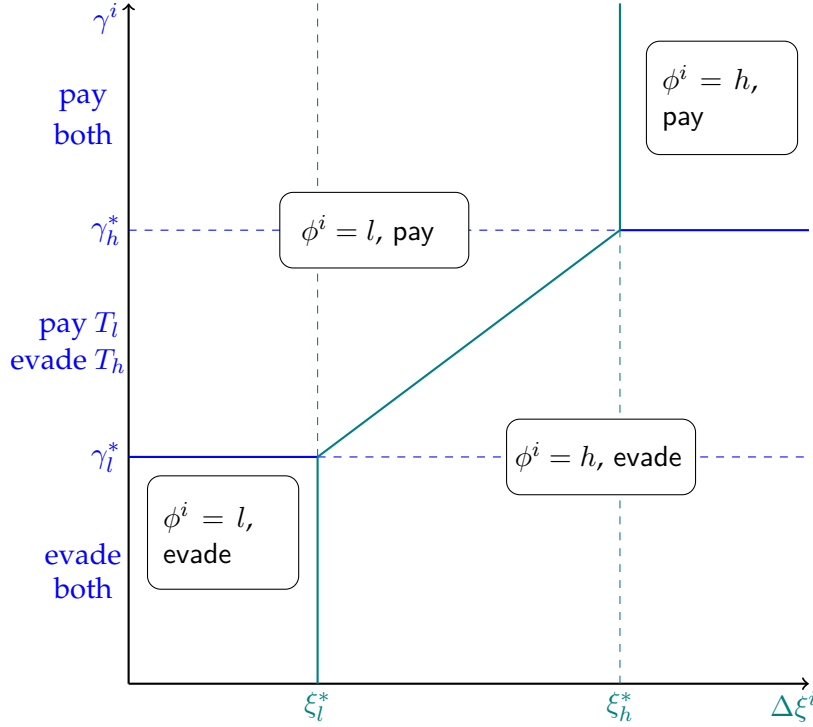
$$Q_h^D = \int_{\xi_{hl}^*}^{\xi_{hh}^*} \int_{-\infty}^{\bar{\gamma}(\xi_h)} j(\gamma, \xi_h) d\gamma d\xi_h + \int_{\xi_{hh}^*}^{\infty} \int_{-\infty}^{\infty} j(\gamma, \xi_h) d\gamma d\xi_h$$

And prices adjust to equilibrate the market such that

$$Q_l^D = Q_l^S = 1 - \psi \quad \& \quad Q_h^D = Q_h^S = \psi \quad (\text{L.7})$$

These pin down the equilibrium prices and hence define the cutoffs $\gamma_l^*, \gamma_h^*, \xi_{hl}^*, \xi_{hh}^*$ and the

FIGURE L.1: LOCATION AND COMPLIANCE CHOICES



function $\bar{\gamma}(\Delta\xi)$. Given these, the compliance rates are given by

$$c_{Ll} = \frac{1}{1-\psi} \left(\int_{-\infty}^{\xi_{ll}^*} \int_{\gamma_l^*}^{\infty} j(\gamma, \Delta\xi) d\gamma d\Delta\xi + \int_{\xi_{hl}^*}^{\xi_{hh}^*} \int_{\bar{\gamma}(\Delta\xi)}^{\infty} j(\gamma, \Delta\xi) d\gamma d\Delta\xi \right) \quad (L.8)$$

$$c_{Lh} = \frac{1}{\psi} \int_{\xi_{hh}^*}^{\infty} \int_{\bar{\gamma}(\Delta\xi)}^{\infty} j(\gamma, \Delta\xi) d\gamma d\Delta\xi \quad (L.9)$$

In this model, changes in taxes affect compliance through three channels. Consider, for example, a small increase in the high tax T_h . This affects compliance through

1. A direct effect: A higher T_h leads to a higher γ_h (holding house prices fixed), reducing compliance.
2. A mobility effect: A higher T_h (holding house prices fixed) makes living in the high-tax sector less attractive (to those who pay it), raising ξ_h^* and causing a set of compliant households in the high-tax sector to move to the low-tax sector.
3. A house-price effect: A higher T_h reduces demand for houses in the high-tax sector. To equilibrate demand and supply, the price of houses in the high-tax sector, p_{Lh} falls, and this affects compliance decisions by lowering the marginal utility of consumption of paying taxes, and dampening the increase in effective inequity $\tilde{\sigma}$ from the increase in T_h .

Our empirical analysis captures the combination of these three mechanisms. For small changes in taxes, the effect of taxes on location choices causes no first-order welfare effects by the envelope theorem, but the overall effects of tax changes on compliance capture the full fiscal externality that is relevant for welfare, and so our empirical analysis captures the relevant

empirical quantities. However, as the model above shows, house price changes have first-order effects on households' welfare, and these can affect the welfare effects of tax policy and the shape of the optimal tax schedule. The next section explores these issues in more detail.

L.2 Welfare and Optimal Policy

As described above, incorporating mobility into the model creates two new channels through which taxes affect compliance: a mobility effect and a house-price effect. However, by the envelope theorem, only the house-price effect has first-order effects on households' welfare. What does matter for policy design is the size of the fiscal externality, and for this we want to capture the net of the three effects.

To achieve this, we generalize the model slightly and instead of committing to a specific model of household residential choice we capture the reduced form effect of taxes on prices through the expression $p_\theta(T_\phi) = p_\theta^0 - \kappa T_\phi$ where the parameter κ governs the degree of capitalization of taxes into house prices. We also continue to consider reduced-form elasticities of compliance ε and η that allow for all channels through which taxes affect compliance.

In this model, the private welfare of the three types of households is given by³⁷

$$\begin{aligned} V_{Ll} &= \int_{-\infty}^{\gamma_{Ll}^*} [u(v_L - p_L(T_l)) - \gamma] dF(\gamma) + \int_{\gamma_{Ll}^*}^{\infty} [u(v_L - p_L(T_l) - T_l)] dF(\gamma) \\ V_{Lh} &= \int_{-\infty}^{\gamma_{Lh}^*} [u(v_L - p_L(T_h)) - \gamma] dF(\gamma) + \int_{\gamma_{Lh}^*}^{\infty} [u(v_L - p_L(T_h) - T_h) - d(\tilde{\sigma})] dF(\gamma) \\ V_{Hh} &= \int_{-\infty}^{\gamma_{Hh}^*} [u(v_H - p_H(T_h)) - \gamma] dF(\gamma) + \int_{\gamma_{Hh}^*}^{\infty} [u(v_H - p_H(T_h - T_h))] dF(\gamma) \end{aligned}$$

Starting with the correctly tagged households, the marginal private welfare effects are now

$$\begin{aligned} \frac{\partial V_L}{\partial T_l} &= (1 - c_{Ll}) u'(y_L(T_l)) \kappa - c_{Ll} u'(y_L(T_l) - T_l) (1 - \kappa) \\ &\simeq (1 - c_L) u'(y_L(T_l)) \kappa - c_{Ll} u'(y_L(T_l)) \left(1 + \rho \frac{T_l}{y_L(T_l)}\right) (1 - \kappa) \\ &= \kappa u'(y_L(T_l)) \left(1 + c_{Ll} \rho \frac{T_l}{y_L(T_l)}\right) - c_{Ll} u'(y_L(T_l)) \left(1 + \rho \frac{T_l}{y_L(T_l)}\right) \end{aligned} \quad (\text{L.10})$$

$$\frac{\partial V_H}{\partial T_h} = \kappa u'(y_H(T_h)) \left(1 + c_{Hh} \rho \frac{T_h}{y_H(T_h)}\right) - c_{Hh} u'(y_H(T_h)) \left(1 + \rho \frac{T_h}{y_H(T_h)}\right) \quad (\text{L.11})$$

where we introduced the notation that $y_\theta(T_\phi) = v_\theta - p_\theta(T_\phi)$ and we used the approximation to marginal utility that $u'(y_\theta(T_\phi) + x) \simeq u'(y_\theta(T_\phi)) \left(1 - \rho \frac{x}{y_\theta(T_\phi)}\right)$.

We get two extra effects:

1. All households have higher utility from the capitalization of tax liabilities into house prices. This is the $u'(\tilde{y}_{\theta\phi})\kappa \times 1$ term. Note, this applies also to the households that don't pay the tax since we assume it affects the market price of houses and that there is no price discrimination by tax evasion.

³⁷In the specific model of household mobility outlined above, the expressions below hold conditional on location taste $\Delta\xi^i$, and the overall welfare integrates across location tastes to yield expressions like the ones below.

2. Households who do pay the tax enjoy even higher utility since they pay the tax on top of gaining utility from the lower house price. That is, the higher house price dampens the utility loss from paying the tax due to the concavity of the utility function (governed by ρ).

This is the $u'(\tilde{y}_{\theta\phi})\kappa \times c_{\theta}\rho\frac{T_{\phi}}{\tilde{y}_{\theta\phi}}$ term.

Turning to the mistagged households, as before, we will want to express their marginal disutility from inequity $d'(\tilde{\sigma})$ in dollar terms and we use the responsiveness of compliance to inequity and the tax liability to do so. To do this, we use the definitions of the reduced-form elasticities ε and η :

$$\eta \equiv -\frac{\partial c}{\partial \sigma} \frac{\sigma}{c} = \frac{\partial c}{\partial \gamma^*} \frac{\partial \gamma^*}{\partial \sigma} \frac{\sigma}{c} = (1 - \kappa) d'(\tilde{\sigma}) \frac{f(\gamma^*)}{1 - F(\gamma^*)} \sigma \quad (\text{L.12})$$

$$\begin{aligned} \varepsilon &\equiv -\frac{\partial c}{\partial T_{\phi}} \frac{T_{\phi}}{c} = \frac{\partial c}{\partial \gamma^*} \frac{\partial \gamma^*}{\partial T_{\phi}} \frac{T_{\phi}}{c} \\ &= \left[-u'(y_{\theta}(T_{\phi})) \frac{\partial p_{\theta}(T_{\phi})}{\partial T_{\phi}} + u'(y_{\theta}(T_{\phi}) - T_{\phi}) \left(1 + \frac{\partial p_{\theta}(T_{\phi})}{\partial T_{\phi}} \right) \right] \frac{f(\gamma^*)}{1 - F(\gamma^*)} T_{\phi} \\ &= [u'(y_{\theta}(T_{\phi}))\kappa + u'(y_{\theta}(T_{\phi}) - T_{\phi})(1 - \kappa)] \frac{f(\gamma^*)}{1 - F(\gamma^*)} T_{\phi} \end{aligned} \quad (\text{L.13})$$

Where we see that now the elasticity with respect to the tax liability will be stronger since $u(\cdot)$ is strictly concave and $y' < 0$.

It also changes how we use the relationship between the two elasticities to express $d(\tilde{\sigma})$ in terms of elasticities: Combining (L.12) and (L.13), gives us

$$d'(\tilde{\sigma}) = \frac{\eta}{\varepsilon} \left[u'(y_L(T_h) - T_h) + u'(y_L(T_h)) \frac{\kappa}{1 - \kappa} \right] T_l \quad (\text{L.14})$$

Combining these expressions we can see that the effect of marginal changes in the low-type tax T_l is

$$\begin{aligned} \frac{\partial V_{Lh}}{\partial T_l} &= \int_{\gamma_{Lh}^*}^{\infty} -d'((1 - \kappa)\sigma)(1 - \kappa) \frac{\partial \sigma}{\partial T_l} dF(\gamma) = c_{Lh} d'((1 - \kappa)\sigma)(1 - \kappa) \frac{\sigma}{T_l} \\ &= c_{Lh} \frac{\eta}{\varepsilon} \sigma [u'(y_L(T_h) - T_h)(1 - \kappa) + \kappa u'(y_L(T_h))] \\ &\simeq c_{L,h} \frac{\eta}{\varepsilon} \sigma u'(y_L(T_l)) \left(1 + \rho[\kappa(1 - \sigma) + \sigma(1 - \kappa)] \frac{T_l}{y_L(T_l)} \right) \end{aligned} \quad (\text{L.15})$$

while the effect of a marginal change in the high-type tax T_h is

$$\begin{aligned}
\frac{\partial V_{Lh}}{\partial T_h} &= \int_{-\infty}^{\gamma_{Lh}^*} u'(y_L(T_h)) \frac{\partial y_L}{\partial T_h} dF(\gamma) + \int_{\gamma_{Lh}^*}^{\infty} \left[u'(y_L(T_h) - T_h) \left(\frac{\partial p_L}{\partial T_h} - 1 \right) - d'((1 - \kappa)\sigma)(1 - \kappa) \frac{\partial \sigma}{\partial T_h} \right] dF(\gamma) \\
&= (1 - c_{Lh}) u'(y_L(T_h)) \kappa + c_{Lh} \left[u'(y_L(T_h) - T_h) (\kappa - 1) - d'((1 - \kappa)\sigma)(1 - \kappa) \frac{1}{T_l} \right] \\
&= (1 - c_{Lh}) u'(y_L(T_h)) \kappa - c_{Lh} u'(y_L(T_h) - T_h) (1 - \kappa) \\
&\quad - c_{Lh} (1 - \kappa) \frac{\eta}{\varepsilon} \left[u'(y_L(T_h) - T_h) + u'(y_L(T_h)) \frac{\kappa}{1 - \kappa} \right] \\
&= u'(y_L(T_h)) \kappa \left[1 - c_{Lh} \left(1 + \frac{\eta}{\varepsilon} \right) \right] - c_{Lh} u'(y_L(T_h) - T_h) (1 - \kappa) \left(1 + \frac{\eta}{\varepsilon} \right) \\
&\simeq u'(y_L(T_l)) \left[1 - \rho \kappa \left(1 - \frac{1}{\sigma} \right) \frac{y_H}{y_L} \frac{T_h}{y_L(T_l)} \right] \kappa \left[1 - c_{Lh} \left(1 + \frac{\eta}{\varepsilon} \right) \right] \\
&\quad - c_{Lh} u'(y_L(T_l)) \left[1 + \rho \frac{y_H}{y_L} \left[1 - \kappa \left(1 - \frac{1}{\sigma} \right) \right] \frac{T_h}{y_H(T_h)} \right] (1 - \kappa) \left(1 + \frac{\eta}{\varepsilon} \right) \\
&= u'(y_L(T_l)) \kappa \left[1 - \rho \kappa \left(1 - \frac{1}{\sigma} \right) \frac{y_H}{y_L} \frac{T_h}{y_H(T_h)} \right] \\
&\quad - c_{Lh} u'(y_L(T_l)) \left[1 + \rho \left[(1 - \kappa) - \left(1 - \frac{1}{\sigma} \right) \kappa \right] \frac{y_H}{y_L} \frac{T_h}{y_H(T_h)} \right] \left(1 + \frac{\eta}{\varepsilon} \right) \tag{L.16}
\end{aligned}$$

Marginal Welfare Effects and Optimal Taxes Turning to the social welfare effects and optimal taxation, the equations get uglier, but the intuition is very much the same. Social welfare, as before, is given by

$$W = \omega_L [\psi V_{Lh} + (1 - \psi) V_{Ll}] + \omega_H V_{Hh} + B(r) \tag{L.17}$$

This means that the normalized marginal welfare effect of the low-type tax T_l is

$$\begin{aligned}
\frac{\partial W}{\partial T_l} \frac{1}{b(r)} &= \frac{\omega_L}{b(r)} \left[\psi \frac{\partial V_{Lh}}{\partial T_l} + (1 - \psi) \frac{\partial V_{Ll}}{\partial T_l} \right] + \frac{\omega_H}{b(r)} \frac{\partial V_{Hh}}{\partial T_l} + \frac{\partial r}{\partial T_l} \\
&= \psi g_L c_{Lh} \frac{\eta}{\varepsilon} \sigma \left(1 + \rho [(1 - \sigma) \kappa + \sigma (1 - \kappa)] \frac{T_l}{y_L(T_l)} \right) \\
&\quad + (1 - \psi) g_L \left[\kappa \left(1 + c_{Ll} \rho \frac{T_l}{y_L(T_l)} \right) - c_{Ll} \left(1 + \rho \frac{T_l}{y_L(T_l)} \right) \right] + \psi c_{Lh} \eta \sigma + (1 - \psi) c_{Ll} (1 - \varepsilon) \tag{L.18}
\end{aligned}$$

and the normalized marginal welfare effect of the high-type tax T_h is

$$\begin{aligned}
\frac{\partial W}{\partial T_h} \frac{1}{b(r)} &= \frac{\omega_L}{b(r)} \left[\psi \frac{\partial V_{Lh}}{\partial T_h} + (1 - \psi) \frac{\partial V_{Ll}}{\partial T_h} \right] + \frac{\omega_H}{b(r)} \frac{\partial V_{Hh}}{\partial T_h} + \frac{\partial r}{\partial T_h} \\
&= \psi g_L \left(\kappa \left[1 - \rho \kappa \left(1 - \frac{1}{\sigma} \right) \frac{y_H}{y_L} \frac{T_h}{y_H} \right] + c_{Lh} \left[1 + \rho \left[(1 - \kappa) - \left(1 - \frac{1}{\sigma} \right) \kappa \right] \frac{y_H}{y_L} \frac{T_h}{y_H} \right] \left(1 + \frac{\eta}{\varepsilon} \right) \right) \\
&\quad - g_H \left[\kappa \left(1 + c_{H\rho} \frac{T_h}{y_H} \right) - c_H \left(1 + \rho \frac{T_h}{y_H} \right) \right] + \psi c_{Lh} (1 - \varepsilon - \eta) + c_{Hh} (1 - \varepsilon) \tag{L.19}
\end{aligned}$$

Setting (L.18) and (L.19) to zero and rearranging, the modified optimal tax formulas are given

by equations (8) and (9):

$$\frac{T_l}{\tilde{y}_{Ll}} = \frac{1 - \varepsilon - g_L + \varphi_l \frac{\eta}{\varepsilon} \sigma (g_L + \varepsilon) + \kappa \frac{g_L}{c_{Ll}}}{\rho g_L (1 - \kappa) \left[1 - \varphi_l \frac{\eta}{\varepsilon} \sigma^2 (1 - \tilde{\kappa}) \right]} \quad (\text{L.20})$$

$$\frac{T_h}{\tilde{y}_{Hh}} = \frac{1 - \varepsilon - \bar{g}_h - \varphi_h \frac{\eta}{\varepsilon} (g_L + \varepsilon) + \kappa \frac{\tilde{g}_h}{\tilde{c}_h}}{\rho (1 - \kappa) \left[\bar{g}_h + \varphi_h g_L \left(\frac{\tilde{y}_{Hh}}{\tilde{y}_{Ll}} \left(1 + \frac{\eta}{\varepsilon} \right) (1 - \tilde{\kappa}) - 1 \right) + \varphi_h g_L \frac{\kappa}{c_{Lh}} \tilde{\kappa} \frac{\tilde{y}_{Hh}}{\tilde{y}_{Ll}} \right]} \quad (\text{L.21})$$

where $\tilde{\kappa} = \frac{\kappa}{1-\kappa} \left(1 - \frac{1}{\sigma} \right)$ measures the increase in marginal utility from the loss in house value from being taxed at T_h rather than T_l ; $\tilde{g}_h = (g_H + \phi g_L) / (1 + \phi)$ is the average marginal social welfare weight of those asked to pay the h tax (note this is not the same as the average social marginal welfare weight of those who *do* pay the h -tax \bar{g}_h); and $\tilde{c}_h = (c_{Hh} + \psi c_{Lh}) / (1 + \phi)$ is the fraction of those asked to pay the h tax who comply.

The equations look much as before, but with some new terms. In the numerators we have the $\kappa g/c$ terms. These account for the fact that all households gain house value when taxes increase, benefiting them. The $(1 - \kappa)$ term in the denominators is similarly there to account for the decrease in marginal utility of consumption coming from the loss of home value. The $(1 - \tilde{\kappa})$ terms in the denominator account for the lower marginal disutility from paying taxes, dampened by the additional house-price loss experienced by the overtagged compliant households. Finally, the final term in the denominator in (L.21) accounts for the lower marginal utility of all overtagged households from their higher house prices.

Notably, these effects interact with the channels highlighted for mistagging: The $(1 - \tilde{\kappa})$ terms dampen (but do not eliminate) the forces that made the mistagging make taxes less progressive.

M Proof of Proposition 3

The proof of proposition 3 is a relatively straightforward application of theorem 1 in [Dong et al. \(2023\)](#). We proceed in three steps. First, we show that potential changes in inequity when $D \rightarrow 0$ are independent of ν . Second, we show that the reduced form effect of crossing the boundary is identified. And third, we combine these results to show the proposition.

Our first lemma shows that crossing the boundary can be thought of as an excludable instrument conditional on the expansiveness rank U and the tax liability τ :

Lemma 5 (Excludability). *Let Assumptions 1, 2 & 3 hold. Then for any $u \in [0, 1]$,*

$$\lim_{d \rightarrow 0^-} f_{\nu|\sigma, \tau, D}(\nu, q_0(d, u, t), t, d) = \lim_{d \rightarrow 0^+} f_{\nu|\sigma, \tau, D}(\nu, q_1(d, u, t), t, d) = \lim_{d \rightarrow 0} f_{\nu|U, \tau, D}(\nu, u, t, d) \quad (\text{M.1})$$

for $v \in \mathcal{V}$ and $\tau \in \mathcal{T}$

Proof. By Bayes' rule, assumption 3, that $U_0|(\nu, D = 0, \tau = t) \sim U_1|(\nu, D = 0, \tau = t)$, where we now make explicit the conditioning on distance $D = 0$ and tax liability τ , implies that $\nu|(U_0 = u, D = 0, \tau = t) \sim \nu|(U_1 = u, D = 0, \tau = t)$, i.e. that $f_{\nu|U_1, D, \tau} = f_{\nu|U_0, D, \tau}$. By invoking our smoothness assumption 2 and the definition relating observed to potential expansiveness ranks $U \equiv U_1 \mathbf{1}[D > 0] + U_0 \mathbf{1}[D < 0]$, we can show that their limits are the same from both sides:

$$\lim_{D \rightarrow 0^+} f_{\nu|U_1, D, \tau}(\nu, u, t) = \lim_{D \rightarrow 0^-} f_{\nu|U_0, D, \tau}(\nu, u, t) = \lim_{D \rightarrow 0} f_{\nu|U, D, \tau}(\nu, u, t)$$

Finally, we exploit the fact that under Assumption 1, for a given $D = d$ and $\tau = t$, whenever $d > 0$ there is a one-to-one mapping between u and $q_1(d, u, t)$ and whenever $d < 0$ there is a one-to-one mapping between u and $q_0(d, u, t)$ so that the same limits apply to the distributions conditional on inequity levels as the distributions conditional on expansiveness ranks

$$\lim_{D \rightarrow 0^+} f_{\nu|\sigma, D, \tau}(\nu, q_1(d, u, t), t) = \lim_{D \rightarrow 0^-} f_{\nu|\sigma, D, \tau}(\nu, q_0(d, u, t), t) = \lim_{D \rightarrow 0} f_{\nu|U, D, \tau}(\nu, u, t)$$

□

Lemma 5 thus show that given an expansiveness rank $U = u$ and a tax liability $\tau = t$, all potential changes in inequity σ when $D \rightarrow 0$ are independent of the unobservables ν . Our second lemma shows that the reduced-form impact of crossing the boundary on compliance is identified:

Lemma 6. *Let Assumptions 1, 2 & 3 hold. Then for any $u \in [0, 1]$,*

$$\begin{aligned} & \lim_{d \rightarrow 0^+} \mathbb{E}[C|U = u, \tau = t, D = d] - \lim_{d \rightarrow 0^-} \mathbb{E}[C|U = u, \tau = t, D = d] \\ &= \int (G(\sigma_1(u, t), t, 0, v) - G(\sigma_0(u, t), 0, t, v)) F_{\nu|U, \tau, D}(dv, u, t, 0) \end{aligned} \quad (\text{M.2})$$

Proof. By assumption 1, we can map from the expansiveness quantiles U to the treatment levels one-to-one:

$$\begin{aligned} & \lim_{D \rightarrow 0^+} \mathbb{E}[C|U = u, D = d, \tau = t] - \lim_{D \rightarrow 0^-} \mathbb{E}[C|U = u, D = d, \tau = t] \\ &= \lim_{D \rightarrow 0^+} \mathbb{E}[C|\sigma = q_1(d, u, t), U_1 = u, D = d, \tau = t] - \lim_{D \rightarrow 0^-} \mathbb{E}[C|\sigma = q_0(d, u, t), U_0 = u, D = d, \tau = t] \end{aligned}$$

And we can substitute in the definition of the potential outcome $C = G(\sigma, \tau, D, \nu)$

$$\begin{aligned} & \lim_{D \rightarrow 0^+} \mathbb{E}[C | \sigma = q_1(d, u, t), U_1 = u, D = d, \tau = t] - \lim_{D \rightarrow 0^-} \mathbb{E}[C | \sigma = q_0(d, u, t), U_0 = u, D = d, \tau = t] \\ &= \lim_{D \rightarrow 0^+} \mathbb{E}[G(q_1(d, u, t), t, d, \nu) | \sigma = q_1(d, u, t), U_1 = u, D = d, \tau = t] \\ & \quad - \lim_{D \rightarrow 0^-} \mathbb{E}[G(q_0(d, u, t), t, d, \nu) | \sigma = q_0(d, u, t), U_0 = u, D = d, \tau = t] \end{aligned}$$

By the smoothness assumption 2 and the compact support of ν , we can exchange the order of the limit and the expectation integral and the expectation above is continuous in D so that

$$\begin{aligned} & \lim_{D \rightarrow 0^+} \mathbb{E}[G(q_1(d, u, t), t, d, \nu) | \sigma = q_1(d, u, t), U_1 = u, D = d, \tau = t] \\ & \quad - \lim_{D \rightarrow 0^-} \mathbb{E}[G(q_0(d, u, t), t, d, \nu) | \sigma = q_0(d, u, t), U_0 = u, D = d, \tau = t] \\ &= \mathbb{E}[G(\sigma_1(u), t, 0, \nu) | U_1 = u, D = 0, \tau = t] - \mathbb{E}[G(\sigma_0(u), t, 0, \nu) | U_0 = u, D = 0, \tau = t] \end{aligned}$$

Finally, by assumption 3 and lemma 5 the two expectations are integrating over the same distribution f_ν so we have that

$$\begin{aligned} & \mathbb{E}[G(\sigma_1(u), t, 0, \nu) | U_1 = u, D = 0, \tau = t] - \mathbb{E}[G(\sigma_0(u), t, 0, \nu) | U_0 = u, D = 0, \tau = t] \\ &= \int (G_1(u), t, 0, v) - G(\sigma_0(u), t, 0, v) F_{\nu|U, \tau, D}(dv, u, t, 0) \end{aligned}$$

□

For the third step to complete the proof of proposition 3, note that by definition $\sigma = q(d, t, u) = q_0(d, t, u)(1 - Z) + q_1(d, t, u)Z$. Assumption 2 implies that $q_z(d, t, u)$, $z = 0, 1$ is smooth and so the right and left limits at $D = 0$ exist: $\lim_{D \rightarrow 0^+} q(d, t, u) = q_1(0, t, u) \equiv \sigma_1(t, u)$ and $\lim_{D \rightarrow 0^-} q(d, t, u) = q_0(0, t, u) \equiv \sigma_0(t, u)$. Combining this with lemmas 5 and 6 shows that equation (11) holds.

To see that the weighted W-LATE also holds note three things. First, the Q τ -LATEs $\eta(u, t)$ are identified. Second, the weighting function $w(t, u)$ is assumed to be known or estimable. Third, the set $\mathcal{U} \equiv \{u \in [0, 1] : |\sigma_1(u) - \sigma_0(u)| > 0\}$ is identified given that the potential treatments $q_z(d, t, u)$, $z = 0, 1$ are identified (and in fact correspond to the quantiles such that $F_{E_z|t, d}^{-1}(u) > 0$).

N Proof of Proposition 4

Our proof proceeds similarly to the proof of proposition 4. We proceed in five steps.

First, note that our relaxed assumptions still allow us to apply 5 to the distribution of ν_1 and so we have that

$$\lim_{d \rightarrow 0^-} f_{\nu_1|\sigma,\tau,D}(v_1, q_0(d, u, t), t, d) = \lim_{d \rightarrow 0^+} f_{\nu_1|\sigma,\tau,D}(v_1, q_1(d, u, t), t, d) = \lim_{d \rightarrow 0} f_{\nu_1|U,\tau,D}(v_1, u, t, d) \quad (\text{N.1})$$

for $v_1 \in \mathcal{V}_1$ and $\tau \in \mathcal{T}$

Second, our relaxed assumptions mean that we cannot apply 5 to the distribution of ν_0 . Instead, the limits are given by the following lemma:

Lemma 7 (ν_0 Limits). *Let Assumptions 1 & 4 hold, Then for any $u \in [0, 1]$, The limiting conditional distributions of ν_0 as $D \rightarrow 0$ from above and from below exist and are given by*

$$\begin{aligned} \lim_{D \rightarrow 0^+} f_{\nu_0|\sigma,\tau,D}(v_0, q_1(d, u, t), t, d) &= \lim_{d \rightarrow 0^+} f_{\nu_0|U_1,\tau,D}(v_0, u, t, d) = f_1(v_0, t) \\ \lim_{D \rightarrow 0^-} f_{\nu_0|\sigma,\tau,D}(v_0, q_0(d, u, t), t, d) &= \lim_{d \rightarrow 0^-} f_{\nu_0|U_0,\tau,D}(v_0, u, t, d) = f_0(v_0, t) \end{aligned}$$

Proof. The proof proceeds in two steps. First, by Assumption 1, we can relate observed treatment σ to the potential expansiveness rank U_z on either side of the boundary. For a given $D = d$ and $\tau = t$, whenever $d > 0$ there is a one-to-one mapping between U_1 and $q_1(d, U_1, t)$ and whenever $d < 0$ there is a one-to-one mapping between U_0 and $q_0(d, U_0, t)$ so that for any $d > 0$, $f_{\nu_0|U_1,\tau,D}(v_0, u, t, d) = f_{\nu_0|\sigma,\tau,D}(v_0, q_1(d, u, t), t, d)$ and for any $d < 0$, $f_{\nu_0|U_0,\tau,D}(v_0, u, t, d) = f_{\nu_0|\sigma,\tau,D}(v_0, q_0(d, u, t), t, d)$.

Second, note that by Assumption 4, the distribution of ν_0 is independent of a taxpayer's potential expansiveness rank, and has both left- and right-limits at $D = 0$, though they need not be the same, as indicated by the subscripts at the end of the equalities. \square

Third, we establish the limiting values of the conditional expectations of compliance.

Lemma 8 (Compliance Limits). *Let Assumptions 1, 4, & 5 hold. Then, for any $u \in [0, 1]$,*

$$\begin{aligned} \lim_{d \rightarrow 0^+} \mathbb{E}[C|U = u, \tau = t, D = d] &= \int_{\mathcal{V}_0} G_0(t, 0, v_0) dF_1(dv_0, t) \\ &\quad + \int_{\mathcal{V}_1} G_1(\sigma_1(u, t), t, 0, v_1) F_{\nu_1|U,\tau,D}(dv_1, u, t, 0) \quad (\text{N.2}) \\ &= m_0^+(t) + m_1^+(u, t) \end{aligned}$$

$$\begin{aligned} \lim_{d \rightarrow 0^-} \mathbb{E}[C|U = u, \tau = t, D = d] &= \int_{\mathcal{V}_0} G_0(t, 0, v_0) dF_0(dv_0, t) \\ &\quad + \int_{\mathcal{V}_1} G_1(\sigma_1(u, t), t, 0, v_1) F_{\nu_1|U,\tau,D}(dv_1, u, t, 0) \quad (\text{N.3}) \\ &= m_0^-(t) + m_1^-(u, t) \end{aligned}$$

(N.4)

Proof. We present the proof for the limit from above in equation (N.2). Exactly analogous steps establish the statement for the limit from below in equation (N.3). By assumption 1, we can map

from the expansiveness quantiles U to the treatment levels one-to-one:

$$\lim_{D \rightarrow 0^+} \mathbb{E}[C|U = u, D = d, \tau = t] = \lim_{D \rightarrow 0^+} \mathbb{E}[C|\sigma = q_1(d, u, t), U_1 = u, D = d, \tau = t]$$

And we can substitute in the definition of the potential outcome $C = G(\sigma, \tau, D, \nu) = G_0(D, \tau, \nu_0) + G_1(\sigma, \tau, D, \nu_1)$

$$\begin{aligned} & \lim_{D \rightarrow 0^+} \mathbb{E}[C|\sigma = q_1(d, u, t), U_1 = u, D = d, \tau = t] \\ &= \lim_{D \rightarrow 0^+} \mathbb{E}[G_0(d, t, \nu_0) + G_1(q_1(d, u, t), t, d, \nu_1) | \sigma = q_1(d, u, t), D = d, \tau = t] \end{aligned}$$

By the smoothness in Assumption 4 with the compact supports of ν_1 and ν_2 , we can exchange the order of the limit and the expectation and the expectation has a right-limit in D at $D = 0$ so that

$$\begin{aligned} & \lim_{D \rightarrow 0^+} \mathbb{E}[G_0(D, \tau, \nu_0) + G_1(\sigma, \tau, D, \nu_1) | \sigma = q_1(d, u, t), D = d, \tau = t] \\ &= \mathbb{E}_{\nu_0}[G_0(0, t, \nu_0) | D = 0, \tau = t] + \mathbb{E}_{\nu_1}[G_1(\sigma_1(u), t, 0, \nu_1) | U_1 = u, D = 0, \tau = t] \end{aligned}$$

Finally, applying lemmas 5 and 7, these are

$$\begin{aligned} & \mathbb{E}_{\nu_0}[G_0(0, t, \nu_0) | D = 0, \tau = t] + \mathbb{E}_{\nu_1}[G_1(\sigma_1(u), t, 0, \nu_1) | U_1 = u, D = 0, \tau = t] \\ &= \int_{\mathcal{V}_0} G_0(t, 0, v_0) F_{\nu_0|U_1, \tau, D}(dv_1, u, t, 0) + \int_{\mathcal{V}_1} G_1(\sigma_1(u, t), t, 0, v_1) F_{\nu_1|U_1, \tau, D}(dv_1, u, t, 0) \\ &= \int_{\mathcal{V}_0} G_0(t, 0, v_0) F_1(dv_0, t) + \int_{\mathcal{V}_1} G_1(\sigma_1(u, t), t, 0, v_1) F_{\nu_1|U, \tau, D}(dv_1, u, t, 0) \end{aligned}$$

□

Fourth, we combine these elements to establish equation (15). For the denominator, note that by definition $\sigma = q(d, t, u) = q_0(d, t, u)(1 - Z) + q_1(d, t, u)Z$. Assumption 2 implies that $q_z(d, t, u)$, $z = 0, 1$ is smooth and so the right and left limits at $D = 0$ exist: $\lim_{D \rightarrow 0^+} q(d, t, u) = q_1(0, t, u) \equiv \sigma_1(t, u)$ and $\lim_{D \rightarrow 0^-} q(d, t, u) = q_0(0, t, u) \equiv \sigma_0(t, u)$. Applying lemma 6 to the terms in the numerator, we have

$$\begin{aligned} & \lim_{d \rightarrow 0^+} \mathbb{E}[C|U = \bar{u}, \tau = t, D = d] = m_0^+(t) + m_1^+(\bar{u}, t) \\ & \lim_{d \rightarrow 0^-} \mathbb{E}[C|U = \bar{u}, \tau = t, D = d] = m_0^-(t) + m_1^-(\bar{u}, t) \\ & \lim_{d \rightarrow 0^+} \mathbb{E}[C|U = \underline{u}, \tau = t, D = d] = m_0^+(t) + m_1^+(\underline{u}, t) \\ & \lim_{d \rightarrow 0^-} \mathbb{E}[C|U = \underline{u}, \tau = t, D = d] = m_0^-(t) + m_1^-(\underline{u}, t) \end{aligned}$$

And inserting these into the definition of $\eta(\underline{u}, \bar{u}, t)$ completes the proof.

Fifth, to see that the weighted WDD-LATE is also identified, note three things. First, the $Q\tau$ DD-LATEs $\eta(\underline{u}, \bar{u}, t)$ are identified. Second, the weighting function $w(\underline{u}, \bar{u}, t)$ is assumed to be known or estimable. Third, the set $\mathcal{U} \equiv \{u \in [0, 1] : |\sigma_1(u) - \sigma_0(u)| > 0\}$ is identified given that the potential treatments $q_z(d, t, u)$, $z = 0, 1$ are identified (and in fact correspond to the quantiles such that $F_{E_z|t, d}^{-1}(u) > 0$).